High throughput breeding for wood quality improvement

Nicholas T. Davies
University of Canterbury

New Zealand School of Forestry
Department of Engineering
University of Canterbury

Doctorate of Philosophy
University of Canterbury
· 2019 ·

Abstract

Eucalypt species are fast-growing and can produce high quality timber for appearance and structural products including Laminated Veneer Lumber (LVL). Their use for solid wood products is hindered by the fact that they can contain large growth-strains, which impose substantial processing costs. Growth-strains are associated with log splitting, warp, collapse and brittle-heart. The body of work presented here focused on the possibility of very-early selection at two years of age, of *Eucalyptus bosistoana* trees for growth-strain and other wood properties, including an in-depth assessment of the accuracy of the methodology used.

Chapter 1 gives an introduction on growth-stresses in trees and how this knowledge developed over the last century. Chapter 2 describes a pilot study assessing wood properties at a young age. Growth-strain was assessed by measuring stem openings after splitting along the pith, which resulted in a left-censored dataset. A Bayesian approach to the analysis was used to increase the accuracy of genetic parameter prediction from the left-censored data. Chapter 3 tested the hypothesis that the reason for the left-censored data was tension wood formed early in growth resulting in a reversed stress profile. The testing showed this was not the case, at least under the given experimental conditions. Chapter 4 describes a very-early selection trial (age 2) of 81 *Eucalyptus bosistoana* families with seven measured traits (growth-strain, under-bark diameter, density, stiffness, volumetric shrinkage, height and acoustic velocity), which yielded heritability estimates of 0.23, 0.57, 0.70, 0.77, 0.39, 0.71, and 0.80 respectively. Following this the precision of the splitting test was investigated. Chapter 5 describes an experimental approach which found that the splitting test could predict surface growth-strains with a precision of ± 1003 micro-strain (Chapter 5). The accuracy of the splitting test was further investigated in Chapter 6 using a classical mechanics model. The effect of differing surface strain fields on the results of both the splitting test and point measurements such as strain-gauges, indicated that the theoretically obtainable maximum accuracy of the splitting test is approximately ± 281 micro-strains. This is similar to four evenly spaced strain-gauges. Finally, Chapter 7 reviews very-early selection and provides guidelines for future breeding projects where reduced cycle times are desired.

Λόγον ἔχεις;' 'ἔχω.' 'τί οὖν οὐ χρᾷ; τούτου γὰρ τὸ ἑαυτοῦ ποιοῦντος τί ἄλλο θέλεις;'

- Marcus Aurelius (4.13)

Contents

List of Figures

List of Tables

Acknowledgments

I would like to acknowledge a number of people and organisations for their monetary, motivational and academic support throughout this research. This work would not have been possible without all of them. The New Zealand tax payer and the other funders of the Sustainable Farming Fund and the T.W. Adams scholarship, both provided financial assistance for running the trials, course fees, living costs, travel and other sundry items. Dr Luis Apiolaza and Dr Clemens Altaner provided supervisory roles for the project, giving advice, criticism, guidance and support even with some of my slightly esoteric or obscure approaches. Nigel Pink for the training and supervision in the laboratory. My academic friends, Hunter, Merel and Christian for the hours of sound-boarding and advice over the years. My friends outside of academia, particularly Louise and Saff for the emotional support and giving me a grounding outside of academia. Last but not least my family Heather, Meric, Rebecca and Elaine Davies for for their continued financial and motivational support.

Prologue

The New Zealand forest industry is approximately 90% *Pinus radiata*, with around 1.3% eucalypt species. The industry produces about 6.7 billion NZD or 12% of the country's annual exports (Forest Owners Association, 2017). The large reliance on a single species clearly has risk management implications for the New Zealand economy as both climate and bio-security risks increase. Further *Pinus radiata*, while a generalist, does not necessarily perform as well as other species in particular environments. Over the last decade, the New Zealand Drylands Forest Initiative (NZDFI) has been investigating some eucalypt species for their suitability in New Zealand environments.

Tree breeding programmes typically have very long breeding cycles as a consequence of the long commercial rotation lengths and reproductive cycles of the organisms. The large space, monetary and time requirements for traditional tree breeding programmes make them very expensive. There is a lot of value to be gained if these breeding cycles can be reduced in time, space and cost requirements. One potential way to reduce all three of these is to harvest and test breeding trials at young ages. However, doing this results in trait measurements which are more removed and hence, less predictive of the final desired commercial properties than the traditional longer cycle.

NZDFI has obtained the largest collection of seed in the world for a number of naturally durable eucalypt species, including *E. bosistoana*, with the aim of establishing a fast-growing, naturally durable, stiff, sustainable plantation timber resource in New Zealand (van Ballekom and Millen, 2017). The basis is a breeding programme which gives wood properties the same priority as growth, form and tree health. This approach to tree improvement also includes very-early screening (age 2) to ensure a timely deployment of improved germplasm (Altaner, 2015).

This work aims to investigate the potential of very-early selection as a breeding strategy

and to develop very-early selection tools. With the splitting test, screening of the entire genetic stock is now a practical solution to remove growth-strain induced wood defects. Three trials in Woodville, New Zealand totalling approximately 10,000 trees from 200 families each with ˜50 half-sibling replicates of *E. bosistoana* were established. Results from the first of these trials are presented in Chapter 4. As the tests are destructive, the superior individuals need to be rescued by coppicing. Propagation of coppice cuttings is also providing a fast route to deploy improved material to the forestry sector. Additionally, a number of long-term field trials have been established (as early as 2009) throughout New Zealand to provide longer term studies of wood properties in particular heartwood formation (van Ballekom and Millen, 2017).

Chapter 1

Background and literature review

1.1 Wood structure and formation

As trees grow they produce wood in order to become taller, wider, and re-orientate stems, branches and roots. Becoming taller or reorienting stems and branches can be an effective way to out-compete other plants for light. Increasing height and width (or stems becoming off axis) increases gravitational force and wind drag on the structure, which requires either enough redundant strength (such as in monocotyledons) or for the tree to strengthen its structure as it increases in size. In woody plants size increase and reorientation occurs in two ways, apical (upwards) growth and cambial (diameter) growth on branches, roots and the stem(s).

Softwoods have a simpler xylem anatomy than hardwoods, consisting mainly of axially elongated tracheids which provide both mechanical support and water transport (Bowyer et al., 2007). A rendition of the cell wall structure of a softwood tracheid is presented in Figure 1.1. Of note are the Middle Lamella (ML) which holds cells together, the Primary wall (P) which is primarily responsible for cellular extension, and the compound Secondary

wall S_{1-3}. A good description of the cell wall structure is available on pages 50-53 of Walker (1993).

Hardwoods are more complex with a number of different cell types. Fibres, similar to softwood tracheids provide structural support, however it is their primary function, with vessels providing conduction. Vessels are comprised of multiple elements joined at the ends to form long conduits, forming a network from the bottom to the top of the tree (Walker, 1993). Both hard and soft woods produce rays which are typically formed by radially orientated parenchyma cells (Walker, 1993) (Figure 1.2). Rays provide a mechanical advantage by diverting the axial force and reducing buckling and shear stresses between fibres (Mattheck and Kübler, 1997). Detailed discussions of wood anatomy can be found in wood anatomy texts such as Fromm (2013).

Growth-stresses in normal wood result from the tendency for cells to contract longitudinally and expand tangentially while developing their secondary cell wall. The effect on the stem as a whole is shown in Figures 1.3 and 1.4. It is thought these stresses develop in normal wood, preloading the wood in tension in order to increase mechanical safety by improving compression strength (Mattheck and Kübler, 1997), which has been showed to be around three times lower than tensile strength depending on the species (Ross and USDA Forest Service., 2010).

The two main independent hypotheses as to how growth-stresses form are the lignin swelling hypothesis and cellulose contraction hypothesis. The lignin swelling hypothesis argues that the cellulose fibril aggregate network in the cell wall starts to be layed down before lignin is deposited. During deposition of lignin into the secondary cell wall the

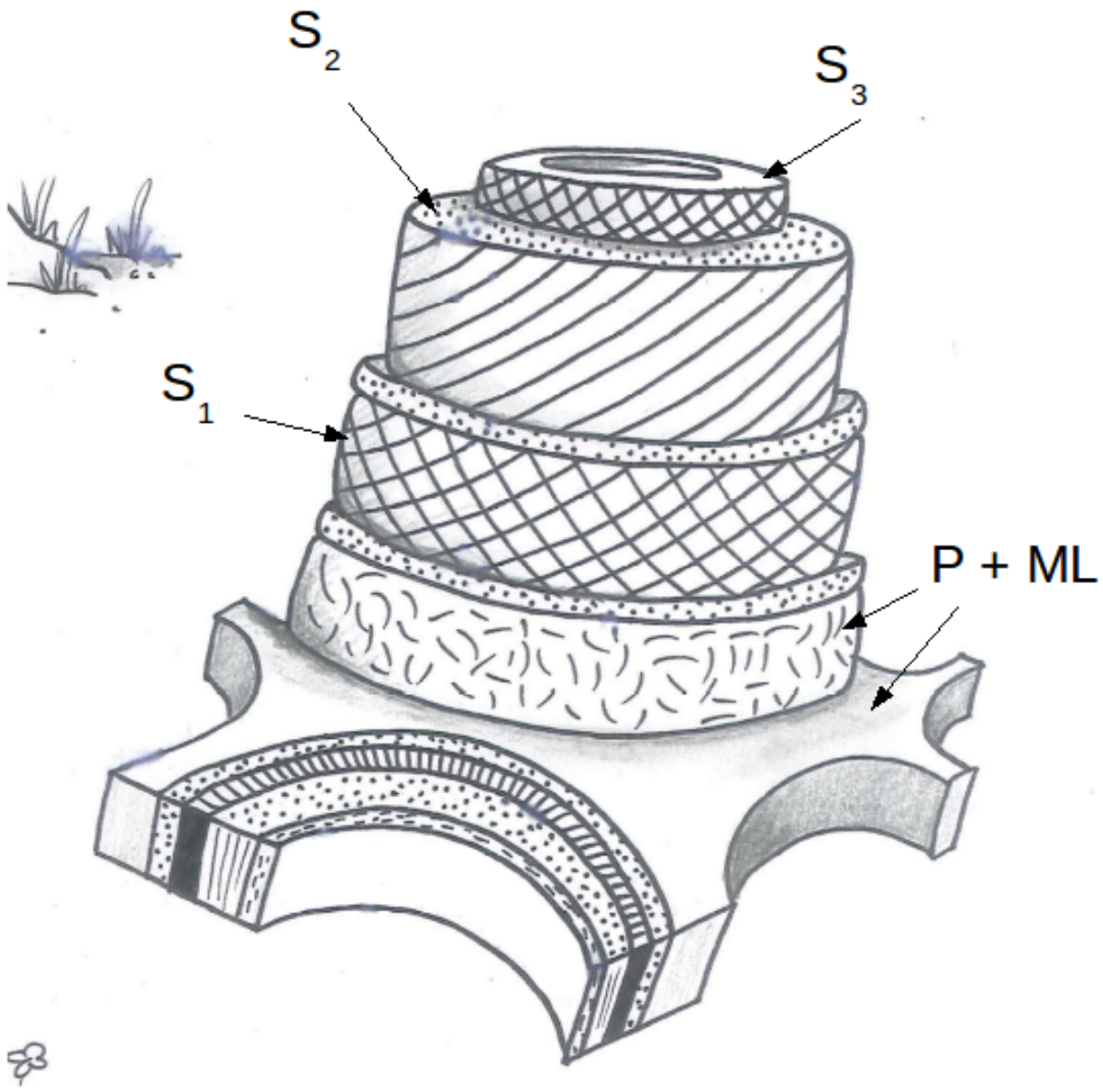

Figure 1.1: Cell wall structure of a tracheid. The middle lamella ML connects cells together. The primary P cell wall is the inital living cell wall which encloses the secondary cell wall, consisting of the S_1, S_2 and S_3 layers. Image courtesy of Eve Baker.

cellulose aggregate is pushed apart (Boyd, 1950). The cellulose contraction hypothesis (Bamber, 1979, 2001) claims the cellulose fibrils change their length after incorporation into the aggregate network resulting in cellular distortion. A combination of the two has

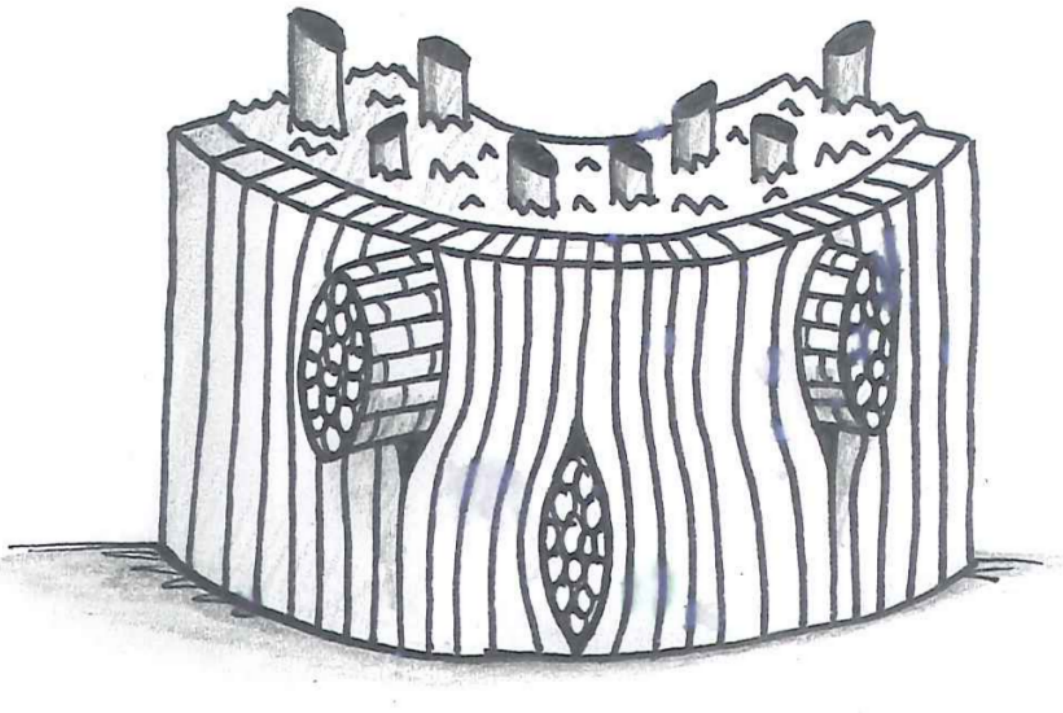

Figure 1.2: Artists' rendition of the ray-fibre structure. Note the rays running toward the viewer and longitudinally aligned tracheids. Image courtesy of Eve Baker.

also been proposed and shown to fit experimental data well (Okuyama et al., 1986, 1994; Yamamoto, 1998; Yamamoto et al., 1992, 1991). Regardless of the mechanism, the result is typically a longitudinal contraction and a tangential expansion of the cells, resulting in the stem periphery being under tension and the pith under compression (Archer, 1987a).

In order to reorientate stems and branches most trees form reaction wood, which produces a force to reorientate the tissue (Gardiner et al., 2014). Reorientation occurs for a number of reasons, it may be upwards as controlled by negative gravitropism or to reorientate toward light or to reduce wind drag (Niklas and Spatz, 2012; Coutts and Grace, 1995). In softwoods this reorientation is caused by the production of compression wood.

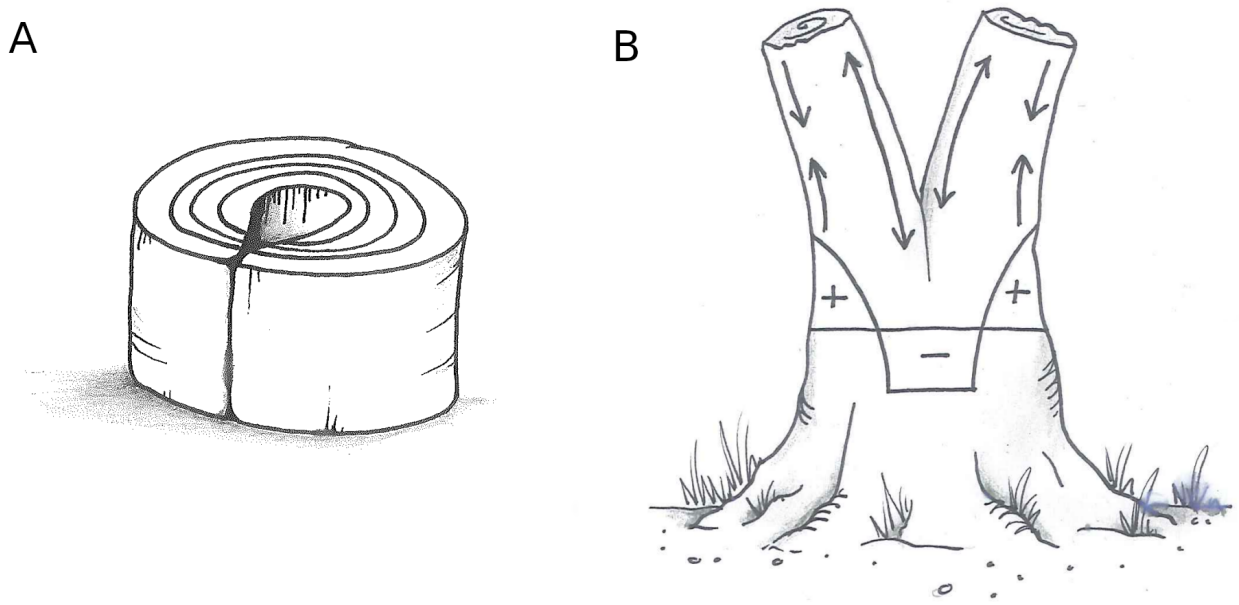

Figure 1.3: Artists' rendition showing the effect of tangential (A) and axial (B) growth-stress on a stem. Positive $+$ sign shows axial tension while the negative sign $-$ shows axial compression. Image courtesy of Eve Baker.

Compression wood forms on the lower side or bottom of the branch and expands longitudinally (Timell, 1986). Hardwoods on the other hand typically produce tension wood on the upper side which contracts longitudinally (Gardiner et al., 2014). An intuitive way of envisioning both compression and tension wood is presented in Figure 1.5.

This work focuses on fibres as they are the structural cells expected to be responsible for growth-stresses in normal and reaction wood within hardwoods (Archer, 1987a). Fibres consist of a number of cell wall layers. Normal wood fibres consist of a middle lamella (ML) connecting the fibre to the surrounding cells and a primary cell wall (P) formed during cell expansion, and a secondary cell wall (S) consisting of S_1, S_2 and S_3 sub-layers formed once expansion is complete (produced in order so the overall composition will change depending on the cells developmental stage) (Barnett, 1981). The S_2 layer is the thickest

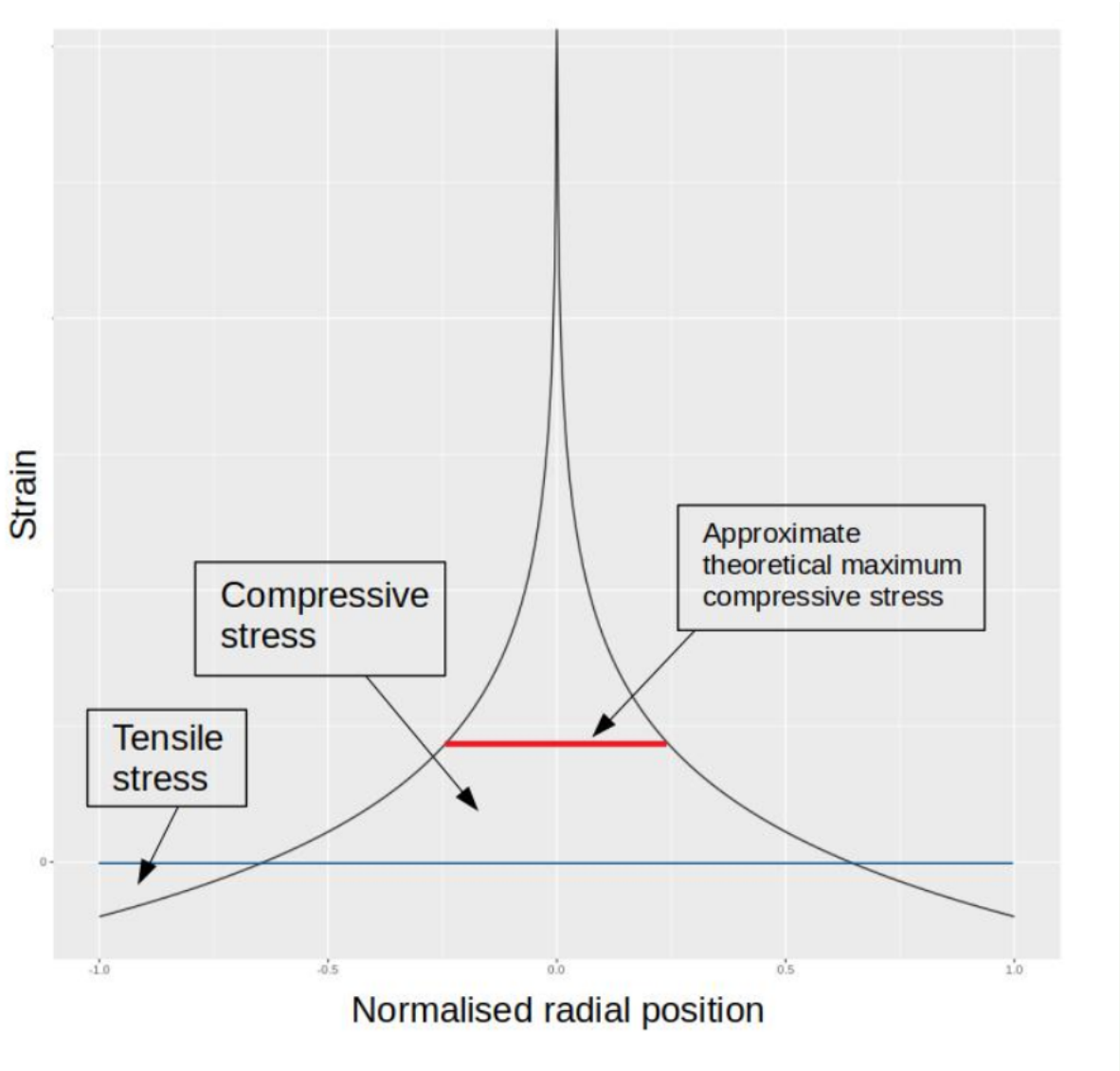

Figure 1.4: Axial stress profile within a normal stem.

layer and consists of cellulose macro-fibrils wrapped in a steep helix around the cells longitudinal axis (Figure 1.1). The cellulose is contained within a matrix of hemicelluloses and lignins giving the cell wall properties of a reinforced composite (Niklas and Spatz, 2012).

In order for the living cambial cells to produce wood, each cell must go through division from its parent cell, growth and death. Because cells in the cambium (and apical meris-

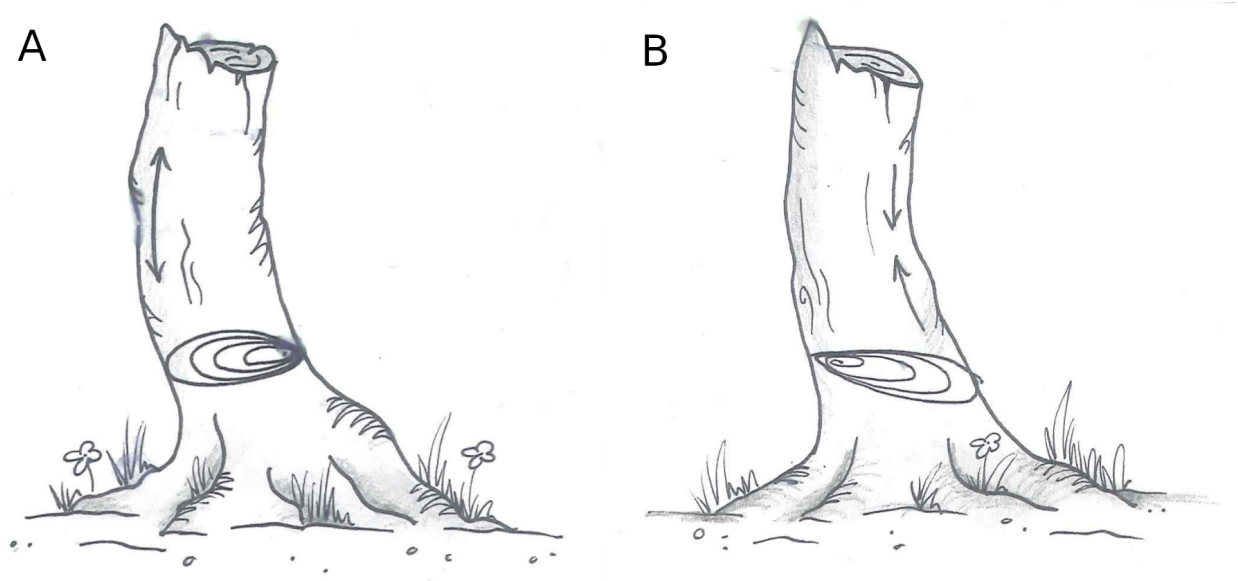

Figure 1.5: Artists' depiction of how compression wood (A) and tension wood (B) reorientate tree stems. Image courtesy of Eve Baker.

tem) are continually dividing, the tree as a dynamic structure is changing form to become better adapted to changing environmental settings (ontogeny), even though large portions (ie the wood) are dead.

1.2 Cell division, formation, elongation and death

Dicotyledons and gymnosperms grow in two main ways, upward by apical growth and outward by cambial growth. As the cambium is forming, fusiform and ray initials are created by the apical meristems. From the cambial initials, cells separate to the inside becoming the elements of xylem (tracheids, vessels, fibres, parenchyma, etc.), while cells to the outside become phloem (Fromm, 2013).

During primary wall formation rapid elongation occurs. The internal hydrostatic (turgor) pressure causes cell expansion controlled primarily by the orientation of the cellulose

micro-fibrils (Tyerman et al., 2002; Cosgrove, 2005). Because the centre of the cell has restricted movement, elongation to dissipate the increasing tensile forces from the turgor pressure occurs by tip growth (Taiz and Zeiger, 2006).

The primary cell wall has randomly orientated micro-fibrils embedded in hemicellulose and pectic compounds, and becomes lignified when the secondary cell wall layers are added. The middle lamella is highly lignified. Often the term compound middle lamella (CML) is used to describe the middle lamella and primary cell wall as one, as it can be hard to distinguish between them. Once the cell has reached its full size biosynthesis of the secondary layers starts (Fromm, 2013).

Typically the S_1 layer is thin and comprised of micro-fibrils winding around the cell axis at a high angle (Figure 1.1). Within the layer many laminates are found. Within each laminate the micro-fibrils are closely aligned, however between each laminate they can differ, or even reverse the direction of the helix, although lower right to upper left orientation tends to be favoured (Fromm, 2013). Close to the S_2 layer the Micro-Fibril Angle (MFA) decreases rapidly. The S_2 layer is typically much thicker and has more axially oriented mirco-fibrils compared to the primary, S_1 and S_3 layers. These S_2 mirco-fibrils circle the cell axis from lower left to upper right. The thin S_3 layer formed on the inside of the S_2 layer is characterised by a high MFA, reversing the direction of the micro-fibril helices to lower right to upper left (Walker, 1993).

In tension wood of some species a gelatinous layer (G-layer) is formed on the inside of the innermost wall (S_1, S_2 or S_3) (Gardiner et al., 2014). The G-layer has near axially oriented micro-fibrils and typically very little lignification. Traditionally the G-layer, a layer primarily consisting of low MFA cellulose fibrils on the inside of the fibres, is credited with forming growth-stresses within tension wood. However some hardwoods produce tension wood without a G-layer such as *Eucalyptus nitens* (Qiu et al., 2008) and a number of other

species (Ruelle et al., 2006). It is suspected that the G-layer plays an important role in the generation of reorientation stresses (Pilate et al., 2004).

At some point during, or soon after the formation of the secondary cell wall, the cell shrinks axially and expands transversely (Boyd, 1972) (The exception is some young softwoods, where the opposite occurs (Jacobs, 1945)). Because of the connectedness between cells a stress profile forms within the stem (Figures 1.3 and 1.4). After the secondary wall formation cell death occurs in fibres and tracheids.

Growth-stresses in trees develop as part of cell formation and are thought to provide a superior mechanical structure (Mattheck and Kübler, 1997). The continual formation of new cells axially contracting on the periphery of the stem causes the older wood, which has completed formation, to contract with each new layer of cells. Older wood near the centre of the stem becomes axially compressed while the newer cells cannot fully contract and remain in axial tension (Archer, 1987a). Growth-stresses in normal wood increase the mechanical stability of the stem by increasing resistance to compression failure, which occurs at a smaller deformation than tensile failure (about half), by pre-tensioning the wood (Mattheck and Kübler, 1997).

Asymmetrical deposition of reaction wood provides the ability for the stem to reorient in order to be best adapted to its environment (Figure 1.5). Growth-stresses are an evolutionary advantage allowing an adaption in a changing environment, however they cause significant value loss when harvesting and milling timber (Kübler, 1987).

1.3 History of work on growth-stresses

Wood workers have known of growth-stresses within trees for centuries, usually referred to as 'a pull towards the sap'. When cutting boards good craftsmen would section logs in such a way as to get straight boards once the growth-stresses were released (Jacobs, 1945). Most early studies on growth-stresses investigated how and why boards changed shape when cut from an intact stem.

Martley (1928) was possibly the first to study growth-stresses in a scientific manner. Initially he argued that the curvature of planks sawn from logs was because the current growth was not able to support the dead weight of the tree until lignification was complete. As a result the centre of the stem is under compression while the periphery had zero stress. However, he showed that the self-weight was not sufficient to cause the observed longitudinal dimension changes of the timber. Later Kübler (1987) stated it would account for approximately one twentieth of longitudinal compression stresses.

After Martley's work a small number of authors investigated growth-stresses through the 1930s and 1940s. Jacobs (1945) tested 34 hardwood species, focusing mainly on Eucalypts. He argued that longitudinal tension stress successively develops in the outer layers of the stem as it grows, and as a consequence of this tension, compression must form in the centre of the stem. Experimentally Jacobs made use of strip planking, measuring the deflection of the board after removal from the log, and the length change when the planks were forced back straight. He showed that wood tended to shrink in the longitudinal direction at the periphery while it extended near the pith (indicating the log is under compression in the centre and tension at the surface).

Further Jacobs (1945), put forward a number of hypotheses to explain how growth-stresses develop. He argued that it is very unlikely that dead cells (wood) could extend within the

core in order to create the observed stress gradient. Instead suggesting several possible mechanisms: weight of the tree, surface tension and sap stream forces, cellulose and colloidal complexes, lignin intercellular substances and action within the primary or secondary cell wall. Without any evidence he did not claim any of these to be the major cause (Jacobs, 1945).

Stresses relating to reaction wood received more attention through the 1930s and 1940s for both soft and hardwoods. Jacobs (1945) stated that the reorientation of stems is caused by a modification of the already existing stress gradient throughout the stem. One option he presented was that the eccentric growth causes larger numbers of cells to be added to the inner side of the curve (in hardwoods). If each cell provides the same contraction force this will result in an angle correction of the stem. Sap tension was also considered, but more importantly Jacobs notes the possibility of tension being formed within the cell walls of tension wood. Jacobs (1945) also found that the amount of reaction wood developed and the stem angle recovery had a poor relationship. Consequently he suggested that the normal axial surface strain pattern in tension corrected the lean, the reaction wood merely acted as a pivot.

Boyd et al. (1950) developed an experimental technique to investigate the stress profile further. Direct extension measurements from inside the stem were obtained by cutting a longitudinal slit in the centre of the log, attaching strain gauges onto the wood inside the slit and successively shortening the log from both ends. He found the point of crossover from longitudinal tension to compression was approximately two thirds the radius out from the pith.

Most commonly, growth-stresses were investigated in the longitudinal direction; however cells also change dimension in the transverse direction, leading to a more complicated three-dimensional stress field even within a straight stem.

Koehler (1933) showed that a radial saw cut through a stem disk had a tendency to close near the periphery (Figure 1.3), suggesting that the peripheral cells are under tangential compression with the inner cells under radial tension. He suggested this could cause shakes (cracks propagating from the periphery towards the pith) in standing trees. Jacobs (1945) removed inner circles from disks of a number of species and found that disk circumference increased when an inner portion was removed. Jacobs again argued that strain in the sap stream along with cells being wider tangentially than radially led to the observed lateral stresses. Jacobs also suggested that secondary cell wall thickening caused by the deposition of lignin was a possible contributing factor. Boyd et al. (1950) investigated radial stress patterns by removing a wedge from a disk and measuring radial expansion, showing that the disks were under radial tension.

The Poisson effect states that the change of dimension of a material in one direction will result in a change of dimension in the perpendicular directions. This relationship is characterised by the Poisson ratio, within the elastic region of deformation. It appears the redistribution of growth-stress through the Poisson ratio from the longitudinal to transverse directions is not sufficient to account for the observed tangential strains, which can also vary for a given longitudinal strain (Kübler, 1987). Boyd et al. (1950) also showed that the longitudinal stresses manifesting as transverse stresses via Poisson ratios are only approximately one tenth of the measured stresses.

Yamamoto et al. (1992) provided an in depth discussion of the available theories describing growth-strain formation at that time, arriving at the conclusion that the cell wall development must control the shape change which results in the formation of the stem wide growth-stress profile. He postulated cellulose, lignin and other carbohydrates all play a role when stresses are formed in normal, compression and tension wood.

Wardrop (1965) commented that a tensile stress generated by cellulose transitioning into

a crystalline state could be the explanation for cells contracting during the formation of the secondary wall. Cellulose contraction aligned well with the observation that the G-layer has a very low MFA and is common in tension wood producing species. Bamber (1979) further argued for the cellulose contraction hypothesis claiming turgor pressure in normal wood cells remained high enough that cells do not contract before the lignin was deposited. During or after lignin deposition the cellulose could become crystalline and shrink, causing the cell wall to contract along the micro-fibril direction. The mechanism for tension wood was suggested to be essentially the same. The mechanism for compression wood development on the other hand was explained by the turgor pressure decreasing before lignification, causing the cell to contract. In turn the cellulose was under compression, resulting in the tendency for the compression wood cells to expand in the direction of the micro-fibrils. Later, Bamber (2001) modified his explanation arguing that the cellulose is laid down in a compressed or extended state to account for both compression wood and tension wood respectively.

Boyd (1972) popularised the alternative and more widely accepted hypothesis of lignin swelling, which was first conceived by Munch (1938) and reviewed by Boyd (1972). Tensile stress is gained in cells of low MFA by lignin deposition into the cell wall, pushing the cellulose fibrils apart, which in turn shrinks the axial length of the cell and increases the transverse dimensions. When the MFA is high, the opposite occurs, lengthening the cell and reducing its transverse dimensions. Note that when cells are part of the larger tissue, some of these cell wall dimension changes may not manifest macroscopically. Cells may be constrained in some directions but not others so may expand into the lumen, or in the radial direction, but not in the tangential directions because neighbouring cells occupy the space.

Around the same time two other lesser known hypothesis were presented. Hejnowicz

(1967) argued that the stresses in compression wood are related to the introduction of water by the cell walls, which results in swelling, because the expansion of compression wood is equal to the shrinkage due to drying. Brodzki (1972) hypothesised strains due to 1,3-linked glucan (callose) deposition within the helical checks of the S_2 cell wall layer could be the most significant factor in longitudinal growth-stress generation. Boyd (1977) refuted this idea arguing (along with other issues) that the callose would expand into the cell lumen not causing any stresses in the cell wall, unless a (non-observed) constraining medium restricted callose expansion.

Through the late 70's and 80's Archer produced a number of papers in the series, 'On the distribution of growth-stresses' (Archer and Byrnes, 1974; Archer, 1976, 1979, 1981, 1985), mainly concerning the mathematical treatment of the stress fields within trees. Advancing on Kübler's (Kübler, 1959a,b) work, Archer introduced an orthotropic solution which allowed for each new growth increment to alter the stress distribution within the stem in a self equilibrating fashion. The other advancement made was the increased accuracy changing the radial crossover point from axial compression to tension, being governed by the moduli in both the radial and tangential directions. Archer went on to develop a numerical approximation to the stress fields generated by asymmetric growth-strains and inclined grains. He used the developed methods to present solutions for a number of hardwood species.

Archer followed up his series 'on the distribution of tree growth-stress' with 'On the origin of growth-stresses' (Archer, 1987b, 1989) where he attempted to mathematically investigate individual cells, presenting an explicit relationship between strains and growth increment of the cell wall. The relationship relates MFA to cell wall swelling strain, and he argued that these results are consistent with the lignin swelling hypothesis for compression wood. In tension wood, assuming an MFA of zero and an increasing ratio of area of the cell wall

to total cell cross sectional area by adding a G-layer could theoretically produce a tensile stress of 36 MPa, with the parameters Archer used. Because there are no measurements of individual cells it is difficult to compare this value with experimental evidence.

A common argument that is made for the cellulose contraction hypothesis is the correlation between cellulose content and strain. Higher proportions of cellulose were found to correlate to tensile strains (Sugiyama et al., 1993; Qiu et al., 2008; Yang et al., 2006), while high lignin content correlates well to compressive strains (Okuyama et al., 1998; Yamamoto et al., 1991). Compression wood is partly characterised by an increased lignin content (Timell, 1986), which has been used as an argument for the lignin swelling hypothesis. Tension wood, however, is often but not necessarily correlated with an increased proportion of cellulose. Within tension wood of G-layer producing species, tensile strain and whole cell cellulose content correlate well as the G-layer has a very low lignin content (Gardiner et al., 2014). The proportions of cellulose and lignin within the cell after the G-layer has been removed do not share this correlation. Timell (1969) found a higher concentration of lignin within the S_2 layer than in normal wood when the G-layer was present.

Bamber (1979, 1987), advocating for the cellulose contraction hypothesis, and Boyd (1972, 1977, 1985) advocating for the lignin swelling hypothesis disputed a number of each others claims; however, no new information was presented, rather a number of issues around interpreting biological data were highlighted. Kübler (1987) provided an in depth review of the hypotheses, evidence and experimental methods at the time, much of which has been discussed above. He presents a table summarising the literature reporting strains for different species, highlighting the large intra and inter tree variation even within a single species.

Yamamoto and coworkers produced a number of papers entitled ‘Generation process of

growth-stresses in cell walls' (Yamamoto et al., 1992, 1991, 1993; Sugiyama et al., 1993; Yamamoto et al., 1995; Okuyama et al., 1990; Yamamoto and Okuyama, 1988). They considered new experimental evidence for both the lignin swelling hypothesis and the cellulose contraction hypothesis and discussed them in detail, concluding that neither hypothesis suitably explained the experimental evidence. In particular, the MFA, where the longitudinal growth-stress switches from contraction to expansion (known as the critical MFA in growth-stress literature) is between 25 and 30 degrees.

Okuyama (1993, in Japanese) and Yamamoto et al. (1995) suggested the unified hypothesis in an attempt to solve the critical MFA discrepancy. Yamamoto et al. (1995) augmented the Barber and Meylan (1964) cell wall model which included an outer radially constraining sheath and an S_2 layer to include an S_1 layer as well. The resulting model was able to account for generation of both tensile and compressive stresses over a wide range of MFAs. However, this was only achievable using unnatural parameter values. The S_1 layer introduced utilises a constant MFA of 90 degrees, with the S_2 layer varying from 0 to 60 degrees. Cell wall maturation occurs in two discrete steps, first the cellulose framework is constructed then the lignin is deposited. The model showed that an increasing S_1 layer thickness reduced the critical MFA. The model was unable to produce realistic tangential strains.

Yamamoto (1998) further refined the model by incorporating time dependence of cell wall maturation. The work showed the failings of both the lignin swelling hypothesis and cellulose contraction hypothesis, even when time dependence was included. Considering time dependence of cell wall maturation within the model provided good agreement between the unified hypothesis and experimental values from *Cryptomeria japonica*. The poor agreement with tangential stresses was explained as being easy to decrease through stress relaxation in comparison to the longitudinal stress.

Guitard et al. (1999) developed an S_2 layer model, which took the transmission of shear between cellulose micro-fibrils into account, resulting in non-zero shear moduli. Previously integral conditions had been used to govern the longitudinal stresses, presumably as they satisfy the necessary condition implicitly required for stress field equilibrium. Guitard et al. (1999) introduced a local condition of zero on every elementary volume, instead of an integral condition on the overall cross section of the cell. They argued that this approach provided better agreement with experimental results when the dimensional changes within the micro-fibril bundle were included. In particular, this model resulted in a better prediction of transverse strains while being less complex than previous attempts discussed above.

Yamamoto (2002) further advanced his 1998 model to include drying stresses and moisture dependence of the Young's modulus. Little changes were made with regard to the growth-stress model.

Alméras et al. (2005) produced the most advanced mechanical model for growth-stress generation. Previously cells had been assumed to either be free (Yamamoto, 1998) or fully restrained (Archer, 1987b, 1989). Various boundary conditions were investigated. The most realistic boundary conditions fully restrained displacement in the longitudinal and tangential direction while were free in the radial direction. The virtually isolated cells were simulated and found to be in good agreement, although with some small discrepancies from Yamamoto (1998), due to the introduction of some second order terms. Their investigation showed that differing boundary conditions had only a small effect on the longitudinal strain, however the tangential strain was significantly affected. This was explained by the cellulose being stiff at the start of maturation and therefore all of the stress within the cellulose can be released as strain. However, in the tangential direction the stiffness of the fibre progressively increases as maturation proceeds, resulting in the re-

leasable strain being only a fraction of the total stress. In order to get good experimental agreement Alméras et al. (2005) used a transverse strain release parameter allowing some strain to be released during maturation. They found that 74% of the transverse stress needs to be released during maturation to provide the best agreement with experimental data.

Many of the previous models have used a physical interpretation of the reinforced matrix hypothesis (Barber and Meylan, 1964), which describes the cell wall as a two phase structure of cellulose fibrils and an isotropic hemicellulose and lignin matrix. Yamamoto and Almèras (2007) applied Mori–Tanaka theory to small fragments of cell wall and when coupled with changes in physical state showed theoretically that the two main phases could exist within the same domain.

More recently theories regarding the nature of hemicelluloses and their bonding have been used in an attempt to address some of the issues associated with the cellulose contraction hypothesis. In its initial form the cellulose contraction hypothesis argued that the crystallisation process of cellulose shortened the chain length (Bamber, 1979). Two theories have been advanced to explain the issue of lengthening during crystallisation in order to retain an updated version of the cellulose contraction hypothesis.

Walker (2006) suggested that at the surface of the cellulose fibrils the cellulose becomes disordered and is consequently able to bond with hemicelluloses, which have a slightly shorter repeat length than the cellulose crystal. Davidson et al. (2004) provided some evidence for the theory showing an increase in the fraction of interior chains to surface chains resulted in an increase in repeat length. Hemicelluloses bonded to the outside of the crystaline centre of the fibril could cause the fibril to be compressed in the crystalline centre. An interesting consequence is the contraction of the cellulose due to the hemicellulose bonding should be dependent on the ratio of surface area to volume of a fibril, as

would be suggested by the results from Davidson et al. (2004).

The second theory put forward in an attempt to explain fibril contraction during cellulose crystallisation is that hemicelluloses are trapped between the fibrils and cause them to bend and longitudinally contract (Mellerowicz et al., 2008). Mechanically this is very similar to the lignin swelling hypothesis. By causing the micro-fibrils to use some of their length to deviate past a cluster of hemicelluloses consequently shortening the over all distance the fibril can cover.

1.4 Outstanding problems

When and how stresses get generated is still debated (Gril et al., 2017). Over the last decades it has been accepted that the generation of the stresses occurs during or immediately after the deposition of the secondary cell wall (Gril et al., 2017). Most commonly either the G-Layer or the S_2 layer are considered responsible. As discussed above, the mechanism(s) within the cell wall which generate stresses have been hypothesised about at great length; however, no theory presented so far is without contrary experimental evidence, or lack the specifics needed to describe the stress generation mechanism fully (Gril et al., 2017). Unfortunately most literature has investigated very few samples and reports high variability within individual trees and tree species.

One of the more debated topics around growth-stress generation is whether or not the generation mechanisms for stress in reaction wood are extreme versions of the same mechanisms in normal wood. The G-layer is not found in normal wood, however not all tension wood producing species produce G-layers (Ruelle et al., 2006; Qiu et al., 2008). Lignin swelling could potentially fit this criteria for normal and compression wood; however, modification of the lignin swelling hypothesis (Boyd, 1950) would be needed to address

the dependence of MFA, as some wood with a lower than 40 degree MFA still produces compressive forces. Typically there is little lignin within the G-layer, the layer suspected to be responsible or at least partly responsible for the generation of axial tension (Walker, 1993).

Growth-stress studies have been largely confined to model, or common species, however, there are a number of species which appear to form intermediates or abnormal forms of reaction wood. For example Hebe and Buxus are angiosperms which appear to form compression wood rather than tension wood (Kojima et al., 2011; Yoshizawa et al., 1992).

1.5 Experimentation

1.5.1 Macroscopic

Currently there are three commonly used experimental methods for measuring surface strains. The Nicholson method, the 'French' (CIRAD) method and the strain gauge method, as reviewed by Murphy et al. (2005); Yoshida and Okuyama: (2002) and Yang et al. (2005). A detailed comparison between the systems was undertaken by Kamarudin (2014), including a new system called GSM10 (similar to Baillères et al. (1995) CIRAD system).

After the developments of Jacobs (1945); Boyd et al. (1950) and Boyd (1950) in testing for growth-stresses it became apparent there was a need for a rapid testing procedure. Nicholson (1971) developed the first of these, measuring the released strain between two metal pins on the surface of a sample, cut from logs. While considered a rapid method in 1971, updated versions of this test are still used for measuring surface strains but not practical (or considered rapid) for testing large numbers of stems in breeding trials. The 'French' or CIRAD method (Baillères et al., 1995) involves drilling a hole in a stem/log

between two reference points, with a gauge measuring the distance change between the two points, taking approximately half an hour per tree.

As reviewed by Kübler (1987), Okuyama et al. (1981) adopted the use of strain gauges to measure stem surface strains of particular layers of wood. Other methods were also derived around the same time, Gueneau and Chardin (1973); Gueneau and Kikata (1973) and Kikata and Miwa (1977) investigated drilling holes near strain gauges to release strains. Gueneau and Saurat (1974) and Saurat and Guneau (1976) introduced an apparatus which utilised two knife blades at a set distance, one knife blade bent as the strain was released via drilling. The strain release was measured on the curved blade.

In an attempt to introduce a rapid measurement for growth-strain screening Chauhan (2008), Chauhan and Entwistle (2010), Entwistle et al. (2014) and Davies et al. (2017) introduced a variant of the pairing test, which involves halving a log through the pith and measuring the resulting deflection, originality developed by Jacobs (1945). Naranjo et al. (2012) and Aggarwal and Chauhan (2013) have used the test for investigating genetic relationships within *Tectona grandis* and *Eucalyptus tereticornis* clones. Chauhan and Walker (2011) used the test during an investigation of juvenile *Eucalyptus regnans* tension wood properties.

There have been a number of studies published where the surface strains of stems have been recorded using various methods (Muneri et al., 1999; Yang et al., 2002; Murphy et al., 2005; Chauhan and Walker, 2004; Raymond et al., 2004). Most recently, Near Infrared spectroscopy (NIR) has been used for non-destructive testing. Watanabe et al. (2011) was able to use NIR to predict surface growth-strain in *Cryptomeria japonica* moderately accurately.

Measuring strains inside the stem has proved to be more difficult. Kikata (1972) adopted Jacob's planking method and electric strain gauges for improved accuracy (presented

in Kübler (1987)). Wilhelmy and Kübler (1973) drilled holes of known diameters into stems and attempted to measure the change in shape of the hole as the log was successively cross cut closer to the measurement site, similar to Boyd et al. (1950). Polge and Thiercelin (1979) attempted to measure the effect of growth-stresses on increment cores. They found that the stresses had an effect on the core itself, deforming it into an oval shape. Ferrand (1982) found a correlation of between 0.67 and 0.77 for the relationship between longitudinal strain and tangential core diameter, showing they can be used for near non-destructive growth-strain testing.

1.5.2 Microscopic

Clair et al. (2006) provided the first direct evidence that cellulose chains are under tension at the periphery of a stem. Using X-ray diffraction they measured the release of wood maturation stress and found a decrease in the repeat length of the cellulose of 0.2% when the surface strains were released.

Individual trachieds of spruce have been investigated for swelling after soaking in a sodium iodide solution. Burgert et al. (2007) found substantial swelling of compression wood tracheids and slight swelling of normal tracheids. They argue these results show the potential for swelling governed only by cell wall architecture to be sufficient to generate the tensile and compressive forces observed.

Chang et al. (2013) investigated differences between normal and tension wood in poplar using Fourier transform infrared spectroscopy. They found that cellulose is more orientated within the S_2 wall of tension wood than normal wood. The orientation of lignin also increases in tension wood, hemicelluloses and pectins in the G-layer are orientated perpendicular to that of the S_2 layer.

There have been a number of attempts to investigate individual fibres and the various cell wall constituents from a micromechanical perspective. For a full review see Eder et al. (2012).

1.6 Cellular modeling not focusing on growth-stresses

A number of mathematical models of wood have been presented from the molecular to cellular and whole organ level. Growth-stress was not usually included, however, these works have made significant advancements in other areas of understanding of plant cell walls which need to be incorporated into growth-stress research (for a review see Mishnaevsky and Qing (2008)).

The first attempt at mathematically defining the mechanical behaviour of a fibre or tracheid was a single layer two phase composite model consisting of the S_2 layer composed of aligned cellulose fibrils and isotropic lignin (Barber and Meylan, 1964). This model was quickly improved on by Mark (1967) and Cave (1968) using continuum mechanics methods. Mark (1967) provides an in depth discussion concerning both experimental and theoretical estimation of the mechanical properties of tracheids. Cave (1968) developed the model to include a Gaussian distribution of the MFA. Bergander and Salmén (2002) developed a nine layer model which emphasised the importance of the inclusion of the S_1 and S_3 layers when estimating transverse elastic properties. Harrington (2002) developed these ideas to incorporate a three-stage homogenization procedure utilizing nanostructural (supramolecular), ultrastructural (cell wall) and microstructural (whole cell) scales in order to estimate a number of material properties of softwood. Further advancements have been made over the last decade. For recent publications see Sun et al. (2014); Flores et al. (2014); Wang et al. (2013) and Faisal et al. (2013).

Hepworth (1998) used a discrete element approach, with limited results. Hydrogen bond dominated solids models have been used to describe paper (Nissan and Batten, 1997; Batten Jr and Nissan, 1987; Nissan, 1987; Batten Jr and Nissan, 1987). Zhan et al. (2014) used a representative volume element method to describe hardwood; however, the limited resolution did not allow for investigation at the cell wall scale. Recently molecular dynamics methods have been used to simulate small volumes of the cell wall in order to investigate their nanostructure (Jin et al., 2015; Charlier and Mazeau, 2012; Sangha et al., 2011; Zhang and LeBoeuf, 2009; Houtman and Atalla, 1995).

Atomic force microscopy, electron microscopy and other spectroscopic techniques have been used to probe the cell wall at the scale of fibril aggregates, showing that the fibrils are not straight and instead meander through the cell wall in a general direction (Fahlén and Salmén, 2005; Kim et al., 2011). Salmén (2014) argued, with the help of various imaging techniques, that cellulose was the most important component when investigating mechanical cell wall properties. The fibril aggregates join and separate creating a distribution of pore sizes and shapes (Yin et al., 2015). The fibril aggregate architecture has yet to be incorporated into cellular models.

1.7 Why growth-stresses exist

Growth-stresses within trees follow a pattern of tension at the periphery and compression in the centre, as discussed by Archer (1987a). Hardwoods typically have larger growth-stresses than softwoods (Barnett, 1981). Some young conifers have been reported to have larger compressive stress at the periphery than at the pith (Jacobs, 1945), this may be due to the abundance of compression wood observed in juvenile conifers, once older they follow the same radial stress profile as hardwoods (Timell, 1986).

The commonly accepted argument for the evolutionary advantage of growth-stress existence is the mechanical hypothesis. The hypothesis argues that a number of wood properties, including the development of growth-stresses evolved in order to increase mechanical stability of trees to improve their survival. The mechanical hypothesis as applied to growth-stresses argues, because wood is stronger in tension than in compression (Mattheck and Kübler, 1997; Ross and USDA Forest Service., 2010), by preloading the periphery of the stem in tension the non-destructive bending radius on the inside of the curve is increased giving a larger safety margin when a force is bending the stem (Barnett and Jeronimidis, 2003). Tangential stresses have been suggested to resist mechanical failure in times of frost (when water inside the cells freezes and expands) and drought (when water tension is very high) (Kübler, 1983).

Typically four hypotheses are used when attempting to explain evolutionary adaptation in wood properties. These are, mechanical, hydraulic, time dependent and a combination of the previous three (Meinzer et al., 2011). Initial speculation for the existence of growth-stresses entertained the mechanical hypothesis based on self weight (Martley, 1928). Jacobs (1945) suggested growth-stresses were a byproduct of sap tension (hydraulic), which he later retracted when sap pressures were recalculated at a much lower value (200 atm reduced to 30 atm) than the generally accepted values at the time (Jacobs, 1965).

1.8 Growth-stresses as a wood defect

Growth-stresses can ruin structural and veneer logs due to splitting, warping, collapse and brittle-heart (Yamamoto, 2007). Growth-stresses also increase the danger for the feller, by binding saws and the stem splitting longitudinally during felling (barber chairing).

When the stem is felled or cross cut, growth-stresses are released around the saw cuts causing shortening at the periphery and extension in the centre. The dimensional change is maximal at the saw cut. Splitting occurs when the contraction/extension force exceeds the plastic limit of the stem. These end-splits, heart-checks, and ring-shakes reduce the value of the stem.

Within mills growth-stresses during processing cause a number of issues leading to reductions in value recovery, an example of this can be seen in Figure 1.6. Because growth-stresses are released when the stem is sawn, the resulting shape change can cause the saws to jam. The main value loss at this stage of processing comes from the need to saw boards multiple times in order to straighten deformed boards. Increasing the number of times the boards are sawed to get their end dimensions gives poor saw use efficiency and major economic loss as the final yield can be reduced up to 30% (Yamamoto, 2007).

Selection for low growth-stress producing families may significantly reduce the occurrence of internal defects. During processing technological remedies such as inline screening or lignin softening may be possible, however, have not become industry standards, probably due to cost. Currently no known attempts have been made to breed specifically for low (or high) growth-stresses. A heritability assessment for growth-strains (and other wood properties) has been carried out on *Tectona grandis* finding low heritability (Naranjo et al., 2012) and on *Eucalyptus dunnii* (Murphy et al., 2005) finding moderate heritability.

Figure 1.6: Freshly sawn *Eucalyptus globulus* displaying splitting caused by growth-stress release during sawing. This is a real world example of the profile presented in Figures 1.3 and 1.4.

Chapter 2

Pilot study and left-censoring

Chapter Prologue

As was discussed in Chapter 1, while growth-stresses and strains have various benefits to tree survival, they can lower the value of wood products. Eucalypt species are generally plagued by high growth-strains and as a consequence they have seen only isolated success as plantation grown species for solid wood products. *Eucalyptus bosistoana* has been identified as a species which may become a successful commercial plantation species for high quality solid wood products. At a species level it displays high stiffness, natural durability and good growth rates. However, it also displays a tendency to distort during sawing as a result of growth-strain, and hence there is an interest in using breeding techniques to lower the level of growth-strain and increase recoverable volume. One of the outstanding problems in tree breeding is reducing the breeding cycle time to increase breeding efficiency. An approach to do this for growth-strain is presented here.

A pilot study measuring *Eucalyptus bosistoana* wood properties at age two was conducted. An important finding was the significant number of individuals with a splitting

test result of zero, because the test cannot measure negative values the dataset was left-censored. The reason why samples were closing during the splitting test within this dataset is still unknown, but larger subsequent trials measuring growth-strain have indicated it is uncommon (Chapter 4). The following chapter presents a method for accounting for the left-censoring to improve the accuracy of heritability estimates and genetic correlations for growth-strain, density, diameter, volumetric shrinkage, acoustic velocity and stiffness.

Parts of Chapter 2 were presented at the 8th Plant Biomechanics International Conference 2015, and the Forest Genetics for Productivity Conference 2016;
These were published as:

Davies, N., Sharma, M., Altaner, C., and Apiolaza, L. (2015). Screening eucalyptus for growth strain. In *Abstracts of the 8th Plant Biomechanics International Conference*

and

Davies, N. T., Apiolaza, L. A., and Sharma, M. (2017). Heritability of growth strain in Eucalyptus bosistoana: a Bayesian approach with left-censored data. *New Zealand Journal of Forestry Science*, 47(1)

2.1 Introduction

Eucalypt species are fast-growing and can produce high quality timber for appearance and structural products, including Laminated Veneer Lumber (LVL). Eucalypts can contain large growth-strains, which are associated with log splitting, warp, collapse and brittle-heart, imposing substantial costs on processing (Yamamoto, 2007). Costly and only partially effective mitigation strategies have been developed to reduce wood defects induced by growth-strain, for example, using hydrothermal recovery, described in more detail by Gril et al. (2017). As growth-strain is heritable, an alternative approach is to select and grow individuals which display low growth-strain. Until now, measurement of growth-strain has been difficult, time consuming and expensive, preventing the assessment of the large number of trees needed by a breeding programme (Altaner, 2015). As an example, the largest sample number in any reported growth-strain study was smaller than 230 trees (Naranjo et al., 2012).

Traditionally selections are made over longer breeding cycles, when the trees are at least one quarter of their expected commercial rotation age. The extended breeding cycle not only increases costs (e.g. trial management, sample handling) but also substantially delays the deployment of improved germplasm (Altaner, 2015). Developments at the University of Canterbury have resulted in a unique growth-strain measurement method supported by theoretical analysis (Entwistle et al., 2014) - termed the 'Splitting' test. It allows for fast growth-strain assessment of small trees (Chauhan and Entwistle, 2010).

The splitting test method was designed to minimise the time taken to measure growth-strain on each tree; however, a consequence of the method is the testing procedure does not account for negative values. These occur when the wood in the centre of the stem is under tension rather than compression, which should produce a negative surface

growth-strain value. However, because the test cannot measure negative values a zero is assigned, resulting in left-censored datasets.

Left-censored data is common in research areas where detection limits are high compared to the measured values, a common example is testing for the presence of drugs in animals. Senn et al. (2012) provides a review of methods for dealing with data below the limit of quantitation. In this Chapter a Bayesian framework was used to impute the missing data from the known data, reducing the error induced by zero inflation. Because of the flexibility of Bayesian approaches, it is easier to include model complexity (e.g. censoring) while accounting for the hierarchical nature of the data. In addition, one can easily obtain complex distributions of functions of covariance components, like heritabilities, as a byproduct of the estimation process (Cappa and Cantet, 2006). There are several examples of Bayesian applications in forest genetics; for example: Soria et al. (1998) (univariate analysis of growth traits), Cappa and Cantet (2006) (multivariate analysis of growth traits) and Apiolaza et al. (2011c) (multivariate analysis of early wood properties).

2.2 Materials and method

2.2.1 Materials

The data was from an open-pollinated *E. bosistoana* progeny trial at an irrigated nursery site in Harewood, Christchurch, New Zealand. The trial represented 40 families from two provenances, with a total of 423 seedlings planted into 100 L bags, which were coppiced after their first harvest. Two separate plantings (trial sections) occurred in 2010 and 2012. The 2010 planting consisted of 200 individuals from 20 families which originated from South-Eastern Australia. They were harvested at age 2 and 196 individuals survived.

After harvest in 2012 they were coppiced and harvested again in December 2014 (165 individuals survived until age 4, 2 years after coppice). The 2012 planting of 3 individuals from 20 families originated from higher elevation in New South Wales and were harvested in 2013, at age 1 (this data was not included in the analysis, due to the magnitude of errors induced by small, malformed stems) and again in October 2015 (119 individuals from 20 families survived until age 3, 2 years after coppice). All seedlings were established following a completely randomised design. Descriptive statistics of the measured wood properties are presented in Table 2.1.

Table 2.1: Descriptive statistics of measured wood properties of two year old *E. bosistoana*.

Property	Mean	Standard Deviation
Growth-Strain $\mu\epsilon$	850	660
Density $\frac{kg}{m^3}$	816	45.5
Diameter mm	28.9	4.88
Volumetric Shrinkage	0.23	0.59
Acoustic Velocity $\frac{km}{s}$	3.16	0.33
Stiffness GPa	8.24	1.74

While all specimens were grown on the same site, they were grown during different time periods, which were confounded with the effect of the two provenances and hence were included as a trial effect. The same trees were assessed as both seedlings and coppice, which was accounted for as a tree effect.

2.2.2 Measurements and Calculations

Growth-strain was measured using a modified version of the Chauhan and Entwistle (2010) and Entwistle et al. (2014) splitting method. The newly developed 'rapid-splitting test' reduced measurement time, enabling larger numbers of samples to be processed. The modified method involved stripping the bark and measuring the under-bark large-end diameter of a clear section of the stem. This resulted in an over estimation of the average diameter used by Chauhan and Entwistle (2010). Diameter was measured perpendicular to the slit using vernier calipers at the big end of the sample. The longest slit length appropriate for the sample (longest length of clear wood without bends or knots, staying at least 100 mm from the small end of the sample) was marked for conducting the rapid-splitting test. Slit length was recorded and the stem cut through the pith with a bandsaw with a kerf of 0.9 mm (see Entwistle et al. (2014) for an analysis of the effect of kerf on error). The small-end of the sample was left intact with the large-end free to distort, which removed the need to clamp the two halves together. Finally, the opening was measured using vernier callipers and recorded. Figure 2.1 shows an example of a sample ready for the opening to be measured. The calculation of strain was unchanged from Chauhan and Entwistle (2010) with the exception that average radius is now large-end radius (Equation 2.1).

After the growth-strain measurements the samples were cross cut 150 mm from the big end, resulting in two half-rounds. These half-rounds were measured for green mass

(using laboratory scales) and green volume using the water displacement (Archimedes) method, also used by Chauhan and Walker (2011). The samples were oven dried at 105℃ until representative samples retained a stable mass for 24 hours. Dry mass and volume measurements were conducted in the same way as the green measurements. In addition, sample length and acoustic velocity (from WoodSpec) were measured as it was on *E. regnans* by Chauhan and Walker (2011).

Growth-strain ϵ was calculated based on Chauhan and Entwistle (2010), using Equation 2.1 where Y_u is the opening, L is the cut length and R is the large end radius. Equation 2.2 is obtained by rearranging Equation 2.1 to take big end diameter (d) rather than radius and output strain directly. Dry density (ρ) was calculated using Equation 2.3 where (m) is dry mass, (V) is dry volume and subscripts represent the sample side. Acoustic velocity (av) from Equation 2.4 and stiffness (k) from Equation 2.5 and volumetric shrinkage (vs) from Equation 2.6 where gV is green volume and V is dry volume were calculated.

$$Y_u = \frac{0.87\epsilon L^2}{R} \tag{2.1}$$

$$\epsilon = \frac{Y_u d}{1.74L^2} \tag{2.2}$$

$$\rho = \frac{m_A + m_B}{V_A + V_B} \tag{2.3}$$

$$av = \frac{av_A + av_B}{2} \tag{2.4}$$

$$k = av^2\rho \tag{2.5}$$

$$vs = \frac{gV_A + gV_B - V_A - V_B}{gV_A + gV_B} \tag{2.6}$$

Figure 2.1: Sketch (A) and photo (B) of a sample after the rapid-splitting test has been performed. The opening is measured and used for the strain calculation along with the sample diameter and cut length. This sample shows significant growth-strain as can be seen from the wide opening. Sketch courtesy of Eve Baker and photo from Clemens Altaner.

2.2.3 Analysis

Data analysis was conducted in R (R Core Team, 2017) and RJAGS (Plummer, 2015), utilising a Bayesian approach to estimate the heritability of growth-strain at the family level. The effect of coppicing was included as a fixed effect. Specimen groups were grown during different time periods and for different rotation lengths, and included as a random effect. The rapid-splitting test is physically constrained to positive values, as the opening cannot be reduced in the presence of compression at the stem surface and tension at the pith, resulting in left-censored data. Bayesian frameworks provide the ability to simulate partially observable data and therefore reduce systematic errors, which occur due to left-censoring. Here the left-censored initial values were sampled from a uniform distribution between -1.5 and 0 (-1500, 0 micro-strains).

The analyses used a Bayesian approach to estimate the posterior distributions for the heritability of growth-strain and other wood properties. A hierarchical model was implemented where y_{ijklm} followed a left-censored normal distribution $N(\omega_{\text{ijklm}}, \tau_{j|i})$ with the predicted value ω_{ijklm} and a trial-dependent precision $\tau_{j|i}$. The precision (reciprocal variance) $\tau[x_1]$ for each trial was given a vague gamma prior $\Gamma(0.01, 0.01)$.

The predicted value for the i^{th} assessment was modelled as a function of an overall intercept, the effect of the j^{th} trial, k^{th} coppicing level, l^{th} family and m^{th} tree, to account for repeated assessment pre- and post-coppicing, Equation 2.7

$$\omega_{jklm|i} = \mu + \alpha[x_{1j|i}] + \beta[x_{2k|i}] + \gamma[x_{3l|i}] + \delta[x_{4m|i}] \tag{2.7}$$

where x_1, x_2, x_3 and x_4 represent indicator variables for the levels of the factors.

The overall intercept (μ), and individual-level coefficients for coppicing (α_j) and site (β_k)

were given vague normal prior distributions (Equation 2.8).

$$\begin{aligned} \mu &\sim N(0.5, 10^{-12}) \\ \alpha &\sim N(0.5, 10^{-12}) \\ \beta &\sim N(0.5, 10^{-12}) \end{aligned} \tag{2.8}$$

The family (γ_l) and tree (δ_m) effects were assumed to come from normal distributions $N(0, \tau_f)$ and $N(0, \tau_t)$, with vague gamma priors $\tau_f \sim \Gamma(0.01, 0.01)$ and $\tau_t \sim \Gamma(0.01, 0.01)$, respectively. The statistical model is presented graphically following Kruschke (2014) in Figure 2.2.

Narrow-sense heritability at the trial level for all properties was calculated using Equation 2.9. The constant of 2.5 used was suggested by Griffin and Cotterill (1988) due to the unknown proportions of selfing, full-siblings and half-siblings within the open-pollinated families (loosely referred to as half-sibling families here). The σ_f^2 and σ_t^2 variances were obtained as the reciprocal of the precisions (τ_f, τ_t).

$$h^2 = \frac{2.5 \times \sigma_f^2}{\sigma_f^2 + \sigma_t^2 + \sigma^2} \tag{2.9}$$

All the models were fitted using RJAGS, an R (R Core Team, 2017) interface to JAGS (Just Another Gibbs Sampler, (Plummer, 2015)), which uses Gibbs Sampling to estimate the marginal posterior distributions for the parameters of interest. Approximately 35% of the strain data was below the limit of quantitation, and was imputed by JAGS as a random value below the limit of detection, using the function 'dinterval' between 0 and -1500

micro-strains; for details see Lunn et al. (2012). A family model rather than an animal model was used as for the purposes of a simple one-generation pedigree, the models are equivalent (*sensu* identical expected values and variance (Henderson, 1985)). The family model was less computationally intensive. The R/JAGS code is available in Appendix A.

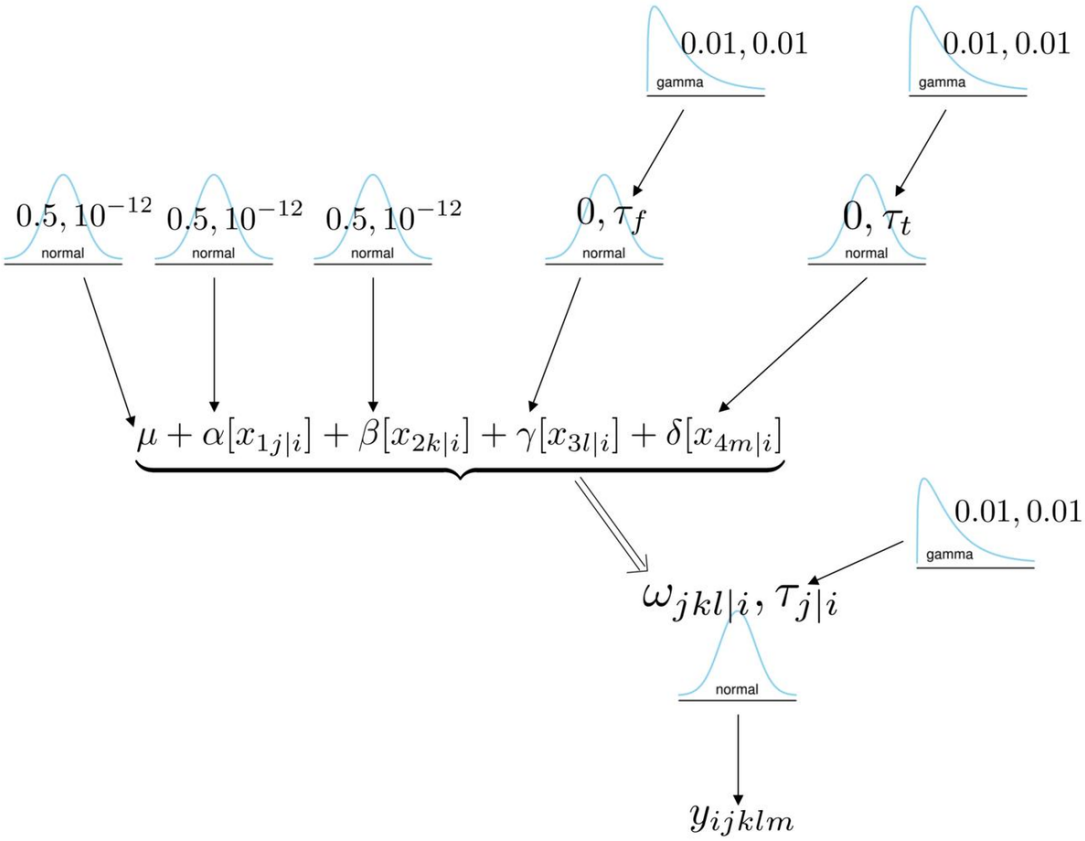

Figure 2.2: Graphical representation of the statistical model (Equation 2.7) used to analyse wood property traits in two year old *E. bosistoana*.

2.3 Results and Discussion

The results showed that growth-strain is heritable, and family rankings varied little whether grown from seed or coppiced from existing root systems, within *E. bosistoana* at age two, grown on a single nursery site. Table 2.2 shows the family mean Spearman rank coefficients of the tested wood properties whether grown from seed or coppice. Figure 2.3 shows 20 families ordered by median growth-strain. The family rankings were similar (Spearman coefficient of 0.77). In particular the top 3rd of the families, i.e. those with the lowest growth-strain, were the best in both trials (Figure 2.3). Growth-strain increased after coppicing. When plants are coppiced from existing root systems they emerge from the side of the old trunk resulting in a hockey-stick shaped lower stem. Given the nature of the testing procedure, it is suspected that the increase in growth-strain with coppicing was due to the formation of tension wood rather than an indicator that older trees will possess significantly higher growth-strain, although this is unconfirmed.

Table 2.2: Spearman rank coefficients between the phenotypic family means when grown from seed or coppiced from the existing root systems (two year old stems). Family mean growth-strain rank showed a strong relationship before and after coppicing (196 plants from seed and 165 of the same plants from coppice of *E. bosistoana* from 20 families).

Property	Spearman coefficient
Diameter	0.44
Dry density	0.30
Acoustic velocity	0.69
Stiffness	0.44
Growth-strain	0.77

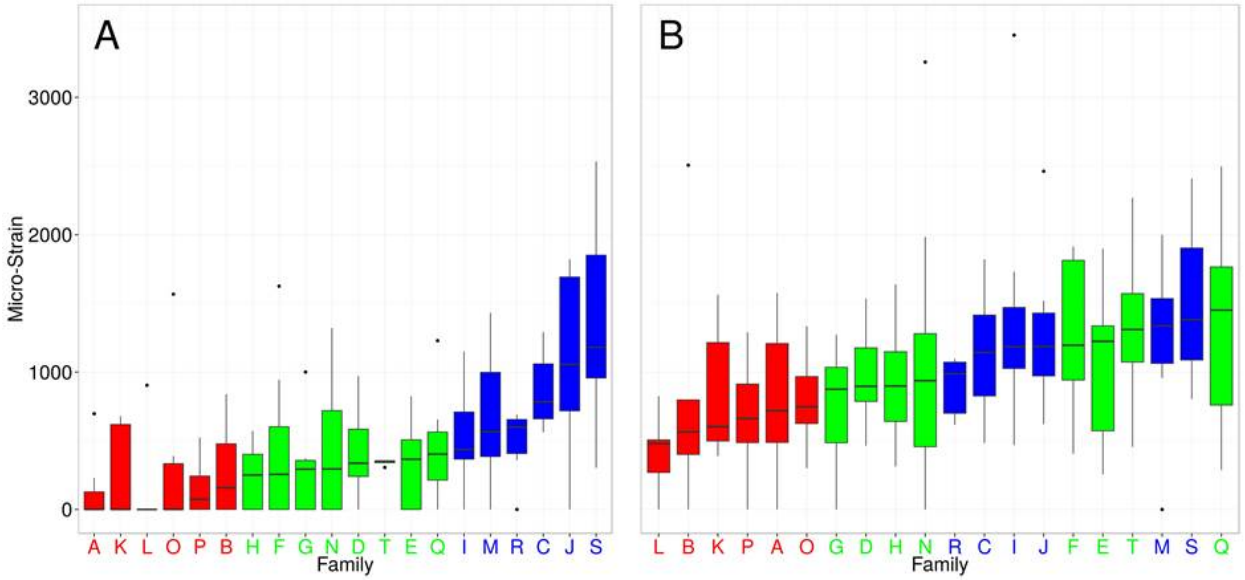

Figure 2.3: Two year old *E. bosistoana* stems from 20 families separated into high (blue), medium (green) and low (red) growth-strain families when grown from seed (A) and the same individuals grown from coppice (B). Note the large number of trees in the low growth-strain families showing closure (zero) during the splitting, test and the higher magnitudes of growth-strain when grown form coppice (196 plants from seed and 165 from coppice).

Testing for all of these properties has been conducted in less than five minutes per sample of 2 year old *E. bosistoana*. While the study was larger than preceding attempts such as Murphy et al. (2005) or Naranjo et al. (2012), the sample number was still small when considering heritability calculations.

The paucity of data resulted in wide 95% credible intervals (Table 2.3), which requires more samples to tighten. The heritability of 0.63 (0.28 - 0.98) indicated that growth-strain can be influenced by breeding, and was in line with the 0.32 reported by Murphy et al. (2005) for nine year old *E. dunnii*, but was significantly higher than the 0.02 value reported by Naranjo et al. (2012) for four-year-old Teak. Density, diameter at age two (growth), volumetric shrinkage, acoustic velocity and stiffness all had significant heritability, suggesting that breeding for these traits is achievable. The heritabilities were similar to those reported

for other eucalypt species at various ages (Hung et al., 2014; Hein et al., 2012; Blackburn et al., 2014; Hamilton and Potts, 2008).

The analysis made use of a residual covariance structure to account for the three different experiments, rather than assuming a single residual distribution. Further it incorporated a tree effect allowing for the identical genetics between pre and post coppicing to be accounted for, meaning a number of genotypes were measured under two slightly different environments, providing a better representation of the genetic control of traits.

Taking into account censored data is important as if it is either ignored or removed, it will (in a left-censored case) artificially inflate the mean and deflate the variance. By simulating the data, which has values below the limit of detection, the true distribution can be more realistically represented (Gelman and Hill, 2007).

Table 2.3: Narrow-sense heritability of measured wood and growth properties of two year old *E. bosistoana*, calculated as per Equation 2.9.

Property	Heritability	95% Credible regions
Growth-strain	0.63	0.28-0.98
Dry Density	0.54	0.11-0.97
Diameter	0.76	0.42-1.0
Volumetric shrinkage	0.29	0.13-0.45
Acoustic velocity	0.97	0.6-1.0
Stiffness	0.82	0.48-1.0

Wood processors pay premiums for stable and stiff timber, while forest growers often prefer to have fast-growing trees to shorten rotation lengths and increase profitability. The preferences for breeding traits are not always aligned, in particular, when traits are un-

favourably correlated. Here stiffness, which is used for grading logs, was positively correlated with growth-strain (0.61) within individual samples (Table 2.4). Unfavourable correlations require trade-offs between traits to maximise overall value. While zero growth-strain is desirable for wood processing, some unknown amount of growth-strain below which little economic loss is experienced exists, this ceiling would be a good target for breeding programmes.

Table 2.5 shows genetic correlations between the properties at the family level. A strong positive Pearson correlation of 0.79 (0.64 - 0.88) was evident between growth-strain and stiffness at the family level. This means that reducing growth-strain will require reducing wood stiffness at the population level. Stiffness is already used for log grades and structural timber in New Zealand requires 8 GPa (Buchanan et al., 2005). Table 2.1 shows the mean *E. bosistoana* stiffness at age 2 was 8.2 GPa in these experiments. Because the wood stiffness is high a reduction may not have practical implications for wood processing within *E. bosistoana* when grown to be large trees where stiffness may be around 21 GPa (Bootle, 2005).

Table 2.4: Phenotypic correlations of wood properties within individual samples of *E. bosistoana* at age two. 95% confidence intervals in brackets.

	Dry density	Volumetric Shrinkage	Acoustic Velocity	Stiffness	Strain
Diameter	0.15 (0.06, 0.24)	-0.10 (-0.19, -0.01)	-0.03 (-0.12, 0.07)	0.02 (-0.07, 0.12)	0.12 (0.03, 0.21)
Dry density		0.13 (0.03, 0.22)	-0.03 (-0.12, 0.06)	0.22 (0.14, 0.32)	0.03 (-0.07, 0.12)
Volumetric Shrinkage			-0.37 (-0.44, -0.29)	-0.33 (-0.41, -0.26)	-0.26 (-0.35, -0.17)
Acoustic Velocity				0.96 (0.95, 0.97)	0.62 (0.56, 0.68)
Stiffness					0.61 (0.54, 0.67)

The original Chauhan & Entwistle (2010) method was modified to adapt it from a research to an operational technique. The effect of these changes should be negligible. The linear error introduced by using large-end diameter rather than average diameter of the stem should have resulted in a slight reduction of reported strains compared to the original

Table 2.5: Genetic correlations between family wood properties from *E. bosistoana* stems at age two (or two years since coppice). 95% credible regions in brackets.

	Density	Volumetric Shrinkage	Acoustic Velocity	Stiffness	Strain
Diameter	-0.17 (-0.46, 0.15)	-0.43 (-0.66, 0.14)	0.27 (-0.04, 0.54)	0.25 (-0.07, 0.52)	0.19 (-0.12, 0.48)
Density		0.27 (-0.04, 0.54)	-0.2 (-0.48, 0.11)	0.01 (-0.30, 0.32)	-0.12 (-0.41, 0.20)
Volumetric Shrinkage			-0.59 (-0.76, -0.34)	-0.55 (-0.73, -0.28)	-0.47 (-0.68, -0.17)
Acoustic Velocity				0.98 (0.95, 0.99)	0.80 (0.65, 0.89)
Stiffness					0.79 (0.64, 0.88)

method. Leaving the small-end intact, that is, not cutting the full length of the sample, did not release as much strain, again lowering the growth-strain value over all samples. Given that a single measurement was taken, rather than two, the measurement error of the opening was reduced. Further work was conducted to estimate the accuracy and precision of both tests and to separate natural within-stem variability from variability between stems, as different openings can be expected depending on the radial plane of the cut. Testing accuracy and precision were investigated and discussed in Chapters 5, 6 and 7.

Heritabilities presented in Table 2.3 are for *E. bosistoana* at age two, at later ages these heritabities may change. From a breeding perspective, these values were calculated from a wild but small (40 families), unimproved population, and hence there is likely larger variability than in older (more breeding cycles) breeding programmes. By removing the worst performing individuals from the breeding population, budgets may be more efficiently spent by only assessing the trees with a higher chance of producing a premium quality product. However this assumes that the rankings at age two correlate sufficiently well with the rankings at older ages. Chapter 7 discusses this and other relevant assumptions further.

The underlying biological reason for the left-censoring, i.e. closing of the two halves during the splitting test is unknown, and has not been discussed previously in literature. Chapter 3 discusses and tests a hypothesis, which suggests the early tension wood formation

could cause the left-censored data.

Genetic gain per unit of time for a breeding programme depends on four elements: variability for the trait under selection, selection intensity (proportion of individuals selected), accuracy of prediction (proportional to heritability) and time required for turning a breeding cycle. New phenotyping techniques, like rapid growth-strain testing, increase selection intensity (as more trees are able to be assessed), and reduce selection time (as trees can be less than two years old when tested), however, accuracy of prediction may decrease. For more details see Chapter 7.

2.4 Conclusion

The modified rapid-splitting test for growth-strain captured population variability in *E. bosistoana* showing that it is was under genetic control. Narrow sense heritability of growth-strain was estimated to be 0.63, with a 0.28 to 0.98 95% credible interval. This suggested that a larger breeding programme may be able to reduce growth-strain in the population.

Heritabilities for wood density, stem diameter, volumetric shrinkage, acoustic velocity and wood stiffness were also presented. All of them were within the range described in previous publications, for more details see Chapter 4. A strong unfavourable genetic correlation, 0.79 (0.64 - 0.88), between growth-strain and stiffness indicated that tree selection will have to find a compromise between those traits when breeding for overall wood quality in *E. bosistoana*.

Due to the nature of the splitting test, strains which result in the closure of the specimen cannot be measured and as a result are recorded as zero. Figure 2.3 shows a number of individuals closed, particularly when grown from seed, indicating an atypical stress

pattern in the stem with greater contraction at the pith than the periphery.

Chapter 3

Experimental investigation of the cause of left-censoring for the splitting test

Chapter Prologue

Chapter 2 presented a Bayesian approach to a left-censored data set of growth-strain from splitting tests on two year old *E. bosistoana*. The reason for the splitting test closing, resulting in left-censored data was unknown. In this Chapter, the hypothesis: if tension wood was developed 'early' in growth (near the pith), followed by the development of normal wood near the periphery, the normal wood may constrain the contraction of the tension wood resulting in a closing during the splitting test, is tested.

3.1 Introduction

The underlying biological reason for the left-censoring is unknown, and has not been discussed previously in literature. If significant quantities of tension wood, which are known to produce large growth-strains (Saranpaa et al., 2014), developed early in life (i.e. near the pith) and were later surrounded by normal wood, the new outer wood would constrain the axial contraction of the tension wood near the pith, creating a growth strain profile where the most tension exists toward the middle-to-centre of the stem, rather than the periphery, as is the typical profile assumed in literature (Archer, 1987a). The result of the inverted profile could be that the two sides pull together during the splitting test resulting in zero values, as some strain could not be released due to the two halves restrained each other. This hypothosis is discussed and investigated here.

3.2 Materials and Methods

A trial of 54 *E. bosistoana* trees was set up, with two treatments and a control each containing 18 individuals. The trees were planted in an irrigated nursery site at Harewood, Christchurch, New Zealand in spring 2015 and grown for 25 months. The manipulation procedure lasted 12 months where the trees were staked on a 45° angle to the vertical and the direction of lean was rotated around the stem axis by either 90° or 180° every 4 to 8 weeks depending on the growing season, in order to maximise tension wood production. The change in lean orientation was chosen to ensure the trees were lent away from seasonal prevailing winds on the site in order to reduce wind damage. One month after planting, all trees were staked, the control remained this way for the next 24 months. The 'early' treatment started the 12 month procedure one month after planting and during the

second 12 month period was staked vertically. The 'late' treatment was staked vertically one month after planting and after 12 months of being staked vertically followed the above procedure for the second 12 months of the experiment.

The survival rate was 78% for the trial. Table 3.1 shows the number of surviving individuals, the mean, standard deviation and the extremes of under-bark diameter and growth-strain for each treatment. An analysis of variance (ANOVA) between the treatments was performed in R using MCMCglmm (R Core Team, 2017; Hadfield, 2010).

3.3 Results and discussion

The 'control' trees produced tension wood as a staked tree would, i.e. where needed to react to changes in the micro-environment. The 'early' treatment should have created trees with tension wood near the pith, and normal wood near the periphery, while the 'late' treatment should have created trees with normal wood near the pith and tension wood near the periphery. Previously tilting in 1 year old *E. regnans* has been used to intentionally form tension wood (Chauhan and Walker, 2011).

Figure 3.1 visualises the variation in the data summarised in Table 3.1 as boxplots for the treatments. Note that there were no zero values in this data. This experiment showed that it was unlikely that tension wood development during 'early' growth was the cause of the zero censored data. Table 3.2 presents the results of the ANOVA between the treatments. The 'early' treatment stunted growth, but had little to no effect on growth strain.

Reaction wood forms to correct the posture of stems (Saranpaa et al., 2014). Chauhan and Walker (2011) tilted the stems of 3 month to 1 year old *E. regnans* to intentionally form tension wood. They found longitudinal growth-strain varied from 708 to 2319 $\mu\epsilon$. The

Table 3.1: Descriptive statistics of two year old *E. bosistoana*. Number of surviving individuals, mean diameter and growth-strain, with standard deviations (in parentheses), and maximum and minimum values. The control was staked for the two year period, while the early treatment was tilted at 45° for the first year and the late treatment was tilted at 45° for the second year. Note that there were no zero values in this data.

Treatment	Number	Diameter (mm)	Min, Max	Growth-strain ($\mu\epsilon$)	Min, Max
Control	15	56 (13)	(32, 72)	2292 (780)	(1325, 3592)
'Early' Leaning	12	43 (13)	(24, 61)	2639 (877)	(1509, 4683)
'Late' Leaning	15	59 (13)	(36, 78)	2518 (764)	(955, 4374)

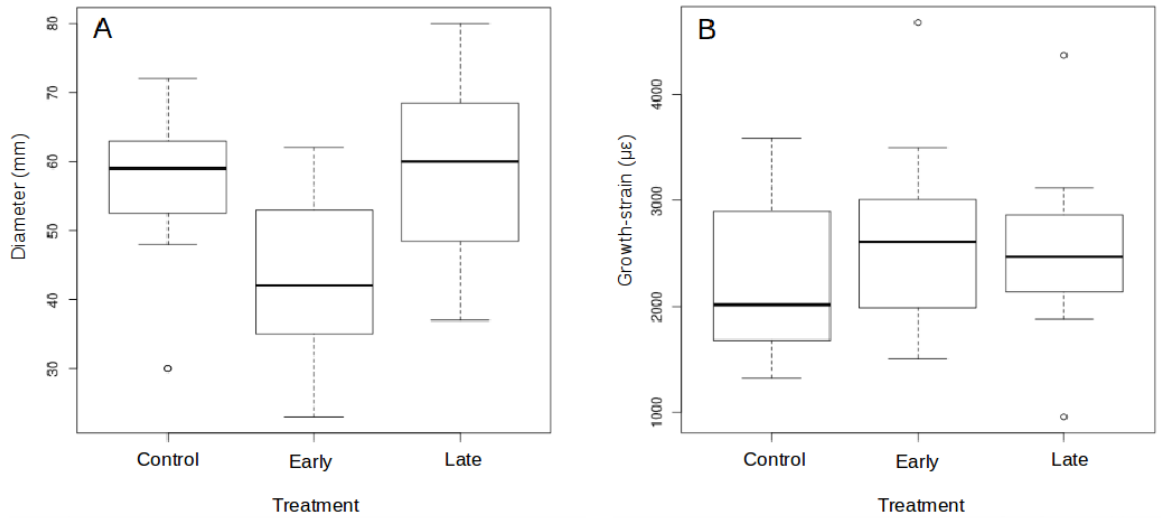

Figure 3.1: Boxplot of two year old *E. bosistoana* for diameter (A) and growth-strain (B) separated into staked (control), bending induced 'early' in life (early) and bending induced 'late' (late) in life.

experiment did not include a non-tilted control, so it is unknown if growth was impeded. Apiolaza et al. (2011a) experimented with *Pinus radiata* seedlings where they were either straight, tilted or set on a rocking table for 6 months. No statistical difference in growth was found between treatments.

Table 3.2: ANOVA results between the leaning treatments for diameter and growth-strain. The 95% credible intervals in brackets suggested that the 'early' treatment stunted growth compared to the control and late treatment. No discernible difference was found between any of the treatments for growth-strain.

Treatment	Comparison	Diameter (mm)	Growth-strain ($\mu\epsilon$)
Control	'Early'	-13 (-23, -3)	352 (-202, 1102)
Control	'Late'	3 (-6, 14)	220 (-431, 777)
'Late'	'Early'	-17 (-28, -7)	118 (-510, 720)

Table 3.1 shows the mean and standard deviation for diameter and growth-strain. The trees in this trial which had mean diameters of between 43 and 59 mm depending on the treatment were larger than the original dataset used in Chapter 2 which had a mean diameter of 28 mm and a standard deviation of 5 mm. They were also larger than the two year old *E. bosistoana* population presented in Chapter 4 which had a mean diameter of 37 mm with a standard deviation of 9 mm. The mean growth-strains of between 2292 and 2639 $\mu\epsilon$ were larger across all treatments than both the Chapter 2 population which had a substantially lower growth-strain with a mean of 848 $\mu\epsilon$ and a standard deviation of 662 $\mu\epsilon$ and the Chapter 4 population with a mean growth-strain of 2072 $\mu\epsilon$ with a standard deviation of 755 $\mu\epsilon$.

It should be noted this trial had no zero values, while the substantially larger two year old *E. bosistoana* breeding trials in Chapter 4 and Appendix B contained a total of two zero values, less than 0.1% of the samples. For comparison, approximately 35% of samples in Chapter 2 were zero.

3.4 Conclusion

The hypothesis that production of tension wood early in growth (near the pith), and normal wood at the periphery would result in a zero value from the splitting test was investigated. Stems were artificially leant to induce tension wood production at different times in their growth. Stems with an early development of tension wood showed a small reduction in growth; however, discernible differences in growth-strain were found between treatments and the control. The reason for the uncharacteristic left-censored dataset in Chapter 2 is still unknown.

Chapter 4

Genetics of *Eucalyptus bosistoana*

Chapter Prologue

Previous to the results of Chapters 2 a breeding trial had been planted in Woodville, New Zealand. A trial consisting of 4032 *Eucalyptus bosistoana* trees from 81 half-sibling families were assessed at age two for growth and wood properties. A selection was conducted identifying the 'top' individuals, while the trial itself provided only minor predicted genetic gains, on a single site, at a very young age, it afforded the chance to characterise the species at age two with many more samples than had been available previously for growth-strain investigation (for any species). The results of this investigation, primarily heritabilities and genetic correlations are discussed with reference to previous literature over numerous of wood properties.

4.1 Introduction

Eucalyptus bosistoana F. Muell. is a eucalypt species native to the Australian east coast and eastern high country. As old-growth timber it has been used in general construction, heavy engineering structures, sleepers, bridges, wharves, flooring, decking, cladding, cross-arms, posts, poles and piles (Bootle, 2005; Poynton, 1979). *Eucalyptus bosistoana* is a good candidate for short rotation high value timber products in New Zealand as it shows high stiffness, class 1 durability (Australia, 2005) and exhibits good growth rates, along with reasonable drought and frost resistance (Poynton, 1979; Altaner et al., 2017). However eucalypts often exhibit excessive growth-strain production causing problems in the production of saw logs (Blackburn et al., 2014; Valencia et al., 2010; Yang et al., 2002).

Recently *E. bosistoana* has been investigated for its potential as a high value commercial timber species within the dry-land areas of New Zealand (Altaner et al., 2017; Apiolaza et al., 2011c; Davies et al., 2017). In order to establish an effective initial breeding population, a 4032 tree breeding trial was conducted using very early screening (at age 21 months) for growth and wood properties; growth-strain, under-bark stem diameter, wood density, volumetric shrinkage, tree height and acoustic velocity. Growth-strain was rarely incorporated in breeding trials as, until recently, with the development of a fast and cheap measurement method (Chauhan and Entwistle, 2010; Davies et al., 2017), it has been too expensive and time consuming to assess. For background information and a review of growth-strain see Chapter 1 and Almras and Clair (2016). The genetic material contained in the trial represents the natural range of the species populations (van Ballekom and Millen, 2017).

Starting from a wild population is not a common occurrence in modern tree breeding, and presents the unique challenge of how the genetic variation be quickly and efficiently

distilled down to only the trees which are likely to be useful in a full-length breeding cycle. Early selection methods provide fast ways to screen out individuals which are detrimental to the breeding programme, without the expenditure of growing them to a mature state; however, less gain is expected, and any gain at rotation age is difficult to predict . Very early selection methods have been studied and used in breeding trials previously (Apiolaza et al., 2011c, 2013; Aggarwal and Chauhan, 2013) and are discussed in detail in Chapter 7.

4.2 Methods

4.2.1 Materials

Open pollinated seeds were collected from 81 mother trees in south eastern Australia, representing all known native populations of *E. bosistoana*. The seeds were germinated and planted into an alpha lattice experimental layout with plots of eight individuals from the same half sibling families, with the plots arranged in replicates. Due to poor germination of some families, only the first two (of eight) replicates were complete. The trials were planted at a uniform, irrigated nursery site in Woodville, New Zealand (40°19'28.9"S 175°52'43.3"E). Soon after planting a wind storm caused 'socketing' (trees swirl in the wind, creating a bowl in the soil around the stem resulting in lowered support from the soil) in one third of the seedlings. These individuals were tethered to bamboo stakes in order to correct their growing posture. Analysis showed that while there was a geographical effect on where socketing and consequently staking, was likely to occur, there was no discernible genetic predisposition to the need for staking (as shown in Table 4.3). The trees were pruned to approximately 500 mm from ground level during growth to ensure

a clean stem section for wood property testing. As part of a pilot study to investigate the usability of wound wood as a proxy for early section of heartwood (Harju et al., 2009), some trees were drilled (to induce a wound-wood reaction) above the clear wood testing zone, approximately one month prior to harvest, no effect was found on growth-strain. In the month preceding harvest the height of each tree was measured using a height pole. Harvesting was undertaken in two batches (1425 individuals in the first batch and 1261 individuals in the second batch two weeks later), the stems were labelled, topped (at the top of the clear wood zone) and felled at ground level. The samples were stored in insulated bins with excess water to avoid any drying and processed within two weeks of harvest. No deterioration of the samples was detectable. At harvest, stems were rejected if they did not met the visually estimated criteria of 400 mm of clear stem and a minimum over bark diameter of 25 mm, which was required for the assessment of growth-strain. Due to resource limitations, two sampling procedures were used. In the first procedure, every individual which met the above criteria was collected for the first five replicates, totalling 2138 individuals. The second procedure was used for the last three replicate plots, selecting only the three largest (visually assessed diameter) individuals with good stem form in each replicate plot of eight trees, totalling 548 individuals.

4.2.2 Measurements and Calculations

The samples were manually debarked, split and dried. Growth-strain, diameter, green and dry density, acoustic velocity, stiffness and volumetric shrinkage were measured and calculated as described in Section 2.2.2 of Chapter 2.

4.2.3 Analysis

A multivariate linear mixed animal model (Equation 4.1) was implemented in the MCMCglmm package (Hadfield, 2010) for the statistical system R (R Core Team, 2017) and used to estimate the genetic parameters of the population. The response variables were; growth-strain, under-bark diameter, dry density, stiffness, volumetric shrinkage, height and acoustic velocity. The 'fixed' effects in the model were: replicate, staking and edge effects, with plot and additive genetic effects included as 'random' effects. Equation 4.1 produced response vectors y_i for all individuals for the i^{th} trait from: m fixed effects, p plot effects, a the individual and e error. The incidence matrices, X, Z_1, Z_2 link the i^{th} trait to the fixed, random plot and random additive genetic effects respectively. It is assumed that the traits were correlated with heterogeneous variances, and hence the variance-covariance (G) and residual variance-covariance (R) matrix structures were not diagonal, using unstructured matrices to model the genetic correlations between traits and residuals. Further, it is assumed that Equation 4.2 holds, where P is the plot variance-covariance matrix and A is the numerator relationship matrix.

Priors for the fixed effects were the default MCMCglmm priors, the expected value of all fixed effects was 0, and the degree of belief matrix was set as I multiplied by 1^{10} where I is the identity matrix of the appropriate dimension (Hadfield, 2014). The priors for both, the plot and additive genetic effects, were vaguely informative, using an inverse Wishart expected variance-covariance matrix obtained by multiplying the phenotypic variance-covariance matrix by 0.25. The residuals prior was set in the same way; however, using a multiplier of 0.5. In a separate instance, an uninformative prior (Hadfield, 2014) was used on the model to ensure that using the phenotypic variance-covariance matrix to inform the priors was not drastically influencing the outcome. The uninformative prior provided similar results, however, took substantially longer to run and did not mix well. A burnin

of 20,000 iterations was used with a total of 100,000 iterations, all models showed good convergence diagnostics.

$$y_i = X_i m_i + Z_{1i} p_i + Z_{2i} a_i + e_i \tag{4.1}$$

$$\text{var} \begin{bmatrix} p_i \\ a_i \\ e_i \end{bmatrix} = \begin{bmatrix} P_i & 0 & 0 \\ 0 & G_i A_i & 0 \\ 0 & 0 & R_i \end{bmatrix} \tag{4.2}$$

4.3 Results and Discussion

Summary statistics of growth and wood properties for two year old *Eucalyptus bosistoana* grown on an irrigated nursery site in Woodville New Zealand are presented in Table 4.1. Table 4.2 presents narrow-sense heritabilities on the diagonal and genetic correlations in upper triangular form. The results were obtained from the model presented in Section 4.2, Equations 4.1 and 4.2. For breeders interested in reducing growth-strain the low to nil correlation between growth-strain and diameter (and height) may provide an opportunity to simultaneously increase growth and decrease strain. The positive correlation between strain and stiffness indicates that some stiffness will need to be sacrificed in order to reduce strain; however, because of the very high stiffness values within *E. bosistoana*, this reduction may not be of practical importance. The stronger correlation between strain and acoustic velocity rather than with stiffness or density suggests the MFA has a larger

impact on growth-strain generation than density. While not measured, grain angle may account for some of the variation which MFA and stiffness cannot explain.

Table 4.1: Summary statistics for the trees used in this study. They were age two *E. bosistoana* grown on an irrigated nursery site in Woodville, New Zealand.

	Mean (standard deviation)	Maximum	Minimum
Strain ($\mu\epsilon$)	2072 (755)	6811	0
Diameter mm	36.6 (8.6)	63.5	10.6
Density ($\frac{kg}{m^3}$)	816 (47)	1056	660
Stiffness GPa	11.2 (1.9)	18.6	5.9
Volumetric Shrinkage	0.2 (0.04)	0.37	0.04
Height m	2.4 (0.6)	3.9	0.1
Acoustic Velocity ($\frac{km}{s}$)	3.7 (0.3)	4.56	2.77

Table 4.2: Narrow-sense heritability (for *E. bosistoana* at age two) presented in bold on the diagonal, with genetic correlations between traits in the upper half of the table, calculated using the model presented above. 95% credible intervals in brackets.

	Strain	Diameter	Density	Stiffness	Volumetric Shrinkage	Height	Acoustic Velocity
Strain	**0.23 (0.13, 0.34)**	0.03 (-0.26, 0.32)	-0.14 (-0.37, 0.1)	0.33 (0.11, 0.54)	-0.16 (-0.49, 0.16)	0.11 (-0.19, 0.41)	0.45 (0.24, 0.66)
Diameter		**0.57 (0.39, 0.74)**	-0.25 (-0.43, -0.08)	-0.3 (-0.44, -0.16)	-0.22 (-0.5, 0.05)	0.93 (0.89, 0.97)	-0.23 (-0.36, -0.08)
Density			**0.7 (0.59, 0.81)**	0.49 (0.38, 0.6)	0.22 (0.01, 0.42)	-0.16 (-0.3, -0.01)	0.18 (0.05, 0.31)
Stiffness				**0.77 (0.67, 0.86)**	-0.05 (-0.26, 0.18)	-0.15 (-0.27, -0.01)	0.94 (0.93, 0.96)
Volumetric Shrinkage					**0.39 (0.23, 0.55)**	-0.38 (-0.63, -0.12)	-0.15 (-0.36, 0.06)
Height						**0.71 (0.56, 0.87)**	-0.08 (-0.2, 0.05)
Acoustic Velocity							**0.8 (0.71, 0.89)**

Table 4.3: Fixed effects of the model, 95% credible intervals in brackets

	Strain	Diameter	Density	Stiffness	Volumetric Shrinkage	Height	AcousticVelocity
Mean	1.95 (1.85, 2.05)	35.2 (34.3, 36.2)	0.82 (0.72, 0.92)	11.2 (10.2, 12.2)	0.21 (0.11, 0.31)	2.49 (2.39, 2.59)	3.68 (3.58, 3.78)
Replicate 2	0.13 (3.02)	-1.7 (-2.7, -0.7)	-0.01 (-0.11, 0.09)	0.1 (-0.9, 1.1)	-0.01 (-0.11, 0.09)	-0.03 (-0.13, 0.07)	0.04 (-0.07, 0.14)
Replicate 3	0.1 (0.0, 0.2)	-1.5 (-2.5, -0.5)	0.0 (-0.1, 0.1)	0.0 (-1.0, 1.0)	0.0 (-0.1, 0.1)	-0.13 (-0.22, -0.03)	0.0 (-0.1, 0.1)
Replicate 4	0.1 (0.0, 0.2)	-1.1 (-2.1, -0.1)	-0.01 (-0.11, 0.09)	0.1 (-0.9, 1.1)	-0.01 (-11.01)	-0.11 (-0.21, -0.01)	0.05 (-0.05, 0.15)
Replicate 5	0.02 (-0.08, 0.12)	-0.4 (-1.4, 0.5)	-0.02 (-0.12, 0.08)	-0.1 (-1.1, 0.9)	-0.02 (-0.12, 0.09)	-0.14 (-0.24, -0.04)	0.03 (-0.07, 0.12)
Replicate 6	0.13 (0.03, 0.23)	2.0 (1.0, 3.0)	-0.02 (-0.12, 0.08)	-0.4 (-1.4, 0.6)	-0.02 (-0.12, 0.08)	-0.15 (-0.25, -0.05)	-0.02 (-0.12, 0.09)
Replicate 7	0.04 (-0.06, 0.14)	2.8 (1.8, 3.8)	0.0 (-0.1, 0.1)	-0.2 (-1.2, 0.8)	-0.01 (-0.11, 0.09)	-0.04 (-0.14, 0.07)	-0.04 (-0.14, 0.06)
Replicate 8	-0.03 (-0.13, 0.07)	4.2 (3.2, 5.2)	-0.01 (-0.11, 0.1)	-0.5 (-1.5, 0.5)	-0.01 (-0.11, 0.09)	-0.09 (-0.19, 0.01)	-0.07 (-0.17, 0.03)
Stake	0.12 (0.02, 0.22)	-1.0 (-2.0, -0.0)	0.01 (-0.09, 0.11)	-0.1 (-1.1, 0.9)	0.0(-0.1, 0.1)	-0.04(-0.14, 0.06)	-0.03(-0.13, 0.07)
Edge S	-0.18 (-0.28, -0.08)	3.0 (2.0, 4.0)	0.02 (-0.08, 0.12)	0.1 (-0.3, 1.7)	0.0(-0.1, 0.1)	0.14(0.04, 0.24)	0.08(-0.02, 0.18)
Edge E	0.1 (0.0, 0.2)	-0.4 (-1.4, 0.6)	0.0 (-0.1, 0.1)	0.1 (-0.9, 1.1)	0.0(-0.1, 0.11)	-0.08(-0.18, 0.02)	0.01(-0.09, 0.11)
Edge N	0.36 (0.26, 0.46)	0.5 (-0.5, 1.5)	-0.02 (-0.12, 0.08)	0.3 (-0.7, 1.3)	0.0(-0.1, 0.1)	-0.34(-0.43, -0.24)	0.08(-0.02, 0.18)
Edge W	-0.18 (-0.28, -0.08)	1.0 (0.0, 2.0)	0.01 (-0.09, 0.11)	0.0 (-1.0, 1.0)	0.0(-0.1, 0.1)	-0.17(-0.27, -0.07)	0.0(-0.11, 0.09)

The contributing fixed effects in the model are presented in Table 4.3, with the remaining fixed effects tested, but not used in the model presented in Appendix B. The fixed effects of replication showed some differences across the experiment but did not show any particular trend (with the exception of diameter which is due to the sampling constraints described in the Section 4.2). In spite of the high correlation between diameter and height, sampling type (Replicates 6, 7 and 8 in Table 4.3 and Sampling Type in Appendix B) only shows influence over diameter, this is because height was measured pre-harvest on all (living) trees, while diameter was one of the main visual indicators for selection during harvest, and measured under bark post-harvest. It was not surprising that sampling type has little effect on other traits, as (with the exception of height) correlations with diameter are weak, as seen in Table 4.2. Staking had a small effect on growth-strain, but this increase is more likely due to tension wood development while the trees were not staked, but had fallen over in the storm. Staking shows little bias toward particular families, however is concentrated toward the southern end of the experiment where wind funnelled between two hedges. The outer-most rows/columns (Edge effects) of the experiment show a small

effect in growth-strain, diameter and height (see Table 4.3). It should be noted there were buffer rows at the southern end of the block, but not on any other side. Remaining fixed effects all show negligible influence (Appendix B).

Growth-strain had a heritability of 0.23, which was significantly lower than the only (known) previously reported value for the species, 0.63 (Davies et al., 2017)/Chapter 2. But is similar to the 0.32 value for *Eucalyptus dunnii* presented by Murphy et al. (2005). The discrepancy with Davies et al. (2017)/Chapter 2 may come from the individuals used in that trial having significantly more genetic relatedness than was assumed. As both were single site trials the environmental effects cannot be distinguished between studies, however it could also be possible the Davies et al. (2017)/Chapter 2 site caused a much stronger expression of the genes responsible for growth-strain than this trial site. It should be noted that the credible intervals from Davies et al. (2017)/Chapter 2 were large (0.28 - 0.98 $\mu\epsilon$ from a sample size of 423 individuals) and overlap with this study. The modelling procedure made a number of assumptions with respect to the relatedness of families and individuals which were likely inflating the true heritabilities of the traits. Fathers were unknown and assumed to be unrelated to each other, or to the mothers. As a result there was likely less genetic variation within families than the model assumed. Because the fathers were unknown, there was an implicit assumption within the numerator relationship matrix that all individuals in a 'family' shared a common mother, but none shared a common father (half-sibling families). Further because the genetics of the mothers was unknown, they may have been related to each other, the unknown father trees or self-pollinated. Because of these factors, some (or all) families were probably less genetically diverse than was assumed, resulting in over estimation of heritability. It should be noted Griffin and Cotterill (1988) warned breeders about the dangers of open pollinated trials inflating genetic parameters, which occurs because the variation from inbreeding is completely confounded with family effects, inflating estimates of additive genetic variance.

It should also be kept in mind that this experiment was conducted on a single irrigated nursery site which was not growth restricted. It is commonly believed favourable environments allow higher expressions of genetic signals related to growth (Ceccarelli et al., 1994), although no substantial studies have been undertaken to determine if this holds for wood properties. Growth-strain may not be affected to the same degree as growth by site uniformity, it may be the case that environmental effects which influence growth-strain are more site independent, such as branching asymmetry and stem wobble from micro-environmental effects. For example a lopsided crown (and hence uneven stress field within the stem to keep the stem upright), light competition or wind damage may have a much more significant effect on growth-strain than, say a temperature difference, nutrient or water deficiency across sites, as these examples require a mechanical input to restore gravitropy or heliotropy (Saranpaa et al., 2014). Therefore it should not necessarily be assumed that growth-strain heritabilities will reduce as drastically as growth traits when GxE experiments are implemented.

Few studies have been undertaken specifically investigating genetic parameters of *E. bosistoana*. Perhaps the most relevant, Apiolaza et al. (2011c), used a subset of this population and investigated the heritability and across site genetic correlations of height at age two. They found total height to have a heritability of 0.10 - 0.14 and across site genetic correlations to be between 0.74 and 0.99. Two of the three sites had significant mortality rates, indicating they were probably growth limited. Two of these three sites (one with high and one with low mortality) were revisited at age five and comparable height heritabilities were found (0.09 - 0.17), over-bark DBH heritabilities were found to range from 0.11 to 0.18 (Burgess, 2015). These sites display considerable heterogeneity. *E. bosistoana* has been investigated at a young age once before by Davies et al. (2017)/Chapter 2 who found hertiablities of 0.63, 0.54, 0.76 0.29 0.97 and 0.82 for growth-strain, density, diameter, volumetric shrinkage, acoustic velocity and stiffness respectively, although the

study was limited by the narrow genetic base (40 families). There was overlap with all of the credible intervals between the Davies study and results reported here. The only other known studies to report heritability of growth-strain (or stress) were Henson et al. (2004) who found heritability of 0.52 in a breeding population of *E. dunnii* and Murphy et al. (2005) who reported heritabilities of between 0.3 and 0.5 for *E. dunnii* both with population sizes below 200 individuals. Naranjo et al. (2012) reported no genetic control (heritability of 0.02) of growth-strain in 4-year-old *Tectona grandis.*

Previously reported heritabilities in eucalypts exist for a number of the wood and growth properties. Table 4.4 reports relevant studies of heritability in various eucalypt species for the properties investigated here.

Some previously reported heritabilities are significantly lower than the values reported here (Table 4.4). There are a number of factors which may account for the discrepancy, relatedness assumptions are a likely candidate. There was no consistency across studies in assumptions regarding relatedness, as they have differing levels of knowledge of their populations and species. A number of the previous studies were multisite studies and may have included growth restricted sites, high mortality etc. which likely contribute to the comparatively low values. A single nursery site study gives much more control over environmental variation, and hence higher discernible genetic influences (for the particular environment). Davies et al. (2017)/Chapter 2 was a single nursery site study, which produced comparable values to those reported here. Some genetic parameters could be expected to reduce when considered over multiple sites with harsher growing conditions. Given the large variation and limited previous studies, significant conclusions with regard to the previously reported genetic correlations and those reported in this study cannot be drawn. Measurement error reduces calculated heritability as it adds random error to all results, it may have a significant influence on all of the reported traits here.

Genetic correlations require more data and complex statistical modelling than heritability estimates; as a result fewer have been reported. Relevant genetic correlations in various eucalypt species are reported in Table 4.5. Investigating multiple populations to gain an understanding of genotype x environment interaction information is common practice among modern tree breeders. This study dealt with a single site; however, the trial genetics represented multiple provenances, some of which were partially geographically isolated from the remainder of the population. No previous studies have investigated divergent evolution in *E. bosistoana.* While no clear differences existed between provenances within this experiment, further work is needed to identify where true provenance boundaries lie, as a better understanding of the genetic isolation of various sub populations of *E. bosistoana* may help explain the comparatively high heritabilities for some traits in this study.

4.4 Conclusion

Eucalyptus bosistoana was investigated at an age of 21 months on a single irrigated nursery site for growth and wood properties (growth-strain, under-bark diameter, density, stiffness, volumetric shrinkage, height and acoustic velocity). Heritabilities for these properties (0.23, 0.57, 0.70, 0.77, 0.39, 0.71, and 0.80 respectively) and genetic correlations between them were presented and compared to relevant previous literature. A discussion is provided with regards to these high heritabilities, their cause and potential impact on breeding. In particular it is noted that the heritabilities are overestimated due to the assumptions of low relatedness (families have no relationship and all individuals within a family are half-siblings) and that there are no provenance effects, both of which may not be true and result in an overestimate of additive genetic variance. While the posi-

tive genetic correlation between growth-strain and stiffness is unfavourable, a reduction in stiffness may be acceptable for E. bosistoana, as stiffness is generally high. The absence of a genetic correlations between growth-strain and diameter indicates that fast-growing and low growth strain genetics may be identifiable. Future studies are recommended to quantify the impact of ageing and environment effects on the genetic parameters.

Table 4.4: Previously reported values for heritability of studied traits in eucalypts.

Trait	Heritability range	Reported Heritability	Species	Reference
Growth-Strain	0.3 - 0.63	0.63	*E. bosistoana*	Davies et al. (2017)
		0.3 - 0.5	*E. dunnii*	Murphy et al. (2005)
		0.52	*E. dunnii*	Henson et al. (2004)
Diameter	0.0 - 0.98	0.05 - 0.37	*E. regnans*	Suontama et al. (2015)
		0.09 - 0.23	*E. nitens*	Blackburn et al. (2014)
		0.22 - 0.4	*E. dunnii*	Henson et al. (2004)
		0.3	*E. cladocalyx*	Vargas-Reeve et al. (2013)
		0.2 - 0.35	*E. cloeziana*	Li et al. (2016)
		0.15 - 0.29	*E. globulus*	Stackpole et al. (2009)
		0.11 - 0.35	*E. globulus*	Silva et al. (2008)
		0.1	*E. globulus*	Mora and Serra (2014)
		0.14 - 0.33	*E. pellita*	Hung et al. (2014)
		0.16 - 0.33	*E. globulus* and *E. nitens*	Raymond (2002)
		0 - 0.76 (from literature)	*E. nitens*	Hamilton and Potts (2008)
		0.76	*E. bosistoana*	Davies et al. (2017)
		0.12 - 0.44	*E. viminalis*	Cappa et al. (2010)
		0.13 - 0.55	*E. regnans*	Griffin and Cotterill (1988)
		0.01 - 0.54	*E. grandis* x *E. tereticornis*	Madhibha et al. (2013)
		0.01 - 0.54	*E. grandis* x *E. camaldulensis*	Madhibha et al. (2013)
		0.14	*E. urophylla*	Hein et al. (2012)
Density (Basic unless stated)	0.06 - 0.96	0.3 - 0.47	*E. dunnii*	Henson et al. (2004)
		0.06 - 0.39	*E. grandis* and *E. urophyllain*	Retief and Stanger (2009)
		0.52	*E. globulus*	Stackpole et al. (2009)
		0.23 - 0.25	*E. pellita*	Hung et al. (2014)
		0.4 - 0.61	*E. urophylla*	Hein et al. (2012)
		0.67 - 1	*E. globulus* and *E. nitens*	Raymond (2002)
		0.11 - 0.96 (from literature)	*E. nitens*	Hamilton and Potts (2008)
		0.35 - 0.43	*E. nitens*	Blackburn et al. (2014)
		0.21 - 0.67 (from literature, Pilodyn)	*E. globulus*	Potts et al. (2004)
		0.54 (Dry)	*E. bosistoana*	Davies et al. (2017)
Stiffness	0.09 - 0.82	0.09	*E. cloeziana*	Li et al. (2016)
		0.18 - 0.61	*E. dunnii*	Henson et al. (2004)
		0.36 - 0.51	*E. pellita*	Hung et al. (2014)
		0.82	*E. bosistoana*	Davies et al. (2017)
Volumetric Shrinkage	0.97	0.97	*E. bosistoana*	Davies et al. (2017)

Table 4.4 continued.

Trait	Heritability range	Reported Heritability	Species	Reference
Height	0.04 - 0.72	0.04 - 0.23	*E. cloeziana*	Li et al. (2016)
		0.28 - 0.6	*E. dunnii*	Henson et al. (2004)
		0.34	*E. urophylla*	Hein et al. (2012)
		0.04 - 0.33	*E. regnans*	Suontama et al. (2015)
		0.3	*E. cladocalyx*	Vargas-Reeve et al. (2013)
		0.04	*E. globulus*	Mora and Serra (2014)
		0.25 – 0.3 (from literature)	*E. globulus* and *E. nitens*	Raymond (2002)
		0.06 - 0.72 (from literature)	*E. nitens*	Hamilton and Potts (2008)
		0.07 - 0.27	*E. viminalis*	Cappa et al. (2010)
		0.04 - 0.43	*E. regnans*	Griffin and Cotterill (1988)
		0.02 - 0.54	*E. grandis* x *E. tereticornis*	Madhibha et al. (2013)
		0.02 - 0.54	*E. grandis* x *E. camaldulensis*	Madhibha et al. (2013)
Acoustic Velocity (Including MFA from other methods)	0.14 - 0.97	0.14 - 0.48	*E. pellita*	Hung et al. (2014)
		0.53 (from literature)	*E. nitens*	Hamilton and Potts (2008)
		0.33 - 0.45	*E. urophylla*	Hein et al. (2012)
		0.16 - 0.74	*E. nitens*	Blackburn et al. (2014)
		0.27 (from literature)	*E. globulus*	Potts et al. (2004)
		0.97	*E. bosistoana*	Davies et al. (2017)

Table 4.5: Ranges of previously reported genetic correlations between traits in various eucalypts.

Trait – Trait	Genetic correlation range	Reported genetic correlation	Species	Reference
DBH - Height	0.47 – 0.94	0.52	*E. globulus*	Mora and Serra (2014)
		0.55 - 0.94	*E. viminalis*	Cappa et al. (2010)
		0.47	*E. urophylla*	Hein et al. (2012)
		0.61 - 0.89	*E. grandis* x *E. tereticornis* and *E. grandis* x *E. camaldulensis*	Madhibha et al. (2013)
DBH – Density (Basic)	-0.94 - 0.25	-0.07	*E. grandis* and *E. urophyllain*	Retief and Stanger (2009)
		-0.94	*E. urophylla*	Hein et al. (2012)
		0.08 - 0.12	*E. globulus*	Stackpole et al. (2009)
		0	*E. pellita*	Hung et al. (2014)
		-0.18 - 0.24	*E. nitens*	Blackburn et al. (2014)
		-0.5 - 0.25 (from literature)	*E. globulus* and *E. nitens*	Raymond (2002)
		-0.79 - 0.08 (from literature)	*E. nitens*	Hamilton and Potts (2008)
DBH - stiffness	0.26	0.26	*E. pellita*	Hung et al. (2014)
DBH – Acoustic Velocity (MFA)	-0.19 - 0.71	-0.19	*E. pellita*	Hung et al. (2014)
		-0.36	*E. urophylla*	Hein et al. (2012)
		0.56 (from literature)	*E. nitens*	Hamilton and Potts (2008)
		0.18 - 0.71	*E. nitens*	Blackburn et al. (2014)
Density - stiffness	0.78	0.29 (basic)	*E. pellita*	Hung et al. (2014)
Density - Acoustic Velocity (MFA)	-0.63 - 0.87	0.54	*E. urophylla*	Hein et al. (2012)
		-0.26	*E. pellita*	Hung et al. (2014)
		-0.63 (from literature)	*E. nitens*	Hamilton and Potts (2008)
		0.15 - 0.87	*E. nitens*	Blackburn et al. (2014)

Chapter 5

Experimental determination of splitting test precision

Chapter Prologue

Because every tree is unique and non-reproducible, testing identical samples to approximate the test precision is not possible. As the test is destructive, conducting the same test multiple times on a sample is not a possibility either. The non-reproducibility can be overcome by using a proxy test to estimate the precision of the original test, in particular the error associated with the radial orientation of the cut. The following chapter describes how a testing procedure was developed and used to experimentally estimate the precision of the splitting test and discusses the impact of these findings on breeding programmes.

5.1 Introduction

In recent years, wood quality parameters have been included in very-early selection pilot studies for tree breeding programmes (Davies et al., 2017; Chauhan et al., 2013; Apiolaza et al., 2011b; Sharma, 2013). Particular wood properties provide advantages for different applications of timber. For example, high stiffness timber is beneficial for structural uses, and a premium is paid. Growth-strain has been identified as a wood quality parameter which reduces the value of eucalypt species for solid wood processing (Yamamoto, 2007; Chauhan and Entwistle, 2010; Raymond et al., 2004; Murphy et al., 2005; Yang and Waugh, 2001). Species with a tendency to produce high internal strains during growth typically experience excessive value-recovery loss. During processing growth-strains are released causing the cut boards to deform, requiring them to be re-sawn straight. For more details on growth-strain refer to Section 1.3 Chapter 1, Alméras and Clair (2016) or for an older, but more comprehensive review, see Kübler (1987).

Until recently the quickest growth-strain test was the 'French' or CIRAD method, (Baillères et al., 1995) which required approximately half an hour on substantially sized trees. This renders growth-strain too time consuming and expensive to incorporate into a breeding programme, particularly for early selection of small trees. Jacobs (1945) developed the pairing test, splitting stems down the pith and measuring the movement of each side, and reported results from *E. delegatensis* along with a number of other species. He did not take the final steps of calculus required to convert his deformation measurements to surface strains. Chauhan and Entwistle (2010) developed the splitting test, which uses the Jacobs (1945) method with a number of assumptions to complete the calculus required to estimate surface strain from the pairing test. The updated pairing test, now referred to as the splitting test, substantially reduced the time and cost involved in measuring growth-strain. This method was further refined and a pilot study was conducted by Davies

et al. (2017) (Chapter 2), which showed it had potential for production trials. The splitting test essentially involves cutting a stem longitudinally along the pith and measuring the opening, along with diameter and cut length (Figure 2.1). A numerical value related to the surface strain in the sample can be obtained from the measurements (Equation 5.1).

Chauhan and Entwistle (2010) took strain gauge measurements at the surface of *E. nitens* stems, which had a mean diameter of 149 mm, and used them to predict the cut opening, which showed correlations (R^2) of 0.70 for butt logs and 0.81 for upper logs. Figure 5.1 shows how surface strain can vary substantially around the stem. The analysis with strain-gauges placed on the surface parallel to the cut only indicated the reliability of the splitting test to account for strain-gauge values from the two positions which are geometrically the most responsible for the opening, not the mean surface strain of the sample. As a consequence, the predicted mean surface strain from the splitting test will differ depending on the orientation of the radial cut plane. In the case of Figure 5.1 A it would underestimate the surface mean, while 5.1 B would overestimate. Nicholson (1971) presents some real world examples and Aggarwal and Chauhan (2013) found a correlation between two oposing strain-gauges of 0.5 in *Eucalyptus tereticornis* clones.

The work presented in Chapters 2 and 4 were conducted on smaller stems ($< 64\ mm$ in diameter) than the initial work at 111 - 192 mm in diameter (Chauhan and Entwistle, 2010). Cramer (2018) analysed two-year-old *E. nitens* stems with diameters ranging from 58 to 120 mm with the same method as Chauhan and Entwistle (2010), and obtained a correlation of 0.27 between surface strain measured with strain gauges and surface strain predicted from the splitting test. In contrast, Chauhan and Entwistle (2010) reported a correlation of 0.92 for *E. nitens* stems with diameters between 111 and 192 mm. One reason for the difference between the two studies could be the smaller openings observed by Cramer (2018). Therefore, the splitting test is not necessarily suitable for use in very-

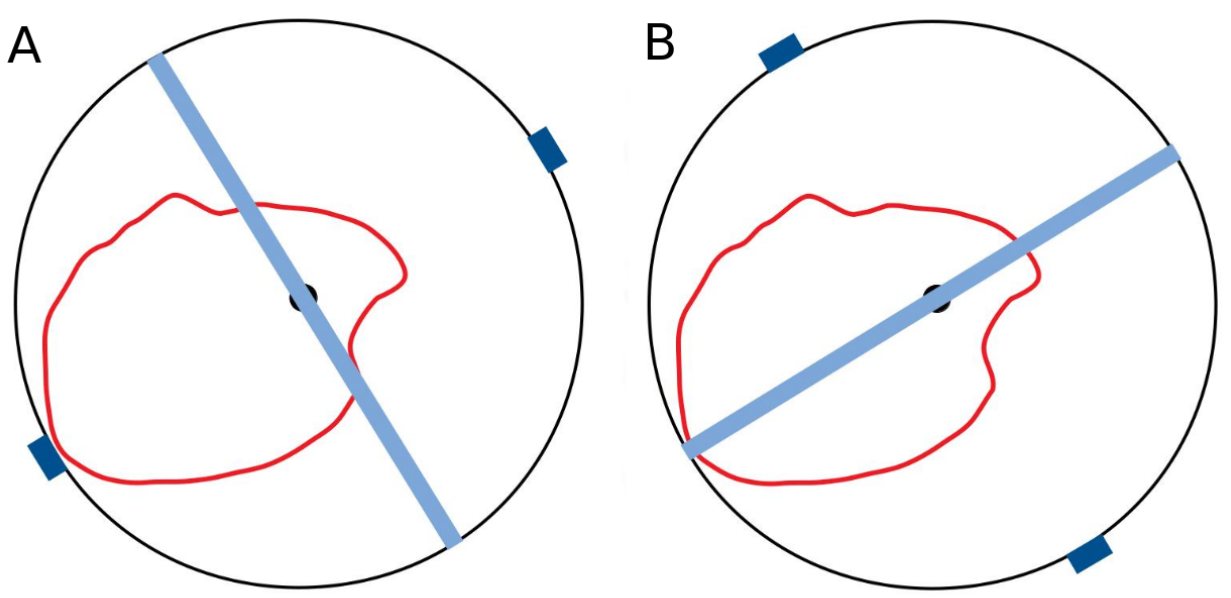

Figure 5.1: The surface strain profile of a single stem (constant strain line in red) and overlaid with two possible orientations for the splitting test. The light blue line represents the cut. The placement of the strain gauges as set up by Chauhan and Entwistle (2010) are in dark blue.

early selection (on small stems) tree breeding programmes.

It has been reported that surface growth-strain can vary markedly over small sectors of a stem (Okuyama et al., 1994; Saurat and Guneau, 1976; Nicholson, 1971). Figure 7 in Nicholson (1971) shows examples of how growth-strain varies around stems. Common protocols for measuring surface strain on logs with the CIRAD tool (Baillères et al., 1995) or strain gauges take eight measurements around the perimeter to account for the variation which can occur over small radial distances on the log surface (Fournier et al., 1994). The major trade-off for the speed of the splitting test is the resolution which can be achieved. Due to the geometry of the test, surface strains near the cut are suppressed, while the strains parallel to the cut are primarily responsible for the opening. Hence placing one strain gauge on each side, parallel to the plane of splitting overestimates how accurately the splitting test predicts the average surface growth-strain of the sample.

It should be noted that the opening in the splitting test is not solely caused by the longitudinal strain, but that tangential and radial strains also play a role (see Section 1.3, Chapter 1). Grain angle likely influences the results of both the splitting and strain gauge tests, although not necessarily in the same way. No known research has investigated this.

The splitting test will produce different outcomes depending on the radial orientation of the cut due to the inhomogeneity of material properties around the stem. It is important to know the accuracy of the estimate, and the proportion of error associated with the orientation as opposed to random measurement error. Reliability of the splitting test is not directly testable due to its destructive nature and inhomogeneity both within and between individuals, precluding repeated measures. It is important for tree breeders to know the accuracy of the splitting test measurements of individuals when deciding on selection weights for various traits.

5.2 Method

5.2.1 Materials

The trees used in this study were thinnings of five-year-old *E. argophloia* grown on a moderately steep, east-facing slope, with a rainfall of approximately 700 mm per year in Marlborough, New Zealand. The 176 samples were selected from 115 suitably straight individual trees, with estimated under-bark diameter of greater than 20 mm and lengths of at least 400 mm. Under-bark diameters ranged from 21 mm to 71 mm with a mean of 40 mm. The samples were cut from the stems in autumn using a chainsaw, packed into air-tight containers with excess water and transported to a cool store, where they were stored at 5 ℃ until assessment, which took place over the following four weeks. No visual

(visible drying or defects) or statistical (time series trends) signs of sample degradation were observed.

Samples were removed individually from their containers and debarked by hand. Care was taken not to damage the underlying wood. The longest sufficiently straight section of sample, which could be obtained from the large end, was marked with a maximum length 50 mm short of the small end. The cut length and diameter of the large end was recorded as was the small end diameter at the marked point.

5.2.2 Measurement

The rapid-splitting test outlined in Chapter 2 involved splitting with a band saw through the pith from the big end to the marked point. The diameter d, slit length L and resulting opening o were measured and recorded. From these, the surface strain ϵ within the sample was estimated using Equation 5.1.

The original-splitting test, presented by Chauhan and Entwistle (2010) involved splitting the whole sample down the pith. This was achieved by docking the remaining intact end from the rapid-splitting test procedure described above. The measuring procedure was slightly modified to reduce measurement error due to the smaller openings compared to the original. The small end was clamped and the opening was measured at the large end, rather than clamping the centre and measuring both ends. When the curvature is sufficiently low, these two methods are approximately equivalent. Growth-strain (ϵ) as calculated from opening (o), average diameter (d) and split length (L) using Equation 5.1.

$$\epsilon = \frac{od}{1.74L^2} \tag{5.1}$$

In order to test the effect of varying growth-strain around the stem the quartering-test was developed. Each of the two halves were halved again into quarter rounds with a band saw. These were reassembled with the small-end in a self-aligning jig and the openings between each adjacent quarter round were measured with callipers. Openings of the same cut plane between adjacent quarter rounds were averaged as there were two measurements for each half round (Figure 5.2).

5.2.3 Analysis

In the splitting tests using half rounds the constant is 1.74, which was derived from the distance to the neutral plane of bending from the outer surface (Chauhan and Entwistle, 2010). Following the same logic, a constant of 2.08 can be calculated for the quarter round test. Assuming the sample possesses a circular cross section, the half-chord of the circle perpendicular to the plane of the cut and through the centroid for each quarter (Distance A in Figure 5.3) can be calculated using Equation 5.2. The distance from the axis to the centroid (B in Figure 5.3) is $\frac{4}{3\pi}r$. The distance from the outer edge of the circle to the centroid (C in Figure 5.3) was calculated as a function of radius (Equation 5.3). Rearranging Equation 5.3 as per Chauhan and Entwistle (2010) gives a constant for quarter round testing of 2.08 (Equation 5.4), and consequently the growth-strain calculation, Equation 5.5.

$$a = \frac{chord}{2} \; = \; \sqrt{r^2 - \left(\frac{4r}{3\pi}\right)^2} = 0.9055r \tag{5.2}$$

$$b = \left(0.9055 \; - \; \frac{4}{3\pi}\right) r \; = \; 0.4811r \tag{5.3}$$

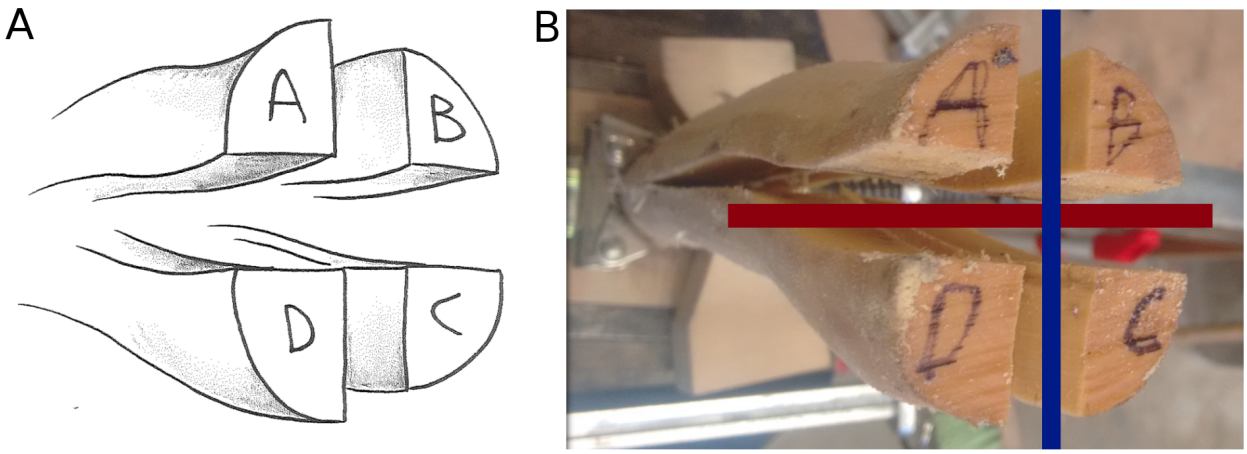

Figure 5.2: Quartering test, where the original cut is displayed as a red line, and the second cut as a blue line. For the original (red) cut the distance between the inner edges of quarters A and D were measured as were the inner edges of quarters B and C. The second cut (blue line) is the perpendicular quartering test and represented by the A-B and C-D distances. The two distances for each plane were then averaged to get the same plane quartering test opening.

$$\frac{1}{0.4811} = 2.08 \tag{5.4}$$

$$\epsilon = \frac{od}{2.08L^2} \tag{5.5}$$

When both cuts of the quartering test are included the differences between the four tests on each sample can be described by six equations, with four error terms (Equations 5.6 to 5.11). Being an over-determined, ill-conditioned system of linear equations, they can be solved simultaneously as a minimisation problem with the Python scipy.optimize minimize algorithm (Jones et al., 2001). Equations 5.6 to 5.11 were solved for means giving estimates on the bias of each test relative to the others (code available in Appendix C)). The system was also solved for variances and used to calculate 95% prediction intervals on an arbitrary measurement.

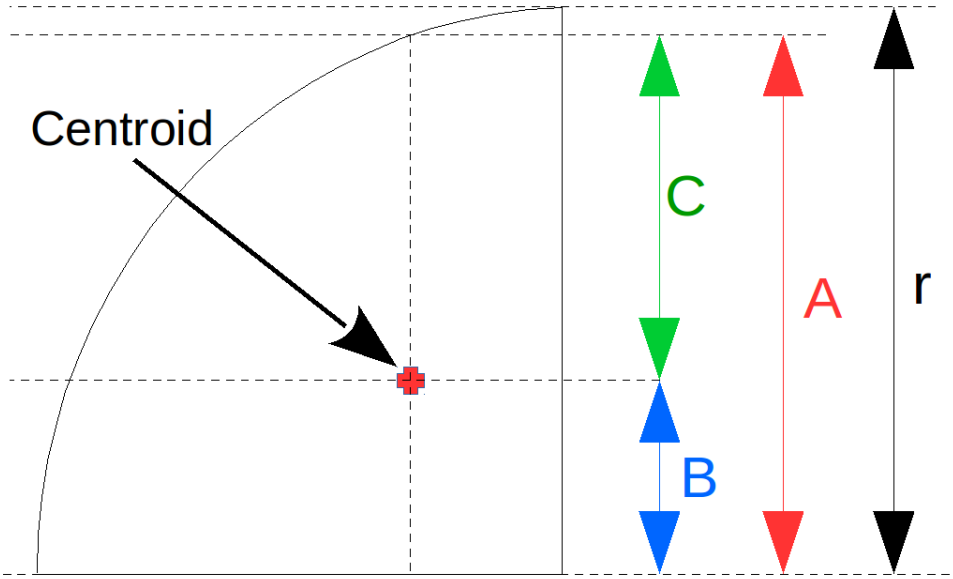

Figure 5.3: Distances required to derive the constant needed for the calculation of surface strain from the quartering test, used in Equations 5.2 to 5.5.

$$RS - OS = e_{rapid} + e_{original} \tag{5.6}$$

$$RS - QS1 = e_{rapid} + e_{quartering} \tag{5.7}$$

$$RS - QS2 = e_{rapid} + e_{quartering} + e_{rotational} \tag{5.8}$$

$$OS - QS1 = e_{original} + e_{quartering} \tag{5.9}$$

$$OS - QS2 = e_{original} + e_{quartering} + e_{rotational} \tag{5.10}$$

$$QS1 \; - \; QS2 \; = \; 2e_{quartering} \; + \; e_{rotational} \tag{5.11}$$

Where RS is the result from the rapid-splitting test, OS is the result of the original-splitting test, $QS1$ is the result from the quartering test along the same plane as the rapid-splitting test and $QS2$ is the quartering test along the plane perpendicular to $QS1$. e_{rapid} and $e_{original}$ are the measurement error associated with the rapid and original-splitting tests, $e_{quartering}$ is the measurement error associated with the quartering test, which is the same regardless of splitting plane and $e_{rotational}$ is the difference resulting from the plane of the cut, but does not include measurement error.

In the absence of measurement error in any of the three testing procedures, Equations 5.6, 5.7 and 5.9 and hence e_{rapid}, $e_{original}$ and $e_{quartering}$ would be zero. Equations 5.8, 5.10 and 5.11 (the equations containing $e_{rotational}$) would only be zero if the stem contains a homogeneous strain field. If e_{rapid}, $e_{original}$ and $e_{quartering}$ are zero, any differences between $QS2$ and other tests would be the result of the change in measured strain due to cutting the sample through a different radial plane. Therefore, assuming the samples were arbitrarily aligned, the difference between the two perpendicular cuts in the quartering test provide a distribution with a mean of zero and a non-zero variance. This allows an estimate of the 95% prediction interval on the growth-strain of another hypothetical cut on the same sample.

Unfortunately, all of these tests have measurement error. However, because there were three measurements which *should* all produce the same result, the error associated with each test could be estimated. Note, that this is not necessarily the error from the 'true' value, but the repeatability of the testing procedure.

5.3 Results and Discussion

Population means ($1341 - 1807\ \mu\epsilon$) and standard deviations ($520 - 662\ \mu\epsilon$) for growth-strain measured by the different tests are shown in Table 5.1 and the Pearson correlations between measurements are presented in Table 5.2. The growth-strain means and standard deviations presented in Table 5.1 are similar to those presented in Chapters 2, 3 and 4, with the exception of the growth-strain mean from Chapter 2 ($850\ (660)\ \mu\epsilon$). Chauhan and Entwistle (2010), using the splitting test on *E. nitens* found a similar mean ($855 - 933\ \mu\epsilon$) and standard deviation ($346 - 454\ \mu\epsilon$) to that of Chapter 2 ($850\ (660)\ \mu\epsilon$) and is the only other published record of the splitting test being used in a similar manner. Others such as Murphy et al. (2005); Chauhan and Walker (2004) and Clair et al. (2013) have studied various eucalypt species with other measurement techniques with means and standard deviations ranging from similar to the results presented here to smaller than the Chapter 2 values. Note that these studies are only remotely comparable due to the differences in species, environments and measurement techniques.

Table 5.1: Surface growth-strain means and standard deviations of the population obtained from the splitting test procedures.

Test	Mean ($\mu\epsilon$)	Standard deviation ($\mu\epsilon$)	Coefficient of variation %
Original-splitting test	1556	610	39.2
Rapid-splitting test	1807	662	36.7
Quartering test (same plane)	1369	534	39.0
Quartering test (perpendicular plane)	1341	520	38.7

Table 5.2: Pearson correlations between different splitting test procedures at the individual sample level (176 samples).

	Original-splitting test	Rapid-splitting test	Quartering test (same plane)	Quartering test (Perpendicular plane)
Original-splitting test	1	0.89	0.88	0.73
Rapid-splitting test		1	0.9	0.78
Quartering test (same plane)			1	0.89
Quartering test (Perpendicular plane)				1

All tests measured the 'same' property, in that they are all numerical proxies for deformation occurring during the sawing of green timber. Consequently all tests should have given the same results. The original, rapid, quartering (same plane) tests, should have provided the same numerical result for each sample. Therefore, differences between them are due to the testing procedures. The quartering (perpendicular plane) test compounded measurement error, which was assumed to be the same as the quartering (same plane) test, with the error resulting from measuring a different radial orientation of the sample (explaining the lower correlations). By comparing these test results over multiple samples an estimate of the proportion of error associated with each measurement was produced. It is worth noting that although the numerical result was called 'growth-strain', the 'strain' measurements from splitting tests and strain gauges do not measure the exact same phenomenon, and are not directly comparable. Strain gauges measure the surface-strain

over a small area, while the splitting test measures a non-uniform consolidation of the three dimensional strain field of the sample. Strain, in the sense it is used here is the numerical proxy for how much deformation can be expected during sawing through the pith of a green log. This is described as an omnibus quantity, a single number summary of a complex system of properties. Van Belle (2011) gives a very concise description of omnibus properties on pages 6 and 7, they warn, omnibus properties are less useful understanding basic mechanics and advice researchers should verify before-hand that the transformations do not compromise the objectives of the analysis. These are important points which are partially addressed here, however, the outstanding problem; is the splitting test a good predictor of timber deformation during sawing is not answered and still remains an open question.

Equations 5.6 to 5.11 were solved simultaneously to estimate the approximate measurement error for each test, and the error resulting from the rotation of the cut plane around the pith. Table 5.3 shows the mean and 95% prediction interval of the theoretical error distributions. The means indicate a systematic error between tests, although there is no evidence this is in relation to the real value. When considering how repeatable the tests are, it is the 95% prediction intervals which are associated with the random error of the testing procedure (i.e. measurement and rotational error).

For example, lets assume that a stem is cut and measurements for the rapid-splitting test are taken, and growth-strain calculated to be the value x. If, hypothetically, the sample could be 'put back together' and re-cut in the exact same way (i.e. through the same plane), the resulting growth-strain will, 95% of the time, be within the interval $x \pm 416\mu\epsilon$. However, this implies that the strain field is axis-symmetric, which as can be seen in Figure 5.1 is not the case. Growth-strain varies around the stem, creating uncertainty in

Table 5.3: Growth-strain precision estimates for the rapid, original and quartering tests. The mean represents the systematic error each test contributed to the difference between the results (across different testing types), when ordered according to Equations 5.6 to 5.11. The order determines the sign. The 95% prediction intervals were calculated from the variance of the difference distributions giving the bounds on a given measurement, i.e. how repeatable the measurement is.

	Mean $\mu\epsilon$	95% Prediction interval $\mu\epsilon$
e_{rapid}	125.7	$\pm$415.8
$e_{original}$	125.7	$\pm$365.2
$e_{quartering}$	11.2	$\pm$400.4
$e_{rotational}$	5.6	$\pm$586.9

the measurement, this is the rotational error. If there was no measurement error (discussed above), and again the sample was 'put back together' and re-cut, but on any radial plane rather than through the original one, then 95% of the time the prediction would be within the interval $x \pm 587\mu\epsilon$. The rapid-splitting test result (x) consists of two errors, first, the reliability of the measurement given a predefined cut ($\pm 416\mu\epsilon$) and secondly the variability of the growth-strain around the stem ($\pm 587\mu\epsilon$). Note the co-variance between test error and rotational error is assumed to be zero as there is no reason to expect that orientation and test are correlated. Adding these gives the rapid-splitting test result $x \pm (416 + 587) = x \pm 1003\mu\epsilon$, i.e. the rapid-splitting test will give a value which if it could be hypothetically remeasured on the same sample would, 95% of the time, be $x \pm 1003\mu\epsilon$. Note that populations of larger trees, and hence larger openings might reduce the measurement error.

From Table 5.3 the original-splitting test appears slightly more reproducible than the rapid version. Note that these values are indicators of precision/reproducibility not accuracy.

For breeding purposes, the accuracy is not of too much concern as the same individuals would be selected as long as it can be assumed that the mapping from the observed values and the real ones is sufficiently linear. Precision is of much higher importance as imprecise measurements will result in unreliable mappings to real values and hence rankings of genotypes will be unreliable.

The accuracy of the splitting tests needs to be considered in regards to the observed variation within breeding trials. Figure 5.4 visualises selecting the top 25% of individuals (filled red circles) from the rapid-splitting test data. A possible distribution of 'true' values (the real values were unknown) was created by adding values randomly sampled from a normal distribution characterised by a mean of 0 and a standard deviation of $513\ \mu\epsilon$ (calculated from the 95% prediction interval $\pm 1003\ \mu\epsilon$), as seen in Figure 5.5. Reordering these 'true' values from lowest to highest showed that some higher growth-strain individuals were included in the selection and some lower growth-strain individuals were missed because of the inaccuracies of the test (Figure 5.6).

These results suggested that using splitting tests on a breeding population similar to those presented in Table 5.1 or Chapter 4, have the potential to remove poor performing individuals as part of a non-intensive breeding selection. For example taking the top 25% of the population would have likely removed the bottom 20% in the next generation. However, the limited resolving power of the splitting tests precluded the ability to select the 'best' individual or top few percent of individuals. Current early selection programmes utilising these tests aim to remove the poorest performing individuals in order to reduce the expense of further more extensive breeding programmes. These tests may be suitable for this purpose; however, without further development, accurately ranking individuals for selection is problematic. Testing populations with significantly different means, variances or physical characteristics than were used here may be more or less successful. A useful

immediate application may be comparing mean differences between sufficiently different species for new breeding programmes, selecting species which will be the most likely to meet the goals of the programme. Selection within species by family or clone may be possible if there is sufficient variation between genotypes exists, however, unless the goal is to remove only the worst individuals, by selecting only the top individuals, significantly more variation between genotypes than found in Chapters 2, 4 and here would be needed. Further, the relationship between measured growth-strain at a young age and timber distortion during sawing at a commercial harvest age is unknown, Chapter 7 discusses this further.

5.4 Conclusion

The precision of the destructive growth-strain measurements obtained by the unrepeatable splitting tests were investigated from experimental data on small trees. The results showed that the rapid-splitting test has a 95% prediction interval of $\pm 1003\ \mu\epsilon$ within a population with a mean of $1807\ \mu\epsilon$ and a standard deviation of $662\ \mu\epsilon$. Splitting tests may potentially be suitable for use in early selection breeding programmes, where identifying the best individual is not of high concern, but rather the removal of the worst individuals to make future programmes more cost effective is. The splitting tests were shown not to be precise enough to be used for intensive selections of top individuals and may not predict timber distortion during sawing at older ages well.

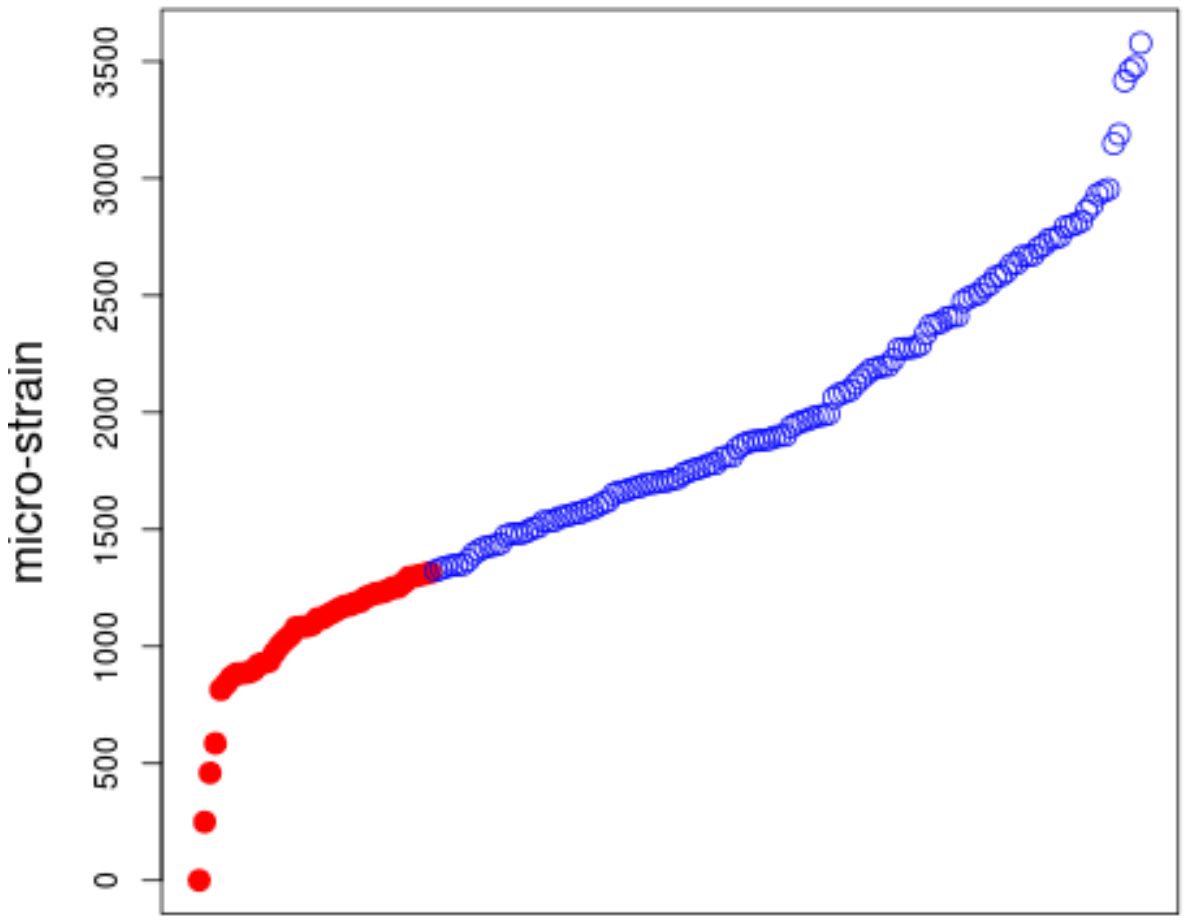

Figure 5.4: Ranked rapid-splitting test results for *E. argophloia* from lowest to highest, with the lowest 25% displayed as filled red circles.

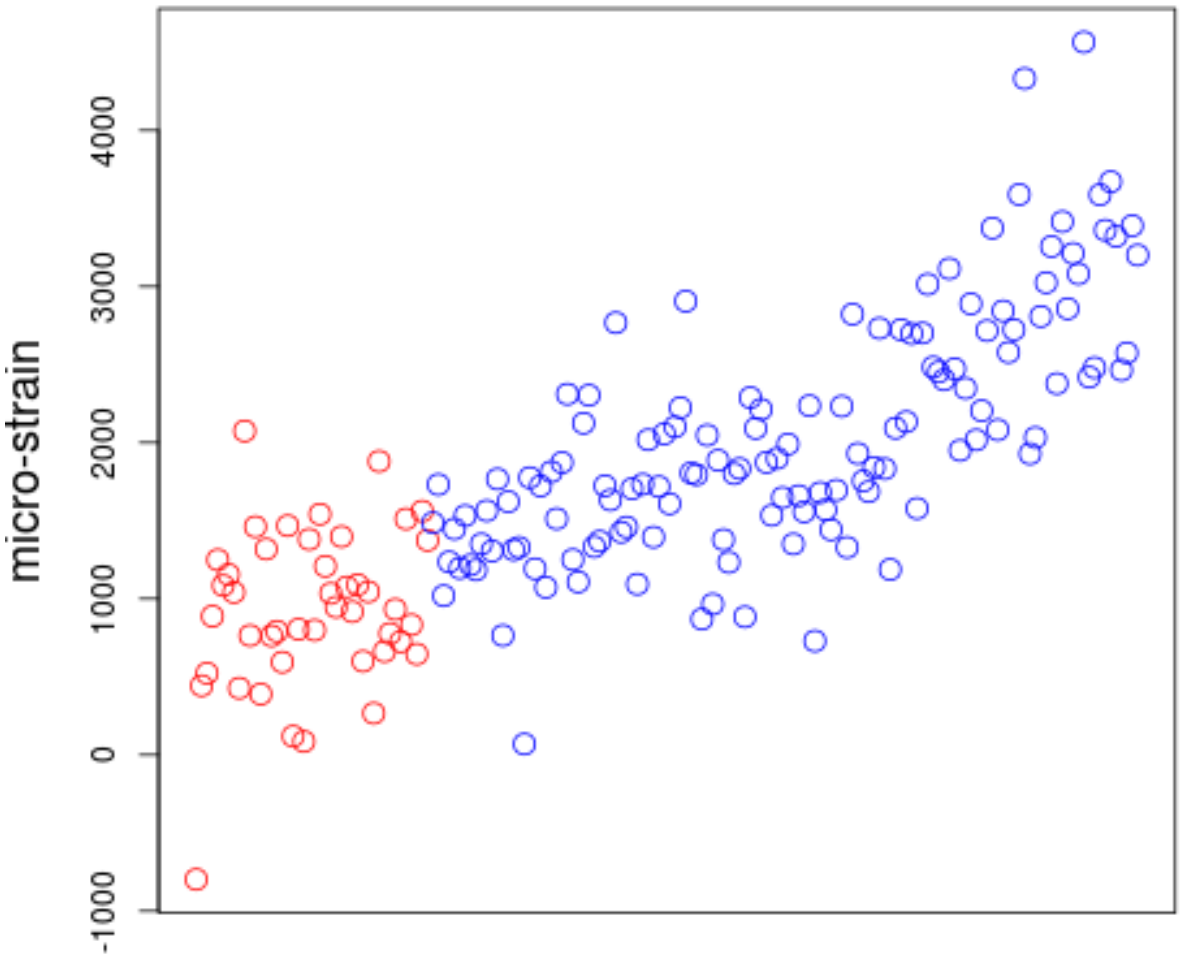

Figure 5.5: *E. argophloia* (order and colouring as in Figure 5.4 samples ranked for rapid-splitting test results after simulated testing error is included. Testing error was simulated by randomly sampling from a normal distribution with a mean of 0 $\mu\epsilon$ (both examples use the rapid-splitting test so there was no systematic error) and a standard deviation of 513 $\mu\epsilon$ (the random error from both the rapid-splitting test procedure and the rotational error, calculated as described in Section 5.3).

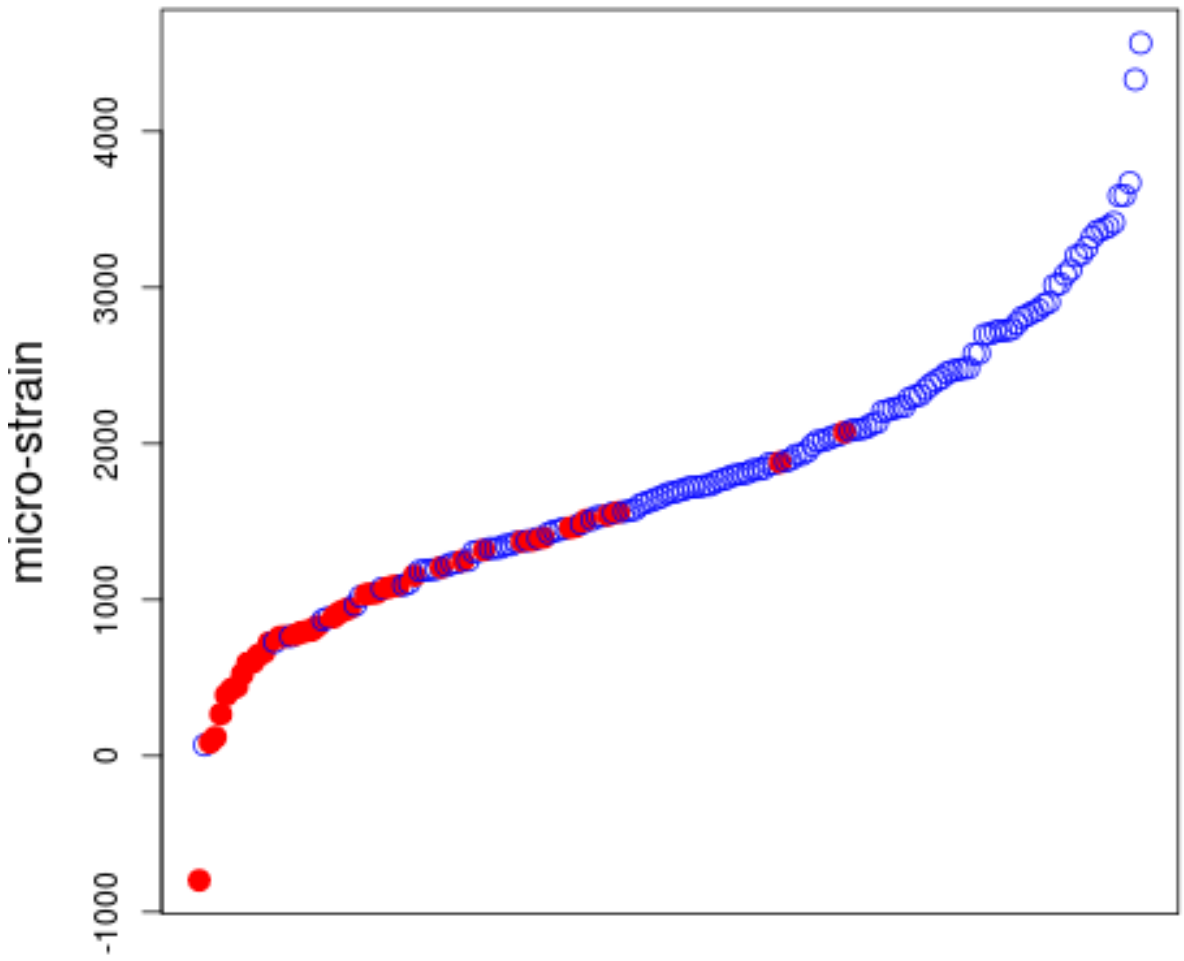

Figure 5.6: Reordered *E. argophloia* samples after the addition of simulated measurement error. The colouring from Figure 5.4 was retained, the top 25% of individuals in filled red circles.

Chapter 6

Theoretical investigation of the accuracy of growth-strain testing methods

Chapter Prologue

Chapter 5 presented an experimental determination of the precision of the splitting test, this chapter theoretically determines the accuracy of the splitting test and compares it to the experimental precision from Chapter 5. Further, the model was used to investigate the effect different surface stress fields have on the splitting test results, as well as on results from strain-gauges. The effect of the strain-gauge layout on predictability of the splitting test outcomes were investigated. Finally, conclusions were drawn regarding likely surface stress profile limitations.

6.1 Introduction

The characterisation of the stress field within stems is not well studied or understood. There is no known technology to directly, or indirectly, measure the surface or volume stress field with the degree of accuracy which would provide insight into the scale of local inhomogeneity. A reliable technology to investigate a stem's stress field would aid applied and theoretical understanding of growth-stresses. Hypothetical stress fields based on conservation of energy have been suggested and reviewed in Chapter 1.

Currently, testing technologies such as strain-gauges are limited to measuring surface strains with an unknown level of accuracy. The lack of non-destructive testing procedures for growth-stress makes repeated testing impossible. Most techniques use multiple measurements of surface strain around the stem, which are then averaged (Archer, 1987b; Kübler, 1987) to provide a single quantification of 'growth-strain'. However, the accuracy of any one of these testing procedures cannot be tested as measurement error and variation on the stem surface are confounded. The same problem exists for the splitting test (Chapter 5). Because other methods require repeated testing on each individual they are quite time consuming. The splitting test is the only growth-strain testing procedure fast enough to be used for tree breeding, so calculating its reliability is of practical importance.

In most previous modelling attempts, the growth-stress field has been assumed to be longitudinally axis-symmetric and follow similar curves to those presented by Gillis and Hsu (1979) and Archer (1987b). How reliable these curves are at estimating the internal stress field is unknown, and very difficult to quantify. On the surface, however, authors have used the assumption that growth-strain is constant around the periphery, either explicitly or by stating growth-strain values as averages. It is unclear if it is useful to quantify growth-strain as a mean surface strain, whether obtained through multiple surface tests

or through some geometric averaging as is implicit in the splitting tests. This is likely to be a problem specific determination, but in the instance of trying to identify timber which is unlikely to distort during sawing, whether that be developing in-line screening technology for mills or to assist breeders identifying favourable genotypes, it is problematic. It is uncertain how surface strains effect sawing stability, or even if an average value is a useful predictor of sawing stability.

6.2 Method

6.2.1 Simulating an individual sample

An orthotropic elastic mathematical model of a typical stem sample used for the splitting test in very-early selection was developed. This was used to investigate how differing surface stress profiles affect the reliability of the rapid-splitting test procedure and 'point' based procedures, such as strain-gauges or CIRAD (for more details see Section 1.5.1). The generated samples were truncated cones with a length of 400 mm, a small-end diameter of 34.8 mm and a big-end diameter of 39.55 mm. Orthotropic material was assumed and the required constants are in Table 6.1. The sample dimensions and assumed material properties were derived from various published and unpublished experiments, including those in this this thesis. E_l was obtained as an average over these experements, while the other eight properties were derived from E_l via ratios from Gonçalves et al. (2013), Davies (2014) and the need to retain model stability. The material properties derived from experiments exist in their native cylindrical coordinate system, which is typical in other experiments, such as Gonçalves et al. (2013). Transformation into a Cartesian coordinate system was required for some modelling functions. Davies (2014) describes this trans-

formation to convert the stiffness matrix from cylindrical to Cartesian coordinates at any point in the domain (in Section 3.2.3 using Voigt (engineering) notation).

To simulate the splitting test the software Salome (Ribes and Caremoli, 2007) and Netgen (Schberl, 1997) were used to create a mesh of 6436 vertices and 22506 cells to approximate the sample using tetrahedrons. A slit from the big-end through the pith, with a width of 0.9 mm and a length of 300 mm was added (Figure 6.1). A second mesh was created with the slit rotated 90 degrees about the longitudinal axis, but the sample was otherwise identical to the first.

Table 6.1: Orthotropic wood properties assumed for all individuals modelled. These properties are constant within and amongst stems.

Property	Value
E_l	$11.33\ GPa$
E_t	$1.74\ GPa$
E_r	$2.52\ GPa$
G_{tl}	$1.74\ GPa$
G_{lr}	$0.17\ GPa$
G_{rt}	$0.44\ GPa$
v_{tr}	0.36
v_{lr}	0.36
v_{lt}	0.56

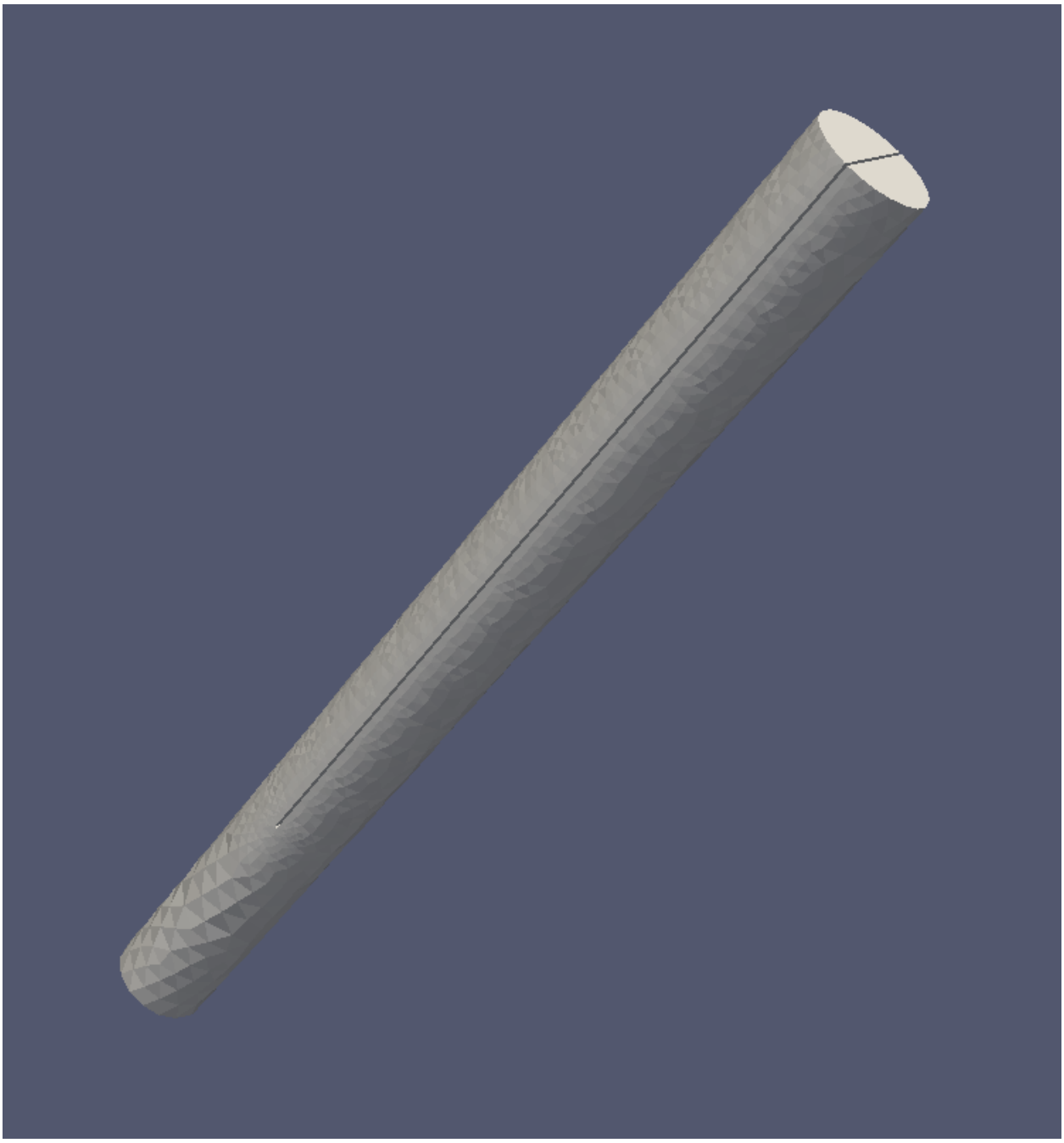

Figure 6.1: Example of a rapid-splitting test sample mesh

At every point the value of the surface stress changes, the non axis-symmetric surface stress is defined by Equation 6.1. The stress field between the pith and periphery is described by Equations 6.1 to 6.5. The maxima and minima of the surface stresses are assumed to be 90 degrees apart and their orientation with the splitting test cut plane, random. In experiments on straight stems it is not known where maxima/minima of the surface stress field are located and hence it can be reasonably assumed that the plane of the cut will be randomly aligned with respect to the surface stress pattern. Figure 6.2 shows some examples of surface strain values around the circumference of theoretical samples.

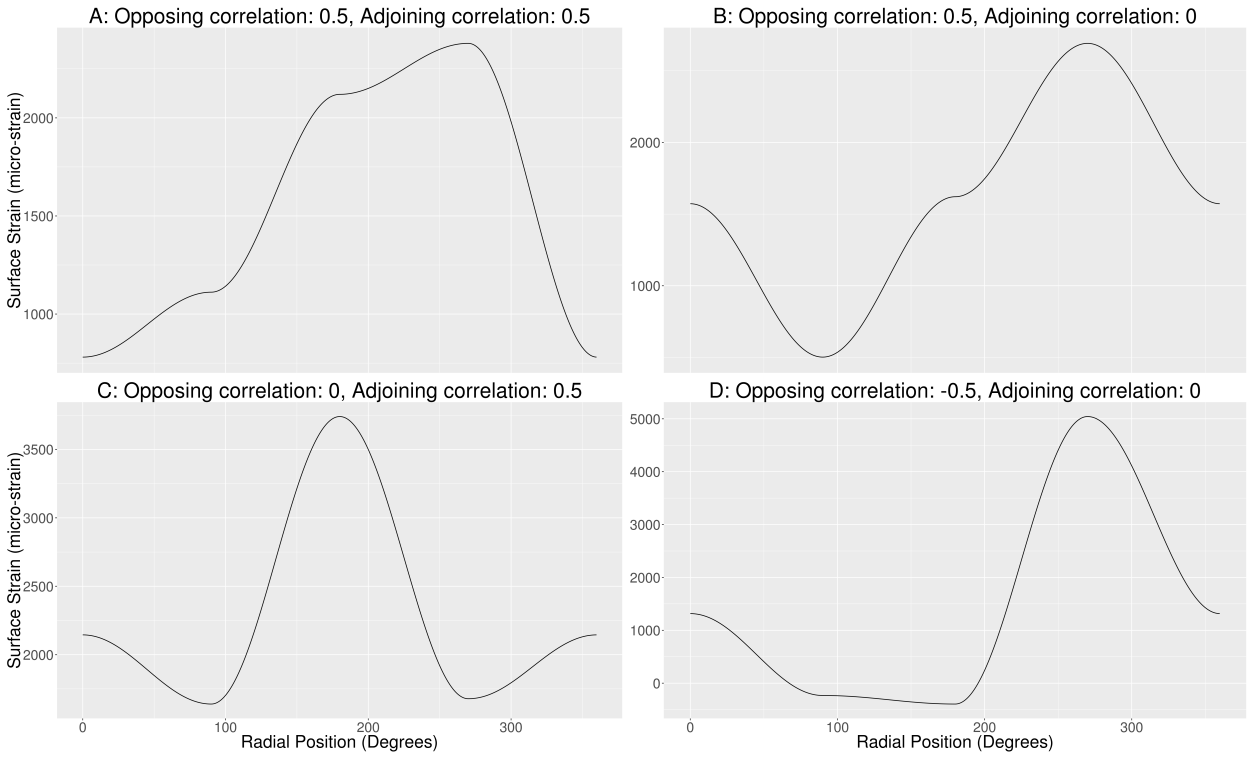

Figure 6.2: Examples of surface strain profiles

In the model, it was assumed that longitudinal stiffness and strain acted parallel to the vertical stem axis, i.e. there was no taper, spiral grain, knots, etc. stems (i.e. the pith of

all samples had the same 9 material constants that the periphery of all samples had). No external forces such as gravity were accounted for on the simulated samples. The only force acting on the samples was the internal stress field.

Equation 6.1 was used to calculate the surface stress σ_{local} for an angular coordinate θ. Where σ_{1-4} were defined in Section 6.2.2 and detailed within Equation 6.12 with visual examples in Figures 6.2 and 6.3.

$$\sigma_{local} = \begin{cases} \sigma_2 sin(\theta)^2 + \sigma_4 cos(\theta)^2, & \text{if } -\pi \leq \theta < -\frac{\pi}{2} \\ \sigma_2 sin(\theta)^2 + \sigma_3 cos(\theta)^2, & \text{if } -\frac{\pi}{2} \leq \theta < 0 \\ \sigma_1 sin(\theta)^2 + \sigma_4 cos(\theta)^2, & \text{if } 0 \leq \theta < \frac{\pi}{2} \\ \sigma_1 sin(\theta)^2 + \sigma_3 cos(\theta)^2, & \text{if } \frac{\pi}{2} \leq \theta < \pi \end{cases} \tag{6.1}$$

The growth-stress G_s at any point in the stem was calculated using Equation 2 in Entwistle et al. (2014) and relied on the caluclated surface stress σ_{local} from Equation 6.1 at the given cylindrical coordinate.

$$G_s = \sigma_{local}(1 + 2.125\ log\frac{r_v}{R_{max}}) \tag{6.2}$$

Because Equation 6.2 tends to infinity if radius alone is used, R_{core} is set to define the radius at which the elastic limit of the material is reached. The constant of 0.244 was taken from Entwistle et al. (2014).

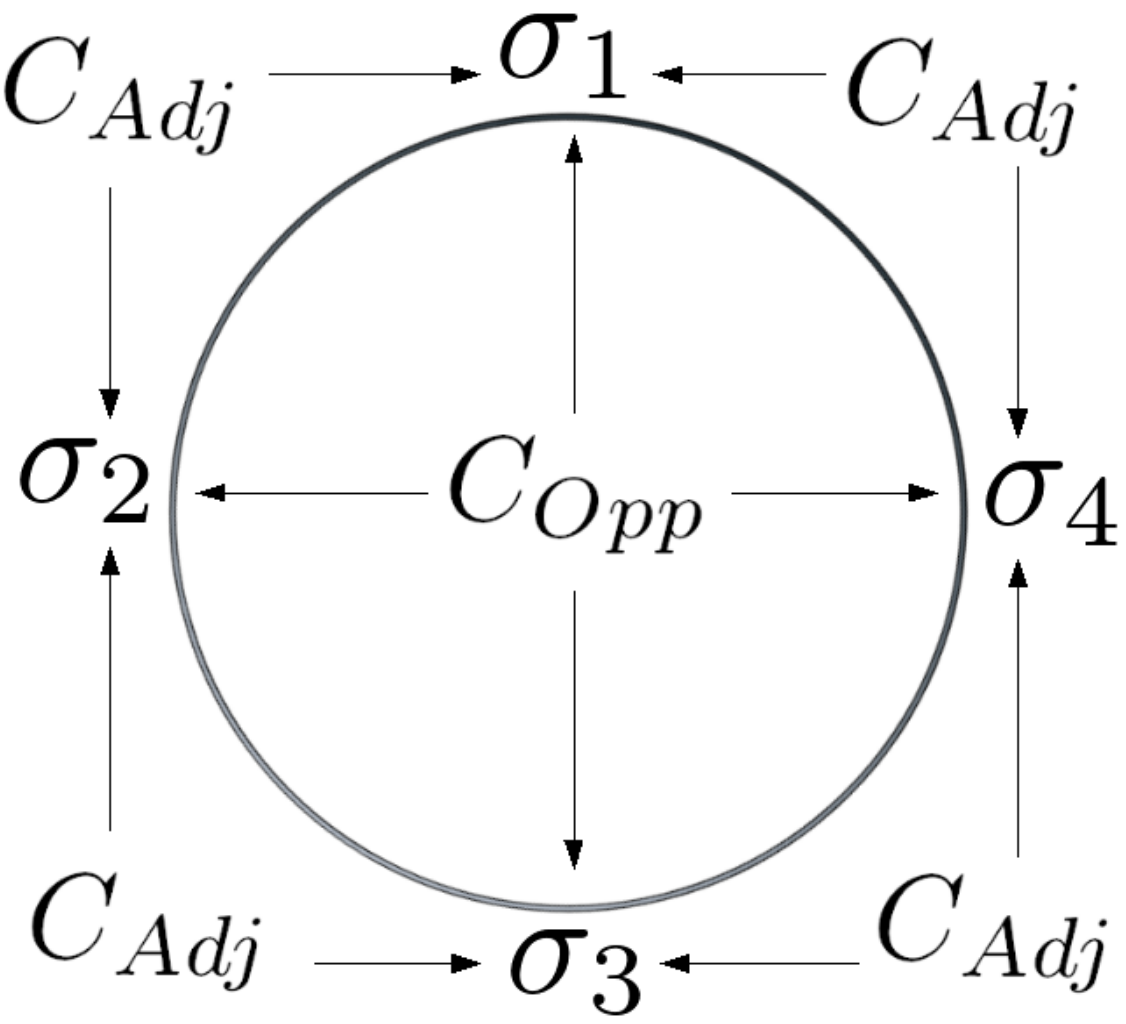

Figure 6.3: Image displaying how the described surface points, σ_{1-4} are related to the correlations, C_{Adj} and C_{Opp}.

$$R_{core} = 0.244 R_{max} \tag{6.3}$$

r is the cylindrical coordinate and r_v is a virtual radius used only for the growth-stress calculations to remove the theoretical discontinuity in the stress field which would otherwise occur when r approaches 0.

$$r_v = \begin{cases} R_{core}, & \text{if } r < R_{core} \\ r, & \text{otherwise} \end{cases} \tag{6.4}$$

Equation 6.2 is then inserted into a zero vector (Equation 6.5) which can be added into the stress calculation in Equation 6.7).

$$\boldsymbol{\sigma_{gs}} = \begin{bmatrix} 0 \\ 0 \\ G_s \\ 0 \\ 0 \\ 0 \end{bmatrix} \tag{6.5}$$

Strain ϵ can be calculated from the displacement vector $\boldsymbol{u}$ as follows

$$\boldsymbol{\epsilon} = \frac{1}{2}(\bigtriangledown \boldsymbol{u} + \bigtriangledown \boldsymbol{u}^T) \tag{6.6}$$

Converted to stress via the stiffness matrix $\boldsymbol{C}$

$$\boldsymbol{\sigma} = \boldsymbol{C}\boldsymbol{\epsilon} + \boldsymbol{\sigma_{gs}} \tag{6.7}$$

Strain energy density W can then be calculated

$$W = \frac{1}{2}\boldsymbol{\sigma}\boldsymbol{\epsilon} \tag{6.8}$$

and the total potential energy $\prod$ found over the whole domain $\boldsymbol{\Omega}$

$$\prod = \int_{\boldsymbol{\Omega}} W \, d\boldsymbol{\Omega} \tag{6.9}$$

The displacement field $\boldsymbol{u}$ can be calculated at the minimum potential energy by taking the directional derivative of $\prod$ with respect to the change in displacement u and setting it to zero.

$$F = \bigtriangledown_{\boldsymbol{u}} \prod(\boldsymbol{u}) = 0 \tag{6.10}$$

Subject to the Dirichlet boundary condition $\boldsymbol{\Omega_{bc}}$

$$\boldsymbol{u}|_{\boldsymbol{\Omega_{bc}}} = \begin{bmatrix} \\ 0 \\ \\ 0 \\ \\ 0 \\ \end{bmatrix} \tag{6.11}$$

$$\boldsymbol{\Omega_{bc}} = \{(x, y, z) \in \boldsymbol{\Omega} : z < 0.001\}$$

From the resulting deformed coordinate positions, the average displacement of the two halves at the inner edge on the big-end of the cut can be calculated. This is the digital equivalent of the opening measurement in the experimental version of the rapid-splitting test. The second mesh, with a cut perpendicular to the first was examined with an identical stress field to the first instance. The two openings provide theoretical results of two distinct tests of the same individual, without one test influencing the other.

6.2.2 Simulating populations

A population refers to one of 41 sets of 1000 simulated individual samples which have a simulated rapid-splitting test mean of $1513 \pm 20\ \mu\epsilon$ and a standard deviation of $630 \pm 5\ \mu\epsilon$. While these values are arbitrary they were chosen to approximate the values found over multiple experiments, some of which were presented in Chapters 4 and 5.

For the theoretical samples described in Section 6.2.1 to be created representing the individuals of the populations, the four input values in Equation 6.1 need to be defined. For each sample they are calculated from a multivariate normal distribution (Equation

6.12). The generation of the normal distribution takes the mean matrix which is constant for all samples regardless of their population, and the covariance matrix which is made up of a population specific input variance and two correlations.

Each of the four evenly spaced stress maxima/minima around the circumference of the sample are related by the adjacent (C_{Adj}) and opposite (C_{Opp}) correlations. Figure 6.3 visually shows the relationships between σ_1, σ_2, σ_3 and σ_4, and Figure 6.2 shows how the surface strain can very around a stem. The input variance is manipulated to give the output population a standard deviation of $630 \pm 5\ \mu\epsilon$.

In Equation 6.12 $16191994\ Pa$ is the mean input population stress equating to the required mean output strain of $1513 \pm 20\ \mu\epsilon$ and ς is the required input variance for a given population to have an output standard deviation of $630 \pm 5 \mu\epsilon$.

By systematically varying C_{Adj} and C_{Opp} (Equation 6.13) along with the population input variance the same descriptive output statistics (mean and standard deviation) can be produced, but the output populations may consist of very different individuals. Note that some populations are not producible statistically, C_{Adj} and C_{Opp} cannot, for example, both equal negative one, as no such statistical distribution can exist. For each individual, the surface stress profile, true mean stress, and two rapid-splitting test values were known, allowing for comparisons of how well different tests predict each other and the true mean value. The models were solved using the finite element solver FEniCS (Alnaes et al., 2015) and Scipy (Jones et al., 2001) (code available in Appendix D). Plotting and interpolation was conducted in R (R Core Team, 2017) using ggplot 2 (Auguie, 2017; Akima and Gebhardt, 2016; Wickham, 2016).

$$\begin{bmatrix} \\ \sigma_1 \\ \\ \sigma_2 \\ \\ \sigma_3 \\ \\ \sigma_4 \\ \\ \end{bmatrix} = \boldsymbol{\mathcal{N}}\left(\begin{bmatrix} \\ 16191994 \\ \\ 16191994 \\ \\ 16191994 \\ \\ 16191994 \\ \\ \end{bmatrix}, \begin{bmatrix} \varsigma & C_{Opp}\varsigma & C_{Adj}\varsigma & C_{Opp}\varsigma \\ C_{Opp}\varsigma & \varsigma & C_{Opp}\varsigma & C_{Adj}\varsigma \\ C_{Adj}\varsigma & C_{Opp}\varsigma & \varsigma & C_{Opp}\varsigma \\ C_{Opp}\varsigma & C_{Adj}\varsigma & C_{Opp}\varsigma & \varsigma \end{bmatrix} \right) \tag{6.12}$$

$$\boldsymbol{C_{Opp}} = \begin{bmatrix} -1 \\ -0.75 \\ -0.5 \\ -0.25 \\ 0 \\ 0.25 \\ 0.5 \\ 0.75 \\ 1 \end{bmatrix} \quad \text{and} \quad \boldsymbol{C_{Adj}} = \begin{bmatrix} -1 \\ -0.75 \\ -0.5 \\ -0.25 \\ 0 \\ 0.25 \\ 0.5 \\ 0.75 \\ 1 \end{bmatrix} \tag{6.13}$$

6.3 Results and Discussion

The results produced from the models presented in Section 6.2.2 where the surface stress is homogeneous (i.e. C_{Adj} and C_{Opp} are both one, the typical axis-symmetric assumption when dealing with growth-stress in a stem), required an input strain mean and standard deviation of 1429 and 597 $\mu\epsilon$ to produce an output population mean and standard deviation of 1520 and 629 $\mu\epsilon$. The differences indicated that either the testing procedure or the model

slightly overestimated surface strain from split opening. In the model both the predicted opening and the surface stress at any given point were known to machine precision, so it was assumed that there was no measurement error in either the opening or strain-gauge measurements. This was in contrast to experimental methods where measurement errors exist with an unknown magnitude (Chapter 5 attempted to quantify this error).

Figure 6.4A shows the relationship between the surface point relatedness and the input standard deviation required to produce the predefined output population standard deviation of $630 \pm 5\ \mu\epsilon$. Figure 6.4B shows the same information but presented as the ratio of input to output population strain standard deviation, i.e. the input strain is divided by $630\ \mu\epsilon$.

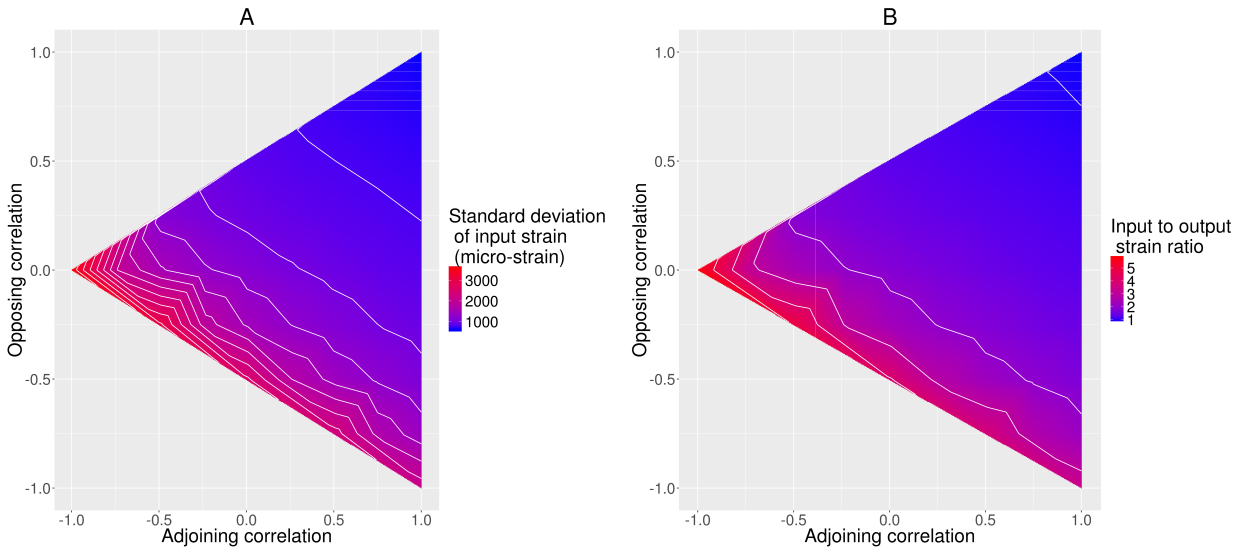

Figure 6.4: Strain standard deviation input (A) and strain standard deviation input to output ratio, where the output standard deviation is $630\ \mu\epsilon$ (B).

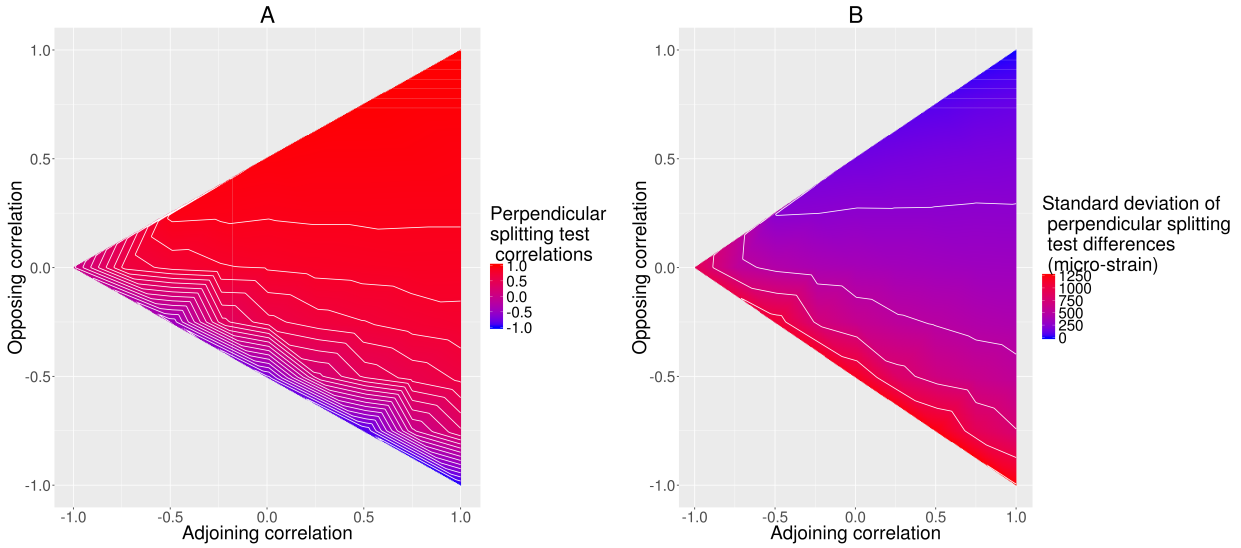

Figure 6.5: Correlation (A) and standard deviation (B) of the differences between perpendicular splitting tests. Contour lines are spaced 0.1 apart where the colour gradient represents a correlation (Sub-figure A) and 250 $\mu\epsilon$ where the colour gradient represents a standard deviation (Sub-figure B).

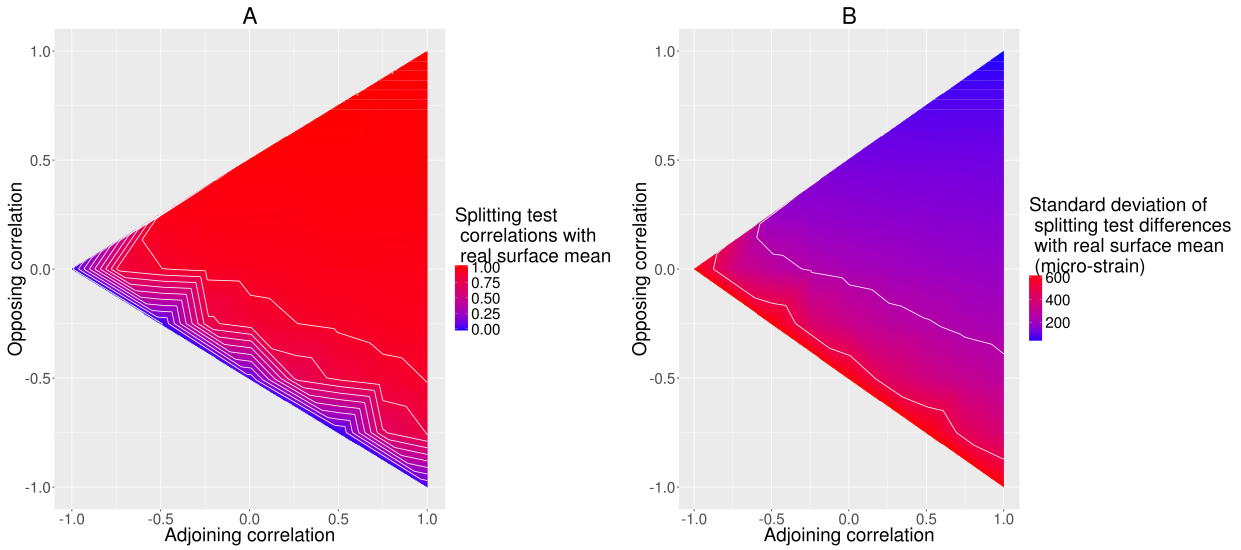

Figure 6.6: Correlation (A) and standard deviation (B) of the differences between the real surface strain mean and splitting test predictions. Contour lines are spaced 0.1 apart where the colour gradient represents a correlation (Sub-figure A) and 250 $\mu\epsilon$ where the colour gradient represents a standard deviation (Sub-figure B).

Investigating splitting test accuracy over different surface stress fields yields Figure 6.5, when comparing how well one splitting test result predicts the perpendicular result on the same sample. In contrast, Figure 6.6 shows how well the test predicts the input surface stress mean.

Chauhan and Entwistle (2010) used two strain-gauges placed parallel to the splitting test cut through the pith (Figure 6.7) and presented a correlation of 0.92 between predicted opening by the strain-gauge measurements and the opening. However, it has been shown that substantial differences in surface strain exist between points around the stem (Nicholson, 1971; Aggarwal and Chauhan, 2013) as was discussed in Chapter 5. The same test was conducted here (Figure 6.8). As was expected from the geometry of the testing procedure, the correlations were high. In contrast, Figure 6.6 shows how well the splitting test predicted the true surface strain, and Figure 6.9 shows how well two strain gauges placed 180 degrees apart predicted the mean surface strain. Note both the splitting test and two strain-gauge averages predicted each other better than the true strain mean.

More typically, 4 or 8 strain-gauges or CIRAD measurements are placed at equal spacing around a stem, Figures 6.10 through 6.12 show the relationship between the number of surface measurements around the stem and how well they predict the surface stress mean for various surface stress profiles.

When C_{Opp} and C_{Adj} are both equal to one, there is no variation of stress on the surface of the stem. Interestingly the input axis-symmetric surface strain of 1429 rises to 1520 $\mu\epsilon$ and the population standard deviation rises from 597 (surface) to 629 $\mu\epsilon$ (splitting test) indicating that the rapid-splitting test slightly over-predicted the real surface strain. These results suggested the rapid-splitting test will predict a surface strain approximately 5% higher than the true value (although this may be different depending on the magnitude of the strain). Note, that this value is insignificant compared to the errors discussed below.

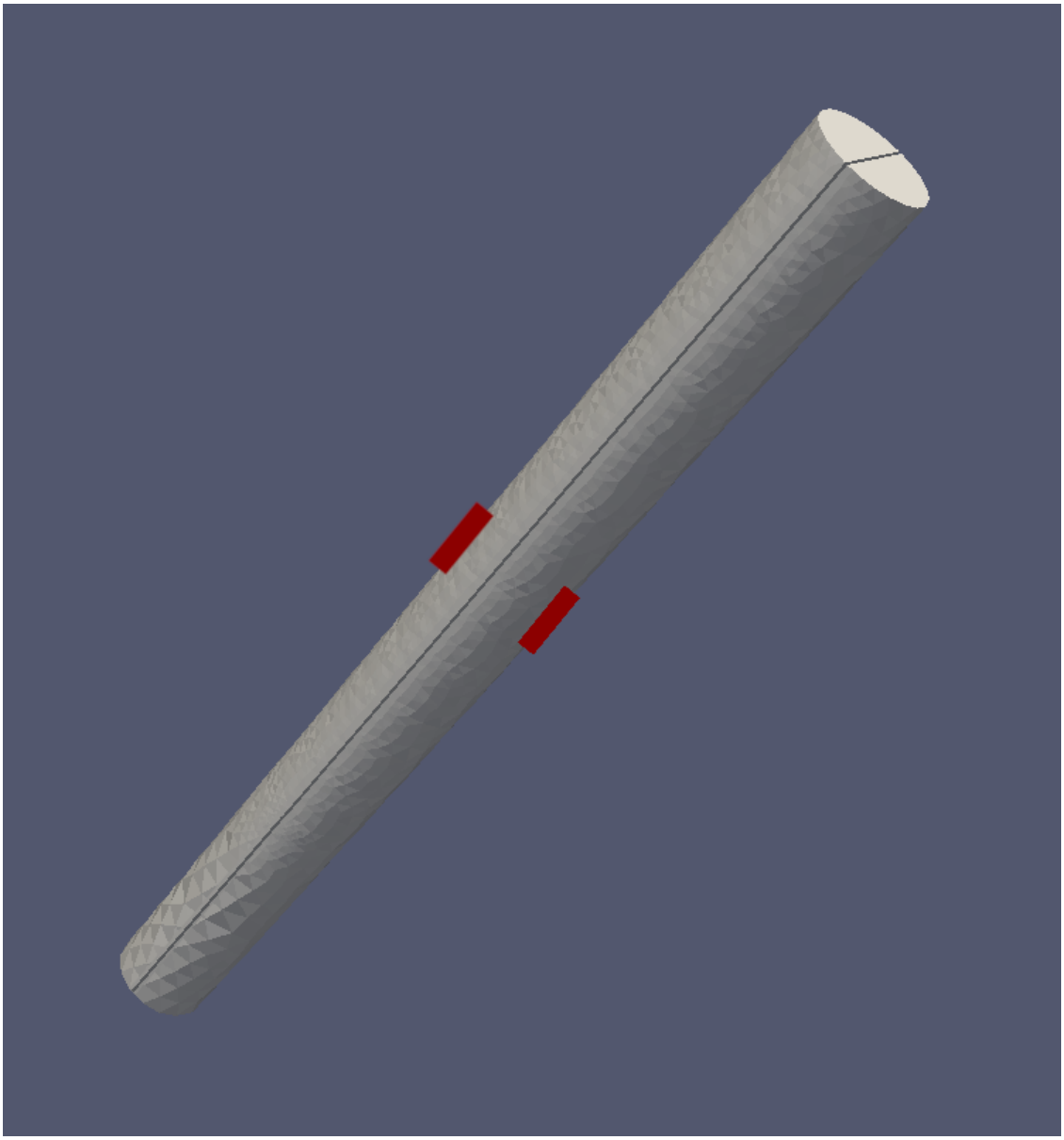

Figure 6.7: A graphical representation of the experimental setup in Chauhan and Entwistle (2010). The two strain-gauges are shown in red and the openings measured at each end.

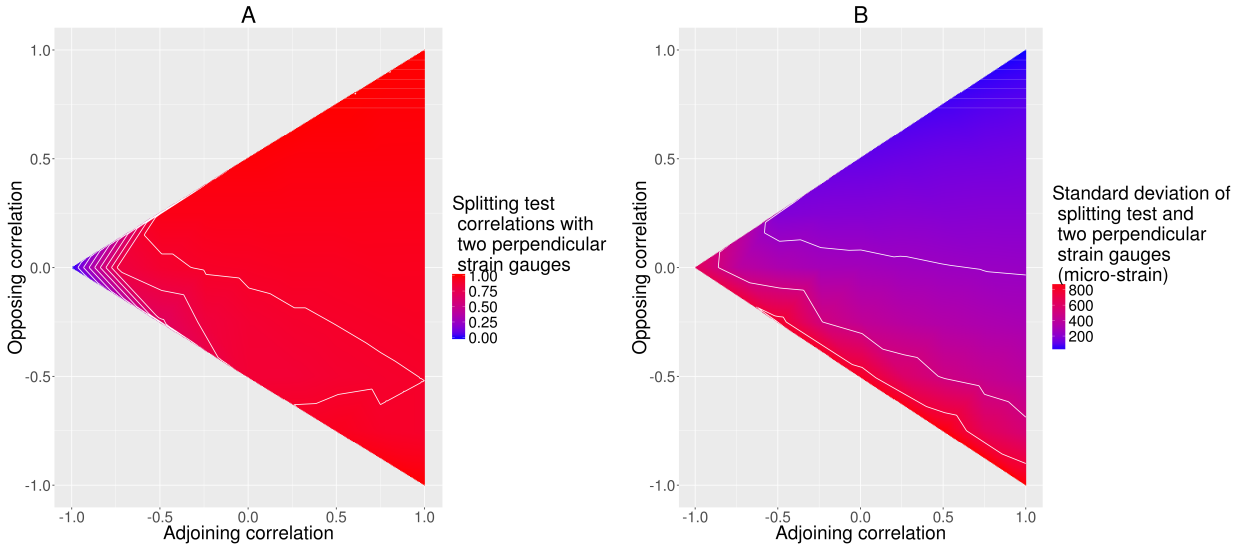

Figure 6.8: Correlation (A) and standard deviation (B) of the differences between the splitting test and the average of two strain-gauges placed as per Chauhan and Entwistle (2010). Contour lines are spaced 0.1 apart where the colour gradient represents a correlation (Sub-figure A) and 250 $\mu\epsilon$ where the colour gradient represents a standard deviation (Sub-figure B).

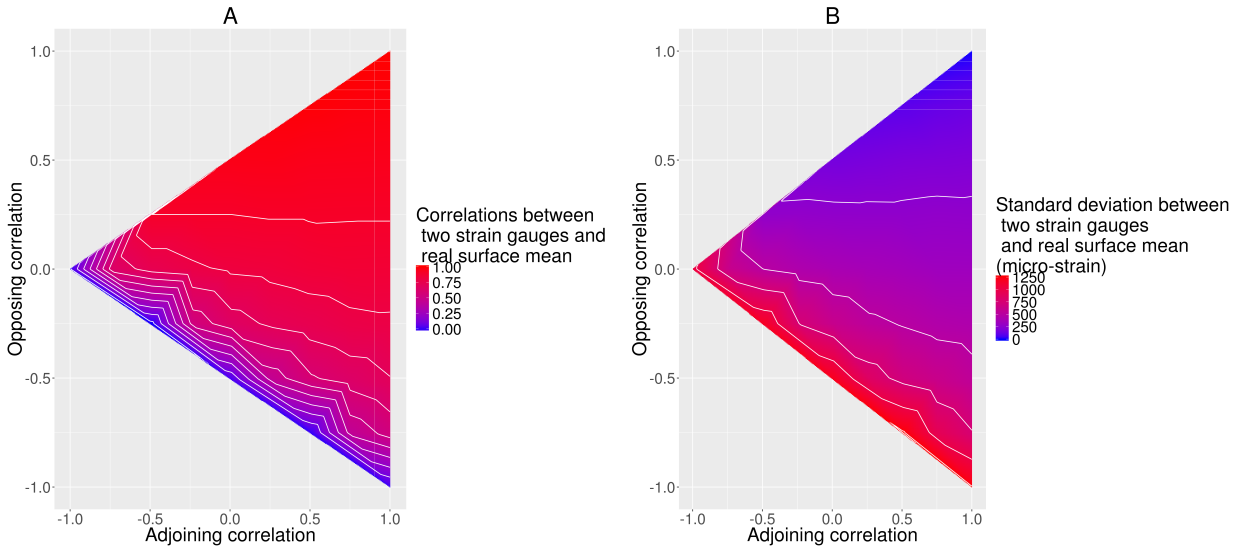

Figure 6.9: Correlation (A) and standard deviation (B) of the differences between the surface strain mean and the average of two strain-gauges placed 180 degrees apart. Contour lines are spaced 0.1 apart where the colour gradient represents a correlation (Sub-figure A) and 250 $\mu\epsilon$ where the colour gradient represents a standard deviation (Sub-figure B).

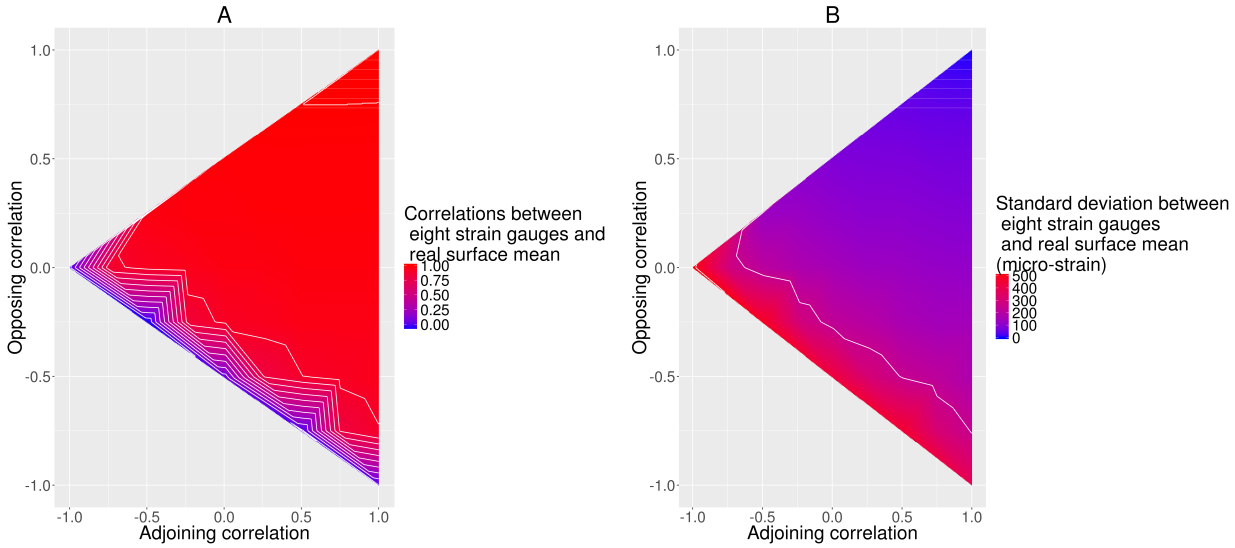

Figure 6.10: Correlation (A) and standard deviation (B) of the differences between the surface strain mean and the average of eight strain-gauges placed 45 degrees apart. Contour lines are spaced 0.1 apart where the colour gradient represents a correlation (Sub-figure A) and 250 $\mu\epsilon$ where the colour gradient represents a standard deviation (Sub-figure B).

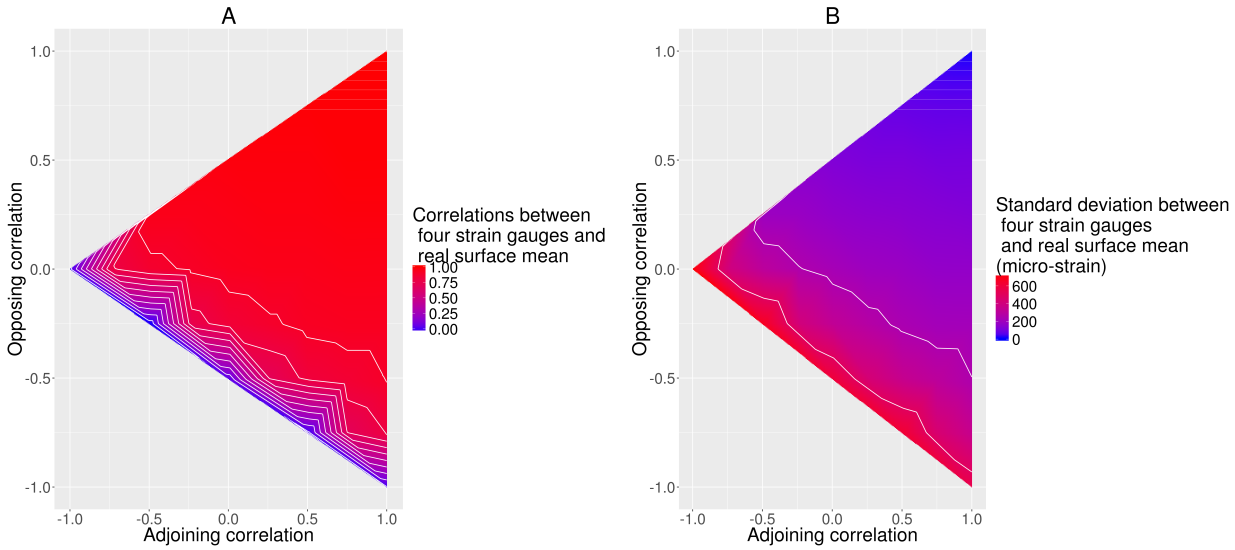

Figure 6.11: Correlation (A) and standard deviation (B) of the differences between the surface strain mean and the average of four strain-gauges placed 90 degrees apart. Contour lines are spaced 0.1 apart where the colour gradient represents a correlation (Sub-figure A) and 250 $\mu\epsilon$ where the colour gradient represents a standard deviation (Sub-figure B).

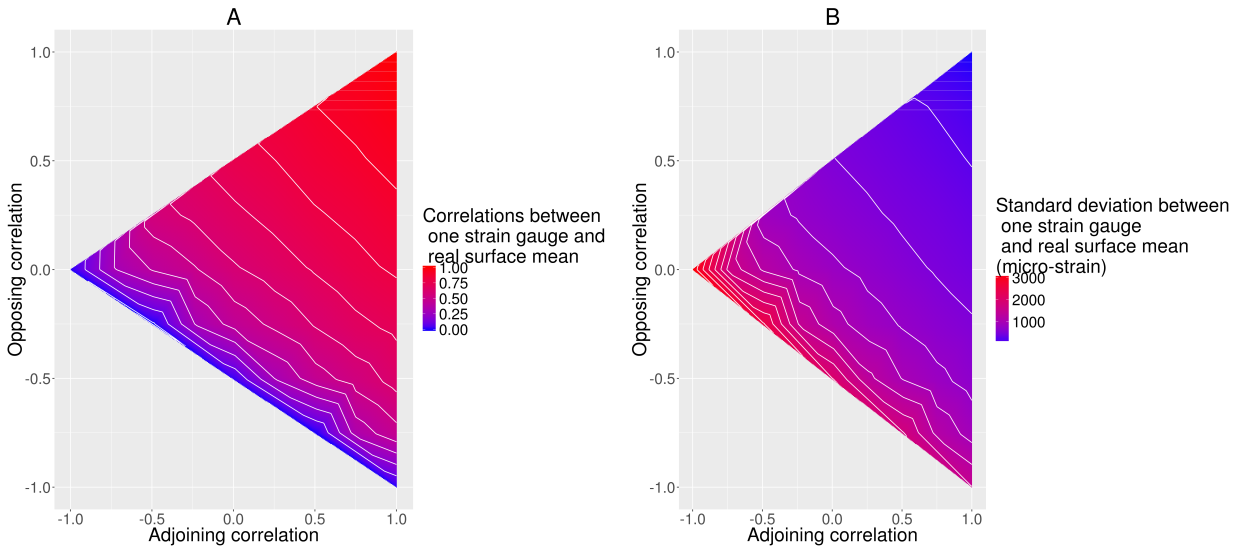

Figure 6.12: Correlation (A) and standard deviation (B) of the differences between the surface strain mean and a single randomly paced strain-gauge. Contour lines are spaced 0.1 apart where the colour gradient represents a correlation (Sub-figure A) and 250 $\mu\epsilon$ where the colour gradient represents a standard deviation (Sub-figure B).

It can be seen in Figure 6.4 that as the correlation between surface points reduces and becomes negative, the required input strain standard deviation increases to provide the same output population statistics. This provided context for how much surface variation must exist for given surface point relationships to obtain a typical output population. The 1:1 contour in Figure 6.4B (the top contour) is where the input strain is equal to the output population strain. The 2:1 contour is where the standard deviation of the input strain was required to be twice that of the output population strain. This occurs because when the surface strain is constant on any given individual, the entire population input strain variation manifests as between tree variation in the output. If there is significant within-tree variation it does not all manifest as between-tree variation in the final population.

Chapter 5 outlined an experimental procedure for estimating the precision of the the splitting test and the magnitude of change in surface strain, associated with the arbitrary angle of the cut during the splitting test. Experimentally, the correlation between the two quar-

tering tests (0.89) and the estimated standard deviation of the difference distribution of $300\ \mu\epsilon$ were obtained (Tables 5.2 and 5.3). These two values were traced as contours on Figure 6.5A and B and rounded to get a window where likely populations would be inside. The experimental results suggested C_{Opp} is greater than 0 and C_{Adj} is greater than -0.5. Repeating Chauhan and Entwistle (2010) within the theoretical framework (Figure 6.8), a similar (although slightly larger) C_{Opp} and C_{Adj} window could have been used, found by tracing the correlation contour of 0.92 as the relationship between predicted and measured opening.

Following from here, two population sets will be referred to, the *full population set* consisting of all of the populations used to make the above figures, and the *limited population set*, which exists inside the lower bounds suggested by the experimental work in Chapter 5. It is worth noting that Nicholson (1971) provided a clear visual representation of the variation of surface strain on some Eucalyptus stems. However their sample size was too small to draw reliable quantitative conclusions.

When splitting test results were compared, most populations produced a moderate to high correlation between perpendicular tests (Figure 6.13, mean correlation of 0.59). The correlations were markedly improved in the limited population set (Figure 6.13, mean correlation of 0.91). However, the differences between the two tests were large enough that identifying or ranking individuals accurately is problematic as the mean difference standard deviation is $473\ \mu\epsilon$ over all populations and $244\ \mu\epsilon$ over the limited population set. If instead the comparison is made between splitting test results and the true surface strain mean, (Figure 6.14) there is substantial movement toward the higher end of strain correlations for both population sets. Again however, the mean difference standard deviations of $262\ \mu\epsilon$ and $143\ \mu\epsilon$ for the full and limited population sets are large enough that accurately identifying individuals is problematic. This can also be seen by comparing Figure Fig-

ure 6.5 and 6.6 where the standard deviation of the difference distribution approximately halves for all populations, along with the correlation between splitting test and true surface strain correlations approximately doubling.

Chauhan and Entwistle (2010) introduced the splitting test for surface growth-strain prediction. One of the experiments they performed involved placing two strain-gauges parallel to the splitting test cut (Figure 6.7). Here this experiment was modelled over the various populations. Figure 6.8 shows a high correlation (0.90 and 0.96) and low difference distribution standard deviation (339 $\mu\epsilon$ and 178 $\mu\epsilon$) between the two strain-gauges and the splitting test, as is expected given the experimental design. However, the mean correlation between the average of two strain-gauges with the real surface strain (Figure 6.9), is significantly lower (0.71 and 0.90) with larger difference distribution standard deviations 492 $\mu\epsilon$ and 258 $\mu\epsilon$.

The more evenly spaced the strain-gauges were placed on the surface of a sample, the more accurately the averaged values predicted the surface strain mean (Figures 6.9 to 6.12). The splitting test and four strain-gauges provided comparable results when predicting the surface mean (Figures 6.6 and 6.11 respectively). The splitting test produced a mean standard deviation of 262 $\mu\epsilon$ and the four strain-gauges of 260 $\mu\epsilon$ in the full populations set and 143 $\mu\epsilon$ and 142 $\mu\epsilon$ in the limited set, while using eight strain-gauges reduced this to 184 $\mu\epsilon$ and 100 $\mu\epsilon$ respectively.

The results for the full and limited population sets are presented in Table 6.2 with maximum, minimum and mean values. Of particular interest is the splitting test standard deviation of the difference between two splitting tests performed on the same sample. Using the limited population set this is 244 $\mu\epsilon$, which equates to a 95% confidence interval

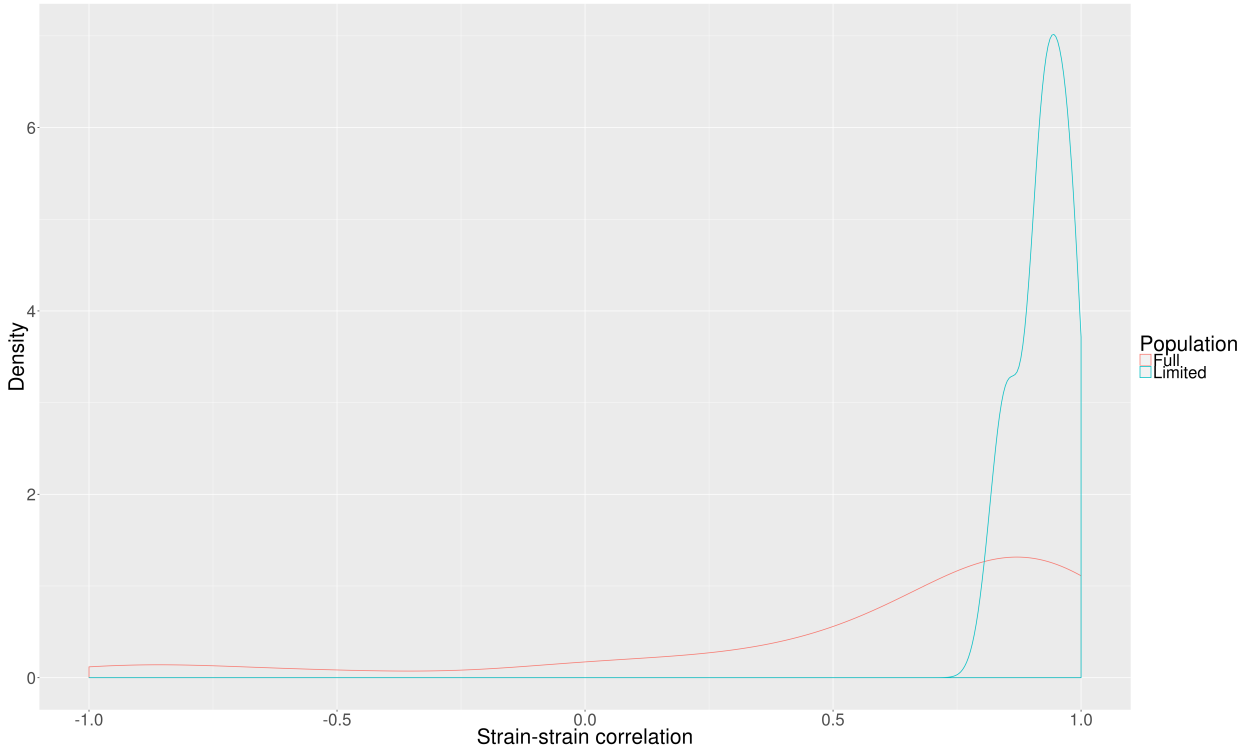

Figure 6.13: Density distribution of the correlations between perpendicular splitting test measurements for the two population sets

of $478\ \mu\epsilon$. This is lower than the $587\ \mu\epsilon$ found using the experimental method in Chapter 5, indicating that some of the populations with fairly consistent surface strains were over represented compared to the experimental data (Chapter 5), or that the experimental data was incorrectly specifying some measurement error as rotational error. The 95% confidence interval of the prediction of the surface strain mean from the rapid-splitting test was $\pm\ 281\ \mu\epsilon$. Any experimentation is likely to be less accurate. Given the limited population set requires a mean standard deviation input surface strain of $878\ \mu\epsilon$ to produce an output population with a standard deviation of $630\ \mu\epsilon$ the within- and between-stems stress variances are partitioned approximately in half, i.e. the standard deviation within a stem $(611\ \mu\epsilon)$ is approximately equal to the standard deviation between stems $(630\ \mu\epsilon)$. However, the within stem variation was probably higher as judged from experimental work (Chapter 5).

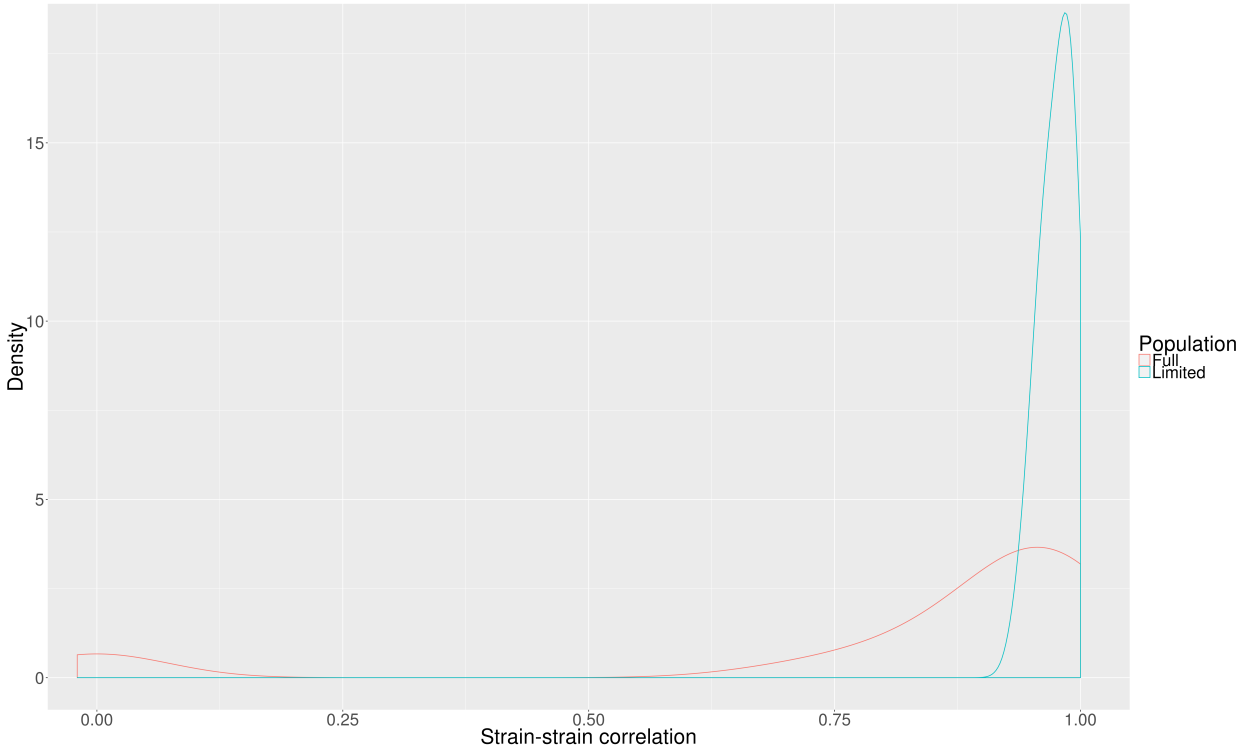

Figure 6.14: Density distribution of the correlations between the real mean surface strain and splitting test measurements for the two population sets

6.4 Conclusion

A computational model was developed to investigate how variation of surface growth-stress effects results of the splitting test and the mean values of various numbers of strain-gauges. By modelling multiple populations with differing stress relationships around the stem surface and comparing the results to experimental work, bounds were estimated for the relatedness of surface stress points. The repeatability of the splitting test rotated around the stem axis was investigated producing a similar result to Chapter 5. The 95% confidence of a splitting test result predicting the mean surface strain of a sample was estimated to be $\pm$ 281 $\mu\epsilon$. It was concluded that the rapid-splitting test provides a similar accuracy in predicting mean surface strain as using four evenly spaced strain-gauges.

Table 6.2: Full and limited population set statistics for the various testing procedures investigated.

Population	Full			Limited		
	Mean	Minimum	Maximum	Mean	Minimum	Maximum
Mean strain input ($\mu\epsilon$)	1435	1417	1449	1439	1423	1449
Standard deviation strain input ($\mu\epsilon$)	1271	597	3680	878	597	1527
Perpendicular splitting test difference SD ($\mu\epsilon$)	473	0	1263	244	0	455
Perpendicular splitting test correlations	0.59	-1.00	1.00	0.91	0.74	1.00
Splitting test difference SD with real value ($\mu\epsilon$)	262	32	634	143	32	279
Splitting test correlation with real value	0.81	-0.02	1.00	0.97	0.90	1.00
Entwistle method difference SD ($\mu\epsilon$)	339	32	896	178	32	322
Entwistle method correlation	0.90	-0.01	1.00	0.96	0.88	1.00
Single strain-gauge difference SD ($\mu\epsilon$)	862	0	3181	501	0	1208
Single strain-gauge correlation	0.58	-0.01	1.00	0.76	0.41	1.00
Two strain-gauges difference SD ($\mu\epsilon$)	492	0	1265	258	0	497
Two strain-gauges correlation	0.71	-0.03	1.00	0.90	0.74	1.00
Four strain-gauges difference SD ($\mu\epsilon$)	260	0	729	142	0	302
Four strain-gauges correlation	0.80	-0.05	1.00	0.97	0.88	1.00
Eight strain-gauges difference SD ($\mu\epsilon$)	185	0	520	101	0	211
Eight strain-gauges correlation	0.84	-0.07	1.00	0.98	0.93	1.00

Chapter 7

A critical review of very-early selection protocols in tree breeding

Chapter Prologue

A reccurring theme throughout the previous chapters has been gaining results without knowledge of accuracy. While the chapters have been presented as investigations into the characterisation of *Eucalyptus bosistoana* properties and the accuracy of the splitting test, the underlying reason for the work was to develop a commercially viable breeding population of *Eucalyptus bosistoana* (presented in Chapter 4). What made this breeding trial unique was that, in an attempt to lower the financial (and time) investment, selections were conducted before two years of age. An in-depth discussion on the suitability of this breeding paradigm, separated by breeding trait, is presented in this Chapter. Recommendations regarding suitable features traits need to possess in order for this paradigm to be considered are provided, along with a brief reiteration of what successful breeding programmes require in general.

7.1 Introduction

Breeding of crops to maximise particular attributes is something humanity has done for generations (Kingsbury, 2009). Examples such as corn and tomatoes are now very different from their wild ancestors. However, in forest trees used for wood products much smaller changes have been made. One of the reasons for the slower advance is the comparatively long breeding cycle. In order to make significant advances in the manipulation of properties of forest trees to maximise their benefits for human use, breeding cycle time needs to be reduced.

Two problems which need to be solved in order to reduce the breeding cycle are, propagation before individuals reach their reproductive age, and reliable selection of individuals for desired properties early in their lifespan. The propagation problem is not of concern here and can be solved through various techniques such as micro-propagation; for background information see Baker (1992) and Watt et al. (2003). The problem of predicting future attributes from very young trees has seen some attention over the last decade, and for convenience this will be referred to as the early selection problem. In essence, trees change a number of properties during their life time as their interaction with the environment evolves, known as ontogenetic change (Dlouh et al., 2013; Meinzer et al., 2011; Burdon et al., 2004). Properties which exist at young ages will not necessarily exist at older ages and vice-versa. Wood formed at a young age is preserved during growth and its properties still exist near the pith if the wood doesn't degrade or get damaged later in life through processes such as creep (from internal stress) or rot (from biological invasion).

There are numerous attributes tree breeders want to select for, including: growth, health, form, durability, density, stiffness, growth-strain and volumetric shrinkage. These can be

broadly separated into two categories: maximisation/minimisation selection and threshold selection. For example, growth is usually maximised, while if form reaches a specific threshold it is considered good enough, and no further breeding is needed. Assuming the payment thresholds in the market do not change there is no value in improving the trait past a given point.

There is an important distinction to be made between maximisation and threshold selection when coupled with tree physiology, as trees present general patterns with some wood properties (such as MFA) which rarely reverse with age (Meinzer et al., 2011). While form is a threshold problem at rotation age, some traits may be a threshold problem at much younger ages due to tree physiology. Threshold selection can be coupled with very-early selection for a trait when that trait is governed by physiological characteristics which follow a known trajectory in a direction that once the threshold is achieved, it will not be reversed. An example is stiffness in *Pinus radiata*, where MFA is known to decrease and density increase with age (Xu and Walker, 2004), resulting in stiffness increasing with age (Sharma et al., 2015). Because a premium is paid once a predefined stiffness is reached it is a threshold problem where once the threshold is reached all later growth can (reasonably) be assumed to be over the threshold. Form on the other hand, while a threshold problem, is not known to strictly become better with time, i.e. meeting a threshold early in life is not a guarantee the threshold will be achieved at full rotation age.

A major problem with very-early selection was discussed in detail by Apiolaza (2009), essentially he argued that even with a high year to year autoregressive correlation for a trait, a 15 year lag between measurement and harvest results in a very low association between selection criterion and objective trait value. A consequence of this argument is that very-early selection cannot be reliably used for maximisation/minimisation selections, e.g. selecting large diameter individuals from a population at age two will not reliably

produce a selected population which is larger than the parent population average at age 20. Apiolaza (2009) pointed out that very-early selection is usable only when the aim is to reach a non-reversible threshold, i.e. a screening problem. The example given was stiffness where he argued that because it is known stiffness (typically) does not decrease with age (Meinzer et al., 2011), and grading of stiffness is a threshold problem, it is advantageous to get wood to the threshold as early in life as possible. Once the threshold is met further gains do not increase value, and there is strong physiological evidence to show that the trait value will not dip back below the threshold later in growth. Myszewski et al. (2004) found non-significant genetic correlations between rings 4-5 and 19-20 for MFA (and therefore likely stiffness and growth-strain as MFA is thought to be a significant factor in both cases) and Dungey et al. (2006) found a reducing correlation as rings were separated for both MFA and stiffness. Donaldson and Burdon (1995) stated *"Corewood microfibril angles appear to be independent of outerwood values in the same tree or clone, so that low corewood angles do not necessarily mean correspondingly low outerwood angles within a clone."* As a hypothetical example; two trees reach a threshold stiffness at age 5 of 2 GPa, and one has a stiffness of 3 GPa at age 10 and the other has a stiffness of 9 GPa at age 10. Both trees met the threshold stiffness at the same time so are worth the same amount, but the correlation between stiffness at age 5 and age 10 is non-existent. For a review of these and other similar studies see Wu et al. (2008).

Currently no trials have been set up specifically to investigate Genotype by Environment interaction (GxE) with very-early selection methods. As a result, little is known about how early selection methods will perform outside of the trial environment in which they were selected, even if only considering properties at the age of selection. GxE is an important factor in breeding programmes, as properties differ from one environment to the next, and the level of genetic control independent of the environment needs to be quantified in order to make a good selection. GxE tends to be lower for wood properties than for

growth traits, for a review see Li et al. (2017). To ensure the appropriate genotypes are matched to the environmental conditions of the desired commercial site, GxE needs to be quantified and used during the decision making processes (White et al., 2007). In the future, investigating how reliably GxE interactions can be predicted at young ages should be a high research priority. Even at older ages, large numbers of trials are needed to accurately separate genetic and environmental effects. Dieters et al. (1995) investigated stem volume from 171 tests of slash pine consisting of over 2,100 full sibling families from 170,000 individuals. They found heritabilities taken from one or a small number of sites can produce almost any heritability between 0 and 0.5. Unbiased heritabilities (heritabilities taking into account GxE effects) ranged from 0.072 to 0.12 depending on age, showing the importance of having large GxE trials and ensuring appropriate age distributions (Dieters et al., 1995). Cullis et al. (2014) investigated 315,581 *Pinus radiata* trees spread over 77 trials in New Zealand and Australia and found substantial additive GxE effects for diameter. Cullis et al. (2014) warned that alternative approaches based on sub-setting trials or genotypes would fail to capture the extent of the interaction. Without significant GxE investigation, genetic parameters can be misleading. Further, along with expressing concern about differing genes being responsible for growth at different ages, Hodge and White (1992) suggested large site index differences between progeny test sites and commercial production land will decrease the reliability of progeny test data in predicting breeding values.

Caution needs to be taken when breeding for traits in trees in general, as without appropriate scrutiny unintended traits may be selected for as a by-product of a legitimate selection due to unfavourable correlations between traits. Wu et al. (2008) suggested a possible solution was to use economic breeding objectives, or preferably breeding out the unfavourable correlations, assuming the unfavourable correlations were known. Unfortunately, this may not always be possible due to the underlying mechanisms.

Targeting particular traits at very young ages may result in unforeseen problems associated with the selection later in their life. For example, breeding stiff trees at very young ages may result in increased mortality from wind throw and animal damage, as the ability to bend in a young stem has been suggested to be a trait which has evolved due to the low second moment of area in the stem (Davies, 2014; Meinzer et al., 2011). By reducing the ability for a small stem to bend, it will be more likely to break or topple in strong wind events or when animals push it over. Another example may be the development of above-ground (stem) growth at the expense of root system development, potentially resulting in increased uprooting during severe wind events. Unfortunately, breeding trial failures due to wind are rarely reported in the literature, and therefore quantifying them is difficult. There is further potential for problems such as these to develop with very-early selection protocols, as unfavourable interactions may also exist between ages as well as traits. Without running both, very-early selection and full length breeding trials in parallel over different environments with the same genetics it will be very difficult to identify negative traits developing as a result of very-early selection.

Dungey et al. (2006) conducted a detailed study of age-age genetic correlations in radiata pine at sites in Australia and New Zealand, concluding that the earliest selection for (whole core) density could be conducted at ring 5 and MFA at ring 8, assuming one was concerned with predictive ability of the measurement for later growth. Similarly Wu et al. (2007) found reasonable selection efficiencies could be obtained between ages 4 and 15 depending on the site and trait. These findings further add to the complexity of selection at early ages as selection efficiency appears to vary markedly across environments for a given age.

As Apiolaza (2009) alluded to, in order for very-early selection to be profitable a switch in thinking is needed to the screening/selection to be only for wood produced early in the

trees lifespan (corewood). Extrapolating that information to older (outer) wood properties can only be done when there is sound physiological reason.

Various wood property traits are addressed in this chapter individually. The appropriateness of very-early selection (arbitrarily defined here as selection at less than 20% of their commercial rotation age or a greater than 10 year lag between selection age and commercial harvest age) is discussed with reference to literature, unpublished pilot trials and thought experiments. Where possible, causes for (un)suitability will be linked to physiological understanding, or lack thereof, and suggestions will be made for future research needs to increase the effectiveness of the tools used.

It should be noted, this chapter does not include selection via genomic data. As technology improves and becomes cheaper, it will become possible to identify genetic markers associated with high performance. At the same time, genomic models need phenotypic information to be developed. Once appropriate technology has been developed these markers could be used to identify individuals at very young ages once calibrated at rotation age (White et al., 2007).

7.2 Growth

Growth, height, diameter and volume are discussed together as they are intertwined. Diameter is often used to predict height and volume is estimated from the two using a taper function. These all fall into a maximisation-class breeding problem; volume is maximised at rotation age. Because growth can be measured non-destructively, research has been conducted investigating the ability to predict a tree's future growth performance at differing ages, and verified on the same tree later in time. Dieters et al. (1995) investigated genetic correlations between volume measurements at differing ages and found the correlations

to vary between 0.56 and 0.97 for lag times of between 3 and 9 years, with young trees showing poorer correlations than older trees even when the lag time was the same. Others have found similar results (Mihai and Mirancea, 2016; Greaves et al., 1997; Stackpole et al., 2009; Osorio et al., 2003).

There is an argument for very-early phenotypic selection of growth and mortality which states something akin to “nurseries pick the top performing individuals at the age of a few weeks; therefore, it stands to reason that the same could be applied at any age” (Walker, 2018). However, nurseries are picking individuals which are the most likely to survive the process of transplanting from the nursery bed to the forest, which requires a much shorter prediction time frame, a few weeks, not decades, as the trees either survive transplant or die during transplant. Physiologically larger individuals likely have more nutrient storage, more developed root systems, and larger canopies, giving them a competitive advantage over smaller individuals in a transplanted situation where they must re-establish and compete with other plants for resources. Lopez et al. (2003) found *Eucalyptus globulus* seed mass had a significant maternal effect, which had a carryover effect on early growth. They suggested that it was unwise to select for very-early growth (less than 3 years) without accounting for seed mass. Further they argued that early age heritability estimates could be inflated by these carryover effects. Nursery selection in this way makes no assumptions regarding how well the tree will perform later in life. It merely takes the individuals which at the time of picking have the physical characteristics which will help them survive transplanting.

Silvicultural practices can have large influences on growth and wood properties. Different genotypes can respond differently to silvicultural practices (Smith et al., 1997; Mason, 2006). Although it should be noted that in *Pinus radiata*, Lasserre et al. (2009) found that *”genotype did not significantly interact with stocking for any of the key wood properties*

considered (MFA, MOE, fibre length)", indicating a lot is still unknown with regards to how silviculture and genetics interact. Very-early selection occurs before trees are large enough for pruning or thinning and are treated differently to typical commercial stands. For example, they may be planted at very high stockings and have irrigation on highly fertile soil to lower mortality. Any genotypes which thrive under these ideal conditions will be selected above others which may be better suited in real plantation conditions. For example, an individual which is slower growing but has high drought tolerance will likely not be selected in an irrigated trial, but the selected fast growing individual may under-perform or die when planted on a dry site.

7.3 Health

Early selection for health appears feasible as a threshold criteria: only select trees which are healthy at the end of the breeding cycle. Once a tree has become sick (or died) it will lag behind other individuals in the stand, giving suboptimal growth and often being suppressed. If trees die or are excluded from very-early selections due to poor health they are not included in the next breeding cycle (even if not directly selecting for health). Any health problem which occurs during the very-early breeding cycle and for which resistance is heritable, can be selected against. However, there is no evidence health problems expressed at older ages can be predicted using this selection method. For example some species of Paropsine attack juvenile foliage while others attack mature foliage De Little et al. (1989). Establishment health is a good candidate for very-early selection, although differing environments will face different biotic and abiotic challenges. Health is used as a broad term, the genetics required to withstand drought are different to those required to withstand frost, or insect attack. Identifying genotypes with resistance or tolerance

to particular environmental pressures at a young age should improve the planting out success, reinforcing the importance of GxE trials.

7.4 Form

Typical form parameters such as a tendency to double leader, large branches or small internodes are measured on larger trees, see Raymond and Cotterill (1990) for an example procedure. Trees used in very-early selection typically have not been growing for long enough to show any repetition of these traits. Because of the lack of repetition, form in the traditional sense is hard to utilise within very-early selection programmes. When domesticating a wild species extremely poor individuals may still be recognisable at young ages, although the concept of form selection needs to be slightly redefined. If an individual is 'bush like', i.e. lacks apical dominance at a small size (assuming no mechanical or disease damage has occurred), it seems reasonable to remove the individual from the breeding population. In this state the individual is likely to become suppressed, and struggle to produce a straight stem of suitable size under a typical single-age single-species commercial stand management strategy. If thinning was part of the stand management strategy the individuals would likely be removed. It seems unlikely that domesticated species, even if only a small number of breeding cycles have been completed, would still have genotypes with form this poor. The strategy does not guarantee remaining trees will possess satisfactory form at older ages or guarantee that removed individuals would never have developed into high quality individuals by commercial rotation age.

7.5 Density

Density is probably the most used wood property in breeding, possibly due to the low measurement cost and high heritability compared to other wood properties (Apiolaza, 2008). When maximising usable biomass is the main concern (for example breeding for carbon sequestration, biofuels and in some cases pulp), maximising density is appropriate. No very-early selection programmes are known to exist for this purpose. If the trait can be expressed as a threshold of density, the potential exists for very-early selection to be valuable as density does not generally reduce with cambial age (Meinzer et al., 2011). Initially, density gained a lot of attention as it was easy to measure and thought to correlate well with wood properties such as stiffness. However in young trees, when stiffness is dominated by high MFA, both eucalypts (Chapters 2 and 4) and radiata pine (Sharma et al., 2015) have a low correlation between stiffness and density. Apiolaza (2009), studying radiata pine, found the relationship to vary markedly between trials even at age 7-8, finding weak, non-significant or negative values for the genetic correlation.

It could be the case that when creating engineered wood products, selecting for a specific density may be of importance (Marra, 1992); e.g. gluing may work best at a given density value. If keeping density above a lower threshold is desired, it may be a good candidate for very-early selection methods, however, if the goal is to maximise or keep density within a window it may not be suitable. There is no evidence that the selected trees will not go though a more rapid density change than the individuals which were not selected after the very-early selection time frame. As a result, the selection could provide a genetic base of trees with steeper density gradients, which depending on the desired commercial application may be counter-productive. It should be noted that if keeping density below a desired threshold was required and the target species reliably reduced density with age, the trait could be considered for very-early selection.

7.6 Stiffness

Stiffness is generally a threshold problem (Apiolaza, 2009). Timber is graded using threshold stiffness values to define a particular price bracket (Standards New Zealand, 2005); as a result, nothing is gained from maximising stiffness above the desired threshold, unless all of the requirements are met in order for the timber to move up to the next grade. Stiffness is governed by MFA (which is approximated using acoustic velocity) and density, under normal circumstances MFA follows a fairly universal pattern of decreasing MFA and increasing density with distance from the pith (Meinzer et al., 2011). If a desired stiffness is reached early in life, it is reasonably assumed the stiffness of wood laid down later will not dip below the threshold. The combination of threshold selection and well established age-related physiological patterns make stiffness a good candidate for very-early selection. Stiffness selection can also be formulated as a minimisation problem; how early in life can a tree reach the desired stiffness? Due to testing constraints, measuring whole breeding populations in this manner is not feasible; however harvesting at predetermined (early) age and selecting individuals which reach the threshold will result in a population reaching threshold stiffness earlier and hence provide stems with more wood usable in the higher value stiffness categories (for a given site, although the argument can be readily extended to multi-environment trials). A potential problem with very-early selection of stiffness is that there will be a reduction in flexibility to resist toppling forces from animals and wind events in young stems. One of the most promising arguments for the evolution of the typical radial pattern of MFA and density is that trees experience differing mechanical loading depending on their size (Mattheck and Kübler, 1997). There is a biological advantage in having low stiffness when a stem has a low second moment of area, allowing for the stem to bend rather than break or topple when external forces are applied. As the second moment of area increases with diameter, the

geometry of the stem plays a proportionally larger role in the flexibility of the stem than the material properties do. Once a stem reaches a significant diameter bending ability becomes compromised and hence the best defence strategy is to stand solid (i.e. resist bending or toppling), making stiffer material more desirable. Breeding stiffer small stems may inadvertently increase toppling or breakage at young ages, possibly outside of the age range of very-early selection trials. The trial may also, by chance, not experience a significant weather event, exposing the issue.

7.7 Extractive Content

Extractive content could use a similar selection type to stiffness as once trees start producing heartwood they (with the exception of some rare cases such as striping) don not stop. Therefore, selection of individuals which have started producing extractives at an early age (assuming that the production of extractives is heritable) could lower the age at which the population starts producing heartwood. Further, evidence exists that the lowest durability heartwood exists in the pith and improves in resistance to decay with increasing radial position (Kokutse et al., 2006; Bhat and Florence, 2003; Australia, 2005) and it is under some genetic control (Li et al., 2018) so it may be possible to set a threshold at a young age for timber durability. There are two conceivable reasons to select for the presence of extractives - one, the presence of extractives is required for natural durability, and two, the colour of the wood may fetch a premium. Alternatively one may want to select for low extractive content for uses such as pulp, unfortunately because this is the reverse of the above problem. Selection would need to be delayed as late as possible to identify the individuals which only start producing extractives late in life.

The presence of extractives at a young age does not guarantee that the individual will

have superior durability, but the presence of extractives is required for durability. Therefore assuming that extractive content and durability are heritable, very-early selection may have potential as a starting point for selection of this trait. However, little is known about the relationship between durability and extractive content, which needs further investigation (currently underway at the University of Canterbury (Altaner, 2018)) before its suitability for very-early selection can be assessed. As heartwood tends to develop later in life (compared to when very-early selection takes place), it is unlikely any trees will be producing heartwood at the time of selection. Any proxy based selections (Harju et al., 2009; Mishra, 2018) should be treated with due caution, and a good understanding of the underlying physiology between the proxy trait and later development of heartwood would be needed.

7.8 Growth-strain

There is a number of issues associated with selecting for growth-strain at any age. First growth-strain, in the sense of a breeding trait needs to be defined. The breeders' desire with this trait is to capture genotypes which produce little or no movement during sawing. Minimisation of movement during sawing (or reducing movement below a threshold), which breeders, growers, processors etc. have been calling growth-strain, is not necessarily the same as what physiologists call growth-strain, derived from growth-stress. Growth-strain in the strict sense is a contraction which happens in the secondary cell wall during cell formation (see Chapter 1). When combined with other geometric and material properties, it produces movement at the macroscopic scale when boundary conditions are relaxed, for example during sawing or a typical strain gauge test, resulting in the deformation breeders have been referring to as 'growth-strain'. This omnibus property needs

to be treated with caution as there is significant disconnect between a splitting test at age two and a log being milled at full rotation age.

Biechele et al. (2009) found experimental evidence of an increase in surface strain with age and concluded that a multivariate approach is needed as all investigated growth parameters (crown width, crown area, crown eccentricity, crown length, tree height, DBH and slenderness) had low correlations with growth-strain. Biechele et al. (2009) suggested interactions among parameters may also be useful, but warns that due to the large number of interactions, growth-strain may not be a useful breeding trait.

Timber movement during cutting is influenced by a number of material and geometric properties such as MFA, reaction wood production, grain angle, crown shape and stem lean. Crown formation, soil conditions, prevailing and extreme wind events could all cause stem lean or an asymmetric crown, which would result in an increase in growth-strain within certain areas of the stem, along with asymmetric stem formations. As a result, this could cause more, less predictable deformation during sawing. It may be that genetic selection for low movement timber at milling is not possible due to the large number of genes responsible for so many properties which affect local growth-strain production, which in turn, creates a complicated three-dimensional strain field within the stem. There are many properties which would need to be simultaneously either maximised or minimised within an individual, and their correlations may not be favourable. For example, low base growth-strain, low tendency to produce reaction wood, poor performance of reaction wood produced, symmetric crown and stem properties. Further complications arise as the traits which influence the magnitude of strain at a given point of development change with time. This implies that different traits would need to be maximised/minimised at different stages of development (ontogeny, there are many tree properties which change with time, books such as Niklas and Spatz (2012) and Mattheck and Kübler (1997) provide a good

overview), in order to manipulate the production of the three dimensional strain field to produce the least amount of movement at the time of harvest and milling. Some of these traits may not have a significant level of heritability, may have strong environmental interactions or may be negatively correlated with other required traits. With the technology and species (*E. bosistoana*, and *E. argophloia*) used in this thesis, there is insufficient data to draw a conclusion in this regard.

An argument could be made that, because growth-strain is so heavily affected by various micro-environmental aspects, site-level characteristics such as rainfall, aspect, soil type, etc. may have less of an effect than on other properties, such as growth, although no evidence exists for this. If it is the case that many different properties influence the production of growth-strain, the variation between individuals within a site compared to the variation between sites would be smaller than other traits. For example, growth can be significantly hindered by a lack of water, and that will affect all cloned individuals equally across a uniform site (both genetics and environment are identical). However, with growth-strain, a broken branch, being pushed over by an animal, etc. could alter the growth-strain from tree to tree even though the site level environment is essentially uniform and the genotypes identical. Whether this argument is valid should be investigated in the future, as it may have a profound effect on the way genotype-environment interactions are considered within breeding programmes as technology advances and individual tree monitoring becomes more realistic.

Currently there is a significant knowledge gap regarding what material and geometric properties result in timber movement during (green) sawing. Further, there is a lack of understanding of the strain field within a given stem, and how the field relates to the deformation of timber during milling. Before very-early assessment of tree-level growth-strain can be considered in a breeding programme, an understanding of what causes

timber deformation during green sawing is needed. Work is needed to investigate the influences which create the strain field, only then can those properties be investigated and tools developed to determine if selection for low growth-strain as a means of reducing sawing deformation is feasible.

Assuming low or even moderate age-age correlation of surface growth-strain, it could be argued that selection for high surface growth-strain of young trees which slowly reduce with growth may be the optimal profile. High surface-strain in small stems (the wood on the surface is under tension) provides a flatter profile over the majority of the stem when the tree is much larger, so the gradient from one side to the other of a board is lower potentially resulting in less deformation. While there is no evidence that strain at a young age is a poor predictor of strain at an old age, the reverse does not have any evidence either. It is much more common in other traits for young cambium properties to be poor predictors of older traits (Apiolaza, 2009). It is worth considering that a potential result of selecting for low surface-strain at a young age may have the unintended consequence of increasing saw-board deformation at commercial harvest age. This argument reaffirms the need to have significant physiological understanding of how a trait is produced before proxy tests, whether they are proxies in time or property or both are used for selection.

7.9 Conclusion

White et al. (2007) presented a list of requirements for a successful tree breeding programme.

1) clear programme and product objectives

2) sound knowledge of biology, silviculture and genetics

3) sound breeding strategy, well trained personnel supported by a stable budget

4) efficient mass propagation nursery and plantation management systems to optimise yield and product quality

5) maintenance of a broad genetic base

6) supportive research programme

These points become even more crucial when considering very-early selection, as additional errors are added in order to shorten breeding cycles. Due to the unknown relationships between properties at different ages and in particular at commercial rotation age, having clearly defined programme and product objectives is strongly linked to a sound understanding of the biology, silviculture and genetics of the species. Both of which can only be achieved with a supportive research programme that focuses on fundamental understanding of how the trees grow and why. Without this knowledge it will be nearly impossible to develop reliable testing procedures for very-early selection.

There are two ways to develop very-early selection methods once a suitable level of understanding of tree development is achieved. One is to have sufficient fundamental understanding that, given the properties at one age, there is a guarantee of the properties at another (for example, stiffness from MFA and density). The second option is a statistical approach, either using periodic non-destructive testing on the same individuals to obtain age-age correlations (DHB or height through time for example) or specifically designing trials to test how well destructive tests at one age predict properties at another, ideally using clones. For this to be successful, environmental factors need to be considered. One option is to clone trees and test both individuals grown to full rotation age and their clones at young ages for the desired properties. Multiple significantly different environments would be needed and the sites would need to all contain the same set of control

genetics. The clones could be grown and tested under the intended very-early selection procedures, typically high stocking within a nursery site. If a sufficient number of individuals, families and environments are represented at full rotation age, a relationship between how well the given very-early selection procedure (for that trial) can estimate outcomes on the different sites at different ages can be obtained. Hence, the site and procedures could be used to accelerate breeding cycles provided none of the above change significantly and the age-age correlations for the traits are sufficiently high.

The above discussion leads to the conclusion that for a trait to be a viable candidate for very-early selection (in addition to significant levels of heritability, genetic variation, environmental variability etc. which are required for success for all breeding programmes) at least one of the following three is required:

1) Extremely high age-age correlations. No known evidence exists that any of the properties discussed here demonstrate significantly high age-age correlations. Confirmation at full-rotation age would be required to estimate age-age correlations over multiple environments.

2) A non-reversible threshold problem governed by physiology; eg. stiffness and possibly heartwood.

3) A trait which is defined within the very-early selection breeding cycle life span, for example planting survival at one year.

If the above can be met, full-rotation age trials are still continually required to ensure inadvertent undesirable selections in other traits are not being made.

Very-early selection may provide some substantial gains in breeding efficiency for a limited number of wood properties. However, development of the procedures needs to come from thorough understanding of the biology, physics and genetics of both the trait and

the testing procedures. Further, it needs to be confirmed with full-rotation age trials from multiple environments. Full-rotation age individuals need to be tested and the population characterised across multiple significantly different sites with shared genetics first, and then a very-early selection test could be developed and the results compared. While commercially it is tempting to reverse this procedure and complete very-early selection first, there is no evidence of any positive or negative gain being made.

Chapter 8

Final conclusions and future research

The work presented here provided a description of a trial breeding programme using a new method. Chapter 2 presented results from a very-early selection pilot trial using the previously proposed testing procedure for surface growth-strain, the splitting test. Chapter 2 applied a new statistical technique to tree breeding in order to statistically accommodate the zero censored data the testing procedure created. A hypothesis to explain the cause of zero censoring, i.e. the development of tension wood early in growth, followed by normal wood production was suggested. Chapter 3 tested the hypothesis by bending the stems at different stages of growth to induce tension wood development. The hypothesis failed under these experimental conditions. Chapter 4 documents a breeding trial of 4032 *Eucalyptus bosistoana* harvested at age two and tested for a number of wood properties. Genetic parameters were presented and compared with literature values. The trial was repeated with different genotypes and the results presented in Appendix B. Chapters 5 and 6 presented experimental and theoretical investigations into the methods used for measuring growth-strain. These Chapters concluded the splitting test (used in the above breeding trials) should be limited to removal of poor performing individuals at young ages,

and that the selection of high performing individuals was not possible due to the error associated with the procedure. Surface point testing, such as strain gauge measurements, were also investigated and it was found the average value from four strain-gauges evenly spaced around a stem performed similarly to the splitting test method. Chapter 7 addresses the very-early selection problem as a whole and provides guidelines as to which traits may be suitable for selection at young ages.

The next practical step which can be taken is to harvest some commercial rotation age Eucalypts, which are known to coppice readily from multiple environments and test them for the wood properties which are of interest, including growth-strain. After harvest the individuals can be left to coppice and grow for two years, at which time the very-early selection procedures could be followed on the coppice to provide valuable information regarding the age-age correlations associated with the traits in the species of interest over multiple environments, including the Chapter 4 trial. Hypothetical selections should also be conducted in reverse order, i.e. on the coppiced, or very-early selection trial samples and the results investigated on the mature population.

For any future very-early selection tool, the top priority needs to be understanding the biological, physical and chemical drivers responsible for the trait. Once a thorough understanding of trait development is gained, methods to leverage the developmental pathways can be investigated, and finally tools created to identify individuals which will reliably perform as expected at full rotation age. The generating mechanisms behind growth-stresses and other traits which cause timber distortion, are not yet well enough understood to develop reliable testing procedures for the output of timber which is stable during green sawing or peeling regardless of testing age. In order to reduce movement during green sawing or peeling more research is needed into what properties can be tested and selected for, which will result in stable green timber. Unfortunately the work presented here

does not provide any direct leads of promising research areas related to growth-stress or timber deformation measurements and prediction. It does, however, provide guidelines for how traits which may be suitable for very-early selection will present.

Appendix A

JAGS code

R code used in Chapter 2.

```
# Analyzing all sites
rm(list = ls())
library('ggplot2')
library('rjags')

df <- read.csv('harewood_EB_data.csv')

#setting unique identifiers for each experiment and tree
df <- within(df, {
                        bcID <- interaction(section, coppice)
                        treeID <- interaction(row, col, section)
                    })
```

```
#removing unwanted sites
df <- subset(df, bcID== 'H1.1' | bcID == 'H2.0' | bcID == 'H2.1')

#remove all records with NAs in the strain vector from df
df1 <- df[!is.na(df$strain),]
# dropping unused family levels
df1$family <- df1$family[drop = TRUE]

# setting left censored data to NA
df1$strain <- with(df1, ifelse(strain > 0, strain, NA ))

# JAGS code
jagsData <- list(N = nrow(df1),
                 M = length(unique(df1$family)),
                 S = length(unique(df1$section)),
                 D = length(unique(df1$treeID)),
                 BC = length(unique(df1$bcID)),
                 isAboveLOD = ifelse(!is.na(df1$strain) > 0, 1, 0)
                    ,
                 y = df1$strain,
                 site = as.integer(factor(df1$section)),
                 bcid = as.integer(factor(df1$bcID)),
                 fam = as.integer(factor(df1$family)),
                 tid = as.integer(factor(df1$treeID)),
                 cop = df1$coppice,
                 LOD = rep(0, nrow(df1)))
```

```
bugsInits = list(list(fe = rep(0, length(unique(df1$family))), ti
    = rep(0, length(unique(df1$treeID)))))
nMissing <- sum(!jagsData$isAboveLOD)
bugsInits[[1]]$y[!jagsData$isAboveLOD] <- runif(nMissing, -1.5,
   0)

modelString = "
                model
                {
                for(i in 1:N)
                {
                        isAboveLOD[i] ~ dinterval(y[i], LOD[i])
                        y[i] ~ dnorm(yhat[i], yres[i])
                        yres[i] <- sires[bcid[i]]
                        yhat[i] <- mu + si[site[i]] + B1*cop[i] +
                            fe[fam[i]]  + ti[tid[i]]
                }
                for(j in 1:M)
                {
                        fe[j] ~ dnorm(0, tauf)
                }
                sires[1] ~ dgamma(0.001, 0.001)
                for(bc in 2:BC)
                {
                        sires[bc] ~ dgamma(0.001, 0.001)
```

```
}
si[1] <- 0
for(k in 2:S)
{
        si[k] ~ dnorm(0.5, 1.0E-12)
}
for(d in 1:D){
        ti[d] ~ dnorm(0, taut)
}
B1 ~ dnorm(0.5, 1.0E-12)
S1 ~ dnorm(0.5, 1.0E-12)
mu ~ dnorm(0.5, 1.0E-12)

taut ~ dgamma(0.001, 0.001)
tauf ~ dgamma(0.001, 0.001)
vare1 <- 1/sires[1]
vare2 <- 1/sires[2]
vare3 <- 1/sires[3]
vare4 <- 1/sires[4]
vare <- vare1+vare2+vare3+vare4
varf <- 1/tauf
vart <- 1/taut
h2 <- 2.5*(varf+vart)/(varf + vart + vare)
}
"
```

```
writeLines(modelString, con = "multisitemodel.jags.R")

# Building JAGS call
jagsModel <- jags.model(file = "multisitemodel.jags.R", data =
   jagsData, inits = bugsInits)
update(jagsModel, n.iter = 10000)

# Choosing parameters to track, sampling and summarizing
parameters <- c('mu', 'vare', 'varf', 'vare1', 'vare2', 'vare3',
   'vare4', 'h2', 'B1', 'S1', 'vart')
#parameters <- c('vare1', 'vare2', 'vare3', 'vare4')
simSamples <- coda.samples(jagsModel,
                  variable.names = parameters,
                  n.iter = 150000)

oldmargin <- par()$mar
par(mar = c(2, 2, 2, 2))
plot(simSamples)
par(mar = oldmargin)
summary(simSamples)
```

Appendix B

Woodville II results

Table B.1: Summary statistics for the trees used in this study. They were age two *E. bosistoana* grown on an irrigated nursery site in Woodville, New Zealand.

	Mean (standard deviation)	Maximum	Minimum
Strain $\mu\epsilon$	1949 (613)	6361	0
Diameter mm	34.3 (7.5)	68.4	12.9
Density $\frac{kg}{m^3}$	814 (46)	967	612
Stiffness Gpa	11.8 (1.7)	19.6	7.2
Volumetric Shrinkage	0.19 (0.04)	0.32	0.009
Acoustic Velocity $\frac{km}{s}$	3.8 (0.3)	4.69	2.92

Table B.2: Narrow sense heritability (for *E. bosistoana* at age two) presented on the diagonal, with genetic correlations between traits in the upper half of the table, calculated using the model presented above. 95% credible intervals in brackets.

	Strain	Diameter	Density	Stiffness	Volumetric Shrinkage	Acoustic Velocity
Strain	0.24 (0.11, 0.37)	0.07 (-0.44, 0.58)	0.17 (-0.03, 0.37)	0.41 (0.14, 0.69)	0.07 (-0.07, 0.22)	0.42 (0.14, 0.70)
Diameter		0.09 (0.01, 0.17)	0.06 (-0.18, 0.31)	0.14 (-0.26, 0.54)	0.02 (-0.13, 0.17)	0.14 (-0.27, 0.70)
Density			0.38 (0.32, 0.45)	0.56 (0.47, 65)	0.38 (0.30, 0.46)	0.31 (0.18, 0.43)
Stiffness				0.68 (0.55, 0.82)	0.13 (0.03, 0.22)	0.94 (0.93, 0.96)
Volumetric Shrinkage					0.31 (0.27, 0.35)	-0.0 (-0.11, 0.11)
Acoustic Velocity						0.68 (0.54, 0.82)

Table B.3: Further fixed effects which were deemed to be negligible and hence not included in the standard model, within the brackets are the 95% credible intervals * Replicates were not used in this model as confound with sampling type.

	Strain	Diameter	Density	Stiffness	Volumetric Shrinkage	Height	Acoustic Velocity
Wounded	0.02 (-0.08, 0.12)	-0.10 (-0.20, -0.00)	0.01 (-0.09, 0.11)	0.07 (-0.03, 0.16)	0.00 (-0.10, 0.10)	0.02 (-0.08, 0.12)	0.09 (-0.01, 0.18)
Harvest	0.013 (-0.10, 0.12)	0.09 (-0.02, 0.20)	0.00 (-0.11, 0.11)	0.00 (-0.11, 0.11)	0.00 (-0.11, 0.11)	-0.08 (-0.19, 0.03)	-0.00 (-0.11, 0.11)
Row	-0.00 (-0.09, 0.09)	-0.00 (-0.09, 0.09)	-0.00 (-0.09, 0.09)	-0.00 (-0.09, 0.09)	-0.00 (-0.09, 0.09)	-0.00 (-0.09, 0.09)	-0.00 (-0.10, 0.09)
Column	-0.03 (-0.18, 0.12)	0.07 (-0.08, 0.22)	-0.00 (-0.15, 0.15)	-0.01 (-0.16, 0.14)	-0.00 (-0.15, 0.15)	0.02 (-0.13, 0.17)	-0.01 (-0.16, 0.13)
Sampling Type*	-0.03 (-0.14, 0.08)	0.25 (0.14, 0.36)	-0.01 (-0.12, 0.10)	-0.03 (-0.14, 0.08)	-0.01 (-0.12, 0.10)	-0.05 (-0.15, 0.06)	-0.03 (-0.14, 0.08)

R code used in Chapter 4

```
rm(list = ls())
library(MCMCglmm)
library(MasterBayes)
library(reshape2)

wv <- read.csv('woodville_experiment_1.csv', skip=12)

wv[is.na(wv$dry_mass_A)==TRUE & !is.na(wv$dry_mass_B)==TRUE,'
    dry_mass_A'] <- wv[is.na(wv$dry_mass_A)==TRUE & !is.na(
    wv$dry_mass_B)==TRUE,'dry_mass_B']
wv[is.na(wv$dry_mass_B)==TRUE & !is.na(wv$dry_mass_A)==TRUE,'
    dry_mass_B'] <- wv[is.na(wv$dry_mass_B)==TRUE & !is.na(
    wv$dry_mass_A)==TRUE,'dry_mass_A']
wv[is.na(wv$dry_vol_A)==TRUE & !is.na(wv$dry_vol_B)==TRUE,'
    dry_vol_A'] <- wv[is.na(wv$dry_vol_A)==TRUE & !is.na(
```

```
    wv$dry_vol_B)==TRUE,'dry_vol_B']
wv[is.na(wv$dry_vol_B)==TRUE & !is.na(wv$dry_vol_A)==TRUE,'
    dry_vol_B'] <- wv[is.na(wv$dry_vol_B)==TRUE & !is.na(
    wv$dry_vol_A)==TRUE,'dry_vol_A']
wv[is.na(wv$green_mass_A)==TRUE & !is.na(wv$green_mass_B)==TRUE,'
    green_mass_A'] <- wv[is.na(wv$green_mass_A)==TRUE & !is.na(
    wv$green_mass_B)==TRUE,'green_mass_B']
wv[is.na(wv$green_mass_B)==TRUE & !is.na(wv$green_mass_A)==TRUE,'
    green_mass_B'] <- wv[is.na(wv$green_mass_B)==TRUE & !is.na(
    wv$green_mass_A)==TRUE,'green_mass_A']
wv[is.na(wv$green_vol_A)==TRUE & !is.na(wv$green_vol_B)==TRUE,'
    green_vol_A'] <- wv[is.na(wv$green_vol_A)==TRUE & !is.na(
    wv$green_vol_B)==TRUE,'green_vol_B']
wv[is.na(wv$green_vol_B)==TRUE & !is.na(wv$green_vol_A)==TRUE,'
    green_vol_B'] <- wv[is.na(wv$green_vol_B)==TRUE & !is.na(
    wv$green_vol_A)==TRUE,'green_vol_A']
wv[is.na(wv$av_A)==TRUE & !is.na(wv$av_B)==TRUE,'av_A'] <- wv[is.
    na(wv$av_A)==TRUE & !is.na(wv$av_B)==TRUE,'av_B']
wv[is.na(wv$av_B)==TRUE & !is.na(wv$av_A)==TRUE,'av_B'] <- wv[is.
    na(wv$av_B)==TRUE & !is.na(wv$av_A)==TRUE,'av_A']


wv <- within(wv, {
                        animal <- factor(10000 + treeID)
                        mother <- factor(family)
                        father <- NA
                        strain <- opening*diameter/(1.74*
```

```
                    slit_length^2)*1000
                diameter <- diameter/10
                dry_dens <- (dry_mass_A + dry_mass_B)/(
                    dry_vol_A + dry_vol_B)
                av <- (av_A + av_B)/2
                vs <- (green_vol_A + green_vol_B -
                    dry_vol_A - dry_vol_B)/(green_vol_A +
                    green_vol_B)
                stiffness <- (av*av*dry_dens)/10
                height <- height/10.0
            })

wv$rep <- as.factor(wv$rep + 1)
wv$stake <- as.factor(wv$stake)
wv <- wv[!is.na(wv$rep),]
wv <- wv[!is.na(wv$stake),]
wv <- wv[!is.na(wv$row),]

wv$edge1 <- 0
wv[wv$row==1,]$edge1 <- 1
wv$edge2 <- 0
wv[wv$col==1,]$edge2 <- 1
wv$edge3 <- 0
wv[wv$row==312,]$edge3 <- 1
wv$edge4 <- 0
wv[wv$col==14,]$edge4 <- 1
```

```
wv$edge1 <- as.factor(wv$edge1)
wv$edge2 <- as.factor(wv$edge2)
wv$edge3 <- as.factor(wv$edge3)
wv$edge4 <- as.factor(wv$edge4)

names(wv)[names(wv)=="family"] <- "fami"

pedi <- wv[, c('animal', 'mother', 'father')]
pedi <- insertPed(pedi)

#prmul <- list(R = list(V=diag(7)*0.02, nu=8),
#              G = list(G1 = list(V=diag(7)*0.02, nu=8), G2 =
   list(V=diag(7)*0.02, nu=8)))

covmat <- cov(wv[, c('strain', 'diameter', 'dry_dens', 'stiffness
   ', 'vs', 'height', 'av')], use="complete.obs")

prmul <- list(R = list(V=covmat*0.5, nu=1),
              G = list(G1 = list(V = covmat*0.25, nu = 1), G2 =
                  list(V = covmat*0.25, nu = 1)))

bm1 <- MCMCglmm(cbind(strain, diameter, dry_dens, stiffness, vs,
   height, av) ~
                                    trait - 1 + trait:rep +
                                       trait:stake + trait:
```

```
                                                edge1 + trait:edge2 +
                                                trait:edge3 + trait:
                                                edge4,
                    random = ~ us(trait):animal + us(trait):plot,
                    rcov = ~ us(trait):units,
                    family = c('gaussian', 'gaussian','gaussian', '
                       gaussian', 'gaussian','gaussian','gaussian'),
                    data = wv,
                    pedigree = pedi,
                    prior = prmul,
                    burnin = 50000,
                    nitt =  200000,
                    thin = 100,
                    pr=TRUE,
                    pl=TRUE)

bvs.post <- apply(bm1$Sol[, ], 2, function(x) quantile(x, 0.5))
bvs.df <- data.frame(bv = bvs.post)
bvs.df$id <- rownames(bvs.df)

ids <- names(bvs.post)

ids.to.df <- function(id) {
        components <- unlist(strsplit(id, split = '[.]'))
        trait <- substr(components[1], 6, 20)
        typeID <- components[2]
```

```
        animal <- components[3]
        row <- data.frame(trait, typeID, animal)
        return(row)
}

a <- lapply(ids, FUN = ids.to.df)
a <- do.call(rbind, a)

bvs.df <- cbind(bvs.df, a)
bvs.df <- bvs.df[!is.na(bvs.df$typeID),]
bvs.df <- bvs.df[bvs.df$typeID == 'animal',]

bvs.df <- dcast(bvs.df, animal ~ trait, value.var = 'bv', mean)
bvs.df$numan <- as.numeric(levels(bvs.df$animal))[bvs.df$animal]

bvs.fam <- subset(bvs.df, numan < 1000)
bvs.fam$numan <- NULL
names(bvs.fam) <- c('family', 'BVstrain', 'BVdiameter', '
   BVdry_dens', 'BVstiffness', 'BVvs', 'BVheight', 'BVav')

bvs.tree <- subset(bvs.df, numan > 10000)
bvs.tree$treeID <- as.factor(bvs.tree$numan - 10000)
bvs.tree$animal <- NULL
bvs.tree$numan <- NULL
bvs.tree <- merge(bvs.tree, wv[,1:2], by='treeID')
names(bvs.tree) <- c('treeID', 'BVstrain', 'BVdiameter', '
```

```
    BVdry_dens', 'BVstiffness', 'BVvs', 'BVheight', 'BVav', '
    family')

write.csv(bvs.fam, "bvs_fams_standed_non.csv", row.names=FALSE)
write.csv(bvs.tree, "bvs_trees_standed_non.csv", row.names=FALSE)
write.csv(bm1$Sol, "bm1Sol_standed_non.csv", row.names=FALSE)
write.csv(bm1$VCV, "bm1VCV_standed_non.csv", row.names=FALSE)

plot(mcmc.list(bm1$VCV[, "traitstrain:traitstrain.units"]))
plot(mcmc.list(bm1$VCV[, "traitdiameter:traitdiameter.units"]))
plot(mcmc.list(bm1$VCV[, "traitdry_dens:traitdry_dens.units"]))
plot(mcmc.list(bm1$VCV[, "traitheight:traitheight.units"]))
plot(mcmc.list(bm1$VCV[, "traitav:traitav.units"]))
plot(mcmc.list(bm1$VCV[, "traitstiffness:traitstiffness.units"]))
plot(mcmc.list(bm1$VCV[, "traitvs:traitvs.units"]))
plot(mcmc.list(bm1$VCV[, "traitstrain:traitstrain.animal"]))
plot(mcmc.list(bm1$VCV[, "traitvs:traitvs.animal"]))
plot(mcmc.list(bm1$VCV[, "traitdiameter:traitdiameter.animal"]))
plot(mcmc.list(bm1$VCV[, "traitstiffness:traitstiffness.animal"])
    )
plot(mcmc.list(bm1$VCV[, "traitav:traitav.animal"]))
plot(mcmc.list(bm1$VCV[, "traitheight:traitheight.animal"]))
```

Appendix C

Python code for Chapter 5

Python code used in Chapter 5.

```
import numpy as np
from scipy.optimize import minimize

def my_fun_means(z): # function to initalise the error terms and
   set up their equations
    eRS = z[0] # error of the RS test
    eOS = z[1] # error of the OS test
    eQS = z[2] #error of the QS test in the same orentation as
       the RS and OS tests
    eROT = z[3] # error induced by changing the testing
       orentation
    f = np.zeros(6)
    f[0] = 251.4 - (eRS + eOS) # the mean difference between
       between the RS and OS measurments, ie mean(RS - OS) where
       RS and OS are vectors, each row represents a given sample,
        eRS and eOS are the two errors responcable for that
       difference.
    f[1] = 438 - (eRS + eQS) # eQS is the error from the
       quartering test
```

```
    f[2] = 466 - (eRS + eQS + eROT) # eROT is the rotational
       error, ie the error asocated with the change in orentation
        of the sample, but not with the quartering test its self
    f[3] = 186.6 - (eOS + eQS)
    f[4] = 214.7 - (eOS + eQS + eROT)
    f[5] =  28.06 - (2*eQS + eROT)
    return np.sum(f)

def my_cons_means(z): # function to set up constraint equations
   for the optermisation problem
    eRS = z[0]
    eOS = z[1]
    eQS = z[2]
    eROT = z[3]
    f = np.zeros(6)
    f[0] = 251.4 - (eRS + eOS) #   the mean difference between
       between the RS and OS measurments, ie mean(RS - OS) where
       RS and OS are vectors, each row represents a given sample,
        eRS and eOS are the two errors responcable for that
       difference.
    f[1] = 438 - (eRS + eQS) # eQS is the error from the
       quartering test
    f[2] = 466 - (eRS + eQS + eROT) # eROT is the rotational
       error, ie the error asocated with the change in orentation
        of the sample, but not with the quartering test its self
    f[3] = 186.6 - (eOS + eQS)
    f[4] = 214.7 - (eOS + eQS + eROT)
    f[5] = 28.06 - (2*eQS + eROT)
    return f

cons_means = {'type' : 'ineq', 'fun': my_cons_means} # creating
   dict for optermisatioin
res = minimize(my_fun_means, (0, 0, 0, 0), method='SLSQP',
   constraints=cons_means) # performing optermisation on the mean
```

```
    difference values.
print("for means")
print(res)
print("means ")
print(res['x'])
import numpy as np
from scipy.optimize import minimize

def my_fun_means(z): # function to initalise the error terms and
   set up their equations
    eRS = z[0] # error of the RS test
    eOS = z[1] # error of the OS test
    eQS = z[2] #error of the QS test in the same orentation as
       the RS and OS tests
    eROT = z[3] # error induced by changing the testing
       orentation
    f = np.zeros(6)
    f[0] = 251.4 - (eRS + eOS) # the mean difference between
       between the RS and OS measurments, ie mean(RS - OS) where
       RS and OS are vectors, each row represents a given sample,
        eRS and eOS are the two errors responcable for that
       difference.
    f[1] = 438 - (eRS + eQS) # eQS is the error from the
       quartering test
    f[2] = 466 - (eRS + eQS + eROT) # eROT is the rotational
       error, ie the error asocated with the change in orentation
        of the sample, but not with the quartering test its self
    f[3] = 186.6 - (eOS + eQS)
    f[4] = 214.7 - (eOS + eQS + eROT)
    f[5] =  28.06 - (2*eQS + eROT)
    return np.sum(f)

def my_cons_means(z): # function to set up constraint equations
   for the optermisation problem
```

```
    eRS = z[0]
    eOS = z[1]
    eQS = z[2]
    eROT = z[3]
    f = np.zeros(6)
    f[0] = 251.4 - (eRS + eOS) # 251 is the mean difference
       between between the RS and OS measurments, ie mean(RS - OS
       ) where RS and OS are vectors, each row represents a given
        sample, eRS and eOS are the two errors responcable for
       that difference.
    f[1] = 438 - (eRS + eQS) # eQS is the error from the
       quartering test
    f[2] = 466 - (eRS + eQS + eROT) # eROT is the rotational
       error, ie the error asocated with the change in orentation
        of the sample, but not with the quartering test its self
    f[3] = 186.6 - (eOS + eQS)
    f[4] = 214.7 - (eOS + eQS + eROT)
    f[5] = 28.06 - (2*eQS + eROT)
    return f

cons_means = {'type' : 'ineq', 'fun': my_cons_means} # creating
   dict for optermisatioin
res = minimize(my_fun_means, (0, 0, 0, 0), method='SLSQP',
   constraints=cons_means) # performing optermisation on the mean
    difference values.
print("for means")
print(res)
print("means ")
print(res['x'])
# in order eRS, eOS, eQS, eROT
# mean value of error, ie, the eXX value needed to satusfy the
   constraints with a minumum devation from zero
# these values show a slight bias in each of the measurment
   systems, but tell us little about how reliably we can use a
```

```
    given measurment



def my_fun_vars(z):
    eRS = z[0]
    eOS = z[1]
    eQS = z[2]
    eROT = z[3]
    f = np.zeros(6)
    f[0] = 93526.22 - (eRS + eOS) # the  varence of the
       difference between RS and OS measurments, ie var(RS - OS),
        the varence of the distrobution from which the means
       above came from
    f[1] = 87239.51 - (eRS + eQS)
    f[2] = 177430 - (eRS + eQS + eROT)
    f[3] = 76899.36 - (eOS + eQS)
    f[4] = 174149.4 - (eOS + eQS + eROT)
    f[5] = 174149.4 - (2*eQS + eROT)
    return np.sum(f)

def my_cons_vars(z):
    eRS = z[0]
    eOS = z[1]
    eQS = z[2]
    eROT = z[3]
    f = np.zeros(6)
    f[0] = 93526.22 - (eRS + eOS) # the  varence of the
       difference between RS and OS measurments, ie var(RS - OS),
        the varence of the distrobution from which the means
       above came from
    f[1] = 87239.51 - (eRS + eQS)
    f[2] = 177430 - (eRS + eQS + eROT)
    f[3] = 76899.36 - (eOS + eQS)
```

```
    f[4] = 174149.4 - (eOS + eQS + eROT)
    f[5] = 174149.4 - (2*eQS + eROT)
    f[0] > 0
    f[1] > 0
    f[2] > 0
    f[3] > 0
    f[4] > 0
    f[5] > 0
    return f

cons_vars = {'type' : 'ineq', 'fun': my_cons_vars}
res = minimize(my_fun_vars, (0, 0, 0, 0), method='SLSQP',
   constraints=cons_vars) # same as above but for varences
print("\n")
print("for vars")
print(res)
print('standard devs')
print(np.sqrt(res['x']))
print(1.96*np.sqrt(res['x']))
```

Appendix D

Python code for Chapter 6

Python code used in Chapter 6 to produce the variables needed to create the theoretical populations.

```
import os as os
import math as math
import csv as csv
import numpy as np

wd_path = "/home/nick/Dropbox/cuddons/split_test_FEM_two_peak/"
os.chdir(wd_path)
mesh_list = os.listdir("./final_xml/")
num_of_samples = 1000

for ii in range(0,len(mesh_list)):
    mesh_list[ii] = ("./final_xml/"+mesh_list[ii])

samp_list = os.listdir("./samples_var/")
num_exist_samps = len(samp_list)

seed_num = num_exist_samps;
th = -1*np.pi/2
```

```
cin  = 1
cout = 0

c = (cin+cout)/2

#pvar   = 4*(6730620**2)/(1 + 2*c + c)#*c) > 909.2346. 3.8 > 892
#/(1 + (cin + cout) + (cin)) #3.8 > 513
#pvar   =  2.7*(6730620**2) > 713
#pvar   =  2.6*(6730620**2) > 733
#pvar   =  3.0*(6730620**2) > 775
pvar   =  8.607237e+13 #1.9*(6730620**2)

#  2*V_in/1+c
cov_in =  cin*pvar     #4*((cin*pvar))/(2 + 2*cin)
cov_out = cout*pvar     #4*((cout*pvar))/(2 + 2*cout)

mean_mat = [16191994,16191994,16191994,16191994]
cov_mat = [[pvar, cov_out, cov_in, cov_out],[cov_out, pvar,
   cov_out, cov_in],[cov_in, cov_out, pvar, cov_out],[cov_out,
   cov_in, cov_out, pvar]]


if num_exist_samps > num_of_samples:
    print("less samples to be processed than exist in the sample
       vars folder, exiting")

for ii in range(num_exist_samps, num_of_samples):
    seed_num = seed_num + 1
    np.random.seed(seed=seed_num)

    rx1, ry1, rx2, ry2 = np.random.multivariate_normal(mean_mat,
       cov_mat, 1).T
```

```
stress_l_x1 = rx1[0]
stress_l_y1 = ry1[0]
stress_l_x2 = rx2[0]
stress_l_y2 = ry2[0]

np.random.seed(seed=seed_num*23)
theta_change = np.random.uniform(0, math.pi/2)

list_out = [[] for kk in range(len(mesh_list))]
for jj in range(0,len(mesh_list)):
    if mesh_list[jj].startswith("./final_xml/cut_first.xml"):
        mesh_path = wd_path+"final_xml/cut_first.xml"
        theta = 0
    elif mesh_list[jj].startswith("./final_xml/cut_second.xml
       "):
        mesh_path = wd_path+"final_xml/cut_second.xml"
        theta = th
    else:
        print("strange file present check dir")
    os.system("python ./split_test_FEM_strain.py "+str(
       mesh_path)+' '+str(theta)+' '+str(stress_l_x1)+' '+str
       (stress_l_y1)+' '+str(stress_l_x2)+' '+str(stress_l_y2
       )+' '+str(theta_change))
    with open('tfile_var.csv', 'r') as fh:
        mes = fh.read()
        fh.close()
    list_out[jj] = [str(mesh_path), str(theta), str(seed_num)
       , str(mes), str(stress_l_x1), str(stress_l_y1), str(
       stress_l_x2), str(stress_l_y2), str(theta_change)]
with open('./samples_var/sample_'+str(ii)+'.csv', 'w+') as f:
    csv_writer = csv.writer(f)
    csv_writer.writerows(list_out)
```

Python code used in Chapter 6 to produce the finite element model of the samples.

```
from dolfin import *
import numpy as np
import math as math
import scipy.interpolate as inp
import sys as sys
from dolfin.cpp._mesh import Cell_get_cell_data,
    Cell_get_vertex_coordinates, Cell_normal, Cell_cell_normal,
    Cell_contains

mesh_path = sys.argv[1]
theta = float(sys.argv[2])
stress_l_x1 = float(sys.argv[3])
stress_l_y1 = float(sys.argv[4])
stress_l_x2 = float(sys.argv[5])
stress_l_y2 = float(sys.argv[6])
theta_change = float(sys.argv[7])

#r_devider = -5.23 #  jacobs 1945 values in psi come to about
    this - stresses and strains in tree tunks as they grow
#t_devider = -10000.0 # stress_l = 5.23* stress_transverse  --
    Patterns of longitudinal and tangential maturation stresses in
     Eucalyptus nitens plantation trees -- find boyd 1950 it has a
     lot more species in it also need to find Emods

#stress_l_mean = 16249852
#stress_sd_l = 6754671



#need to work out the rotation here
#make dependent on theta
```

```
tol = 0.0000001

if(theta == 0):
        stress_l_modifier_1 = stress_l_x1
        stress_l_modifier_2 = stress_l_x2
        stress_l_modifier_3 = stress_l_y1
        stress_l_modifier_4 = stress_l_y2
elif((theta > (-1*math.pi/2.0 - tol)) and (theta < (-1*math.pi
   /2.0 + tol))):
        stress_l_modifier_4 = stress_l_x1
        stress_l_modifier_3 = stress_l_x2
        stress_l_modifier_1 = stress_l_y1
        stress_l_modifier_2 = stress_l_y2
else:
        print("error, theta not defined, defulting to no varation
            around the stem")


#assumed parameters about samples, this is what the meshes are
big_end_height = 400 #assumed small end centred on origin
bed = 39.55
sed = 34.80
#35.99 at end of slit, average R = 37.76875


big_rad = bed/2.0
small_rad = sed/2.0

mesh = Mesh(mesh_path)



def calc_rad(h, small_end_rad, big_end_rad):
    grad = big_end_height/(big_end_rad-small_end_rad)
```

```
    intersept = grad*small_end_rad
    return (h + intersept)/grad


def irads(max_rad):
    iR = float(max_rad)/math.sqrt(num_of_radial_devisions)
    iA = math.pi*iR**2
    rad_array = np.zeros(num_of_radial_devisions-1)
    for ii in range(1,num_of_radial_devisions):
        rad_array[ii-1] = math.sqrt(max_rad**2-(iA*ii)/math.pi)
    return rad_array[::-1]


class vstress(Expression):
    def eval(self, values, x):
        mr = calc_rad(x[2], small_rad, big_rad)
        rad = sqrt(x[0]**2+x[1]**2)

        if(rad < 0.244*mr):
                rad = 0.244*mr

        theta_c = np.arctan2(x[1], x[0]) + theta_change

        if(theta_c >= 0):
                if(theta_c >= np.pi/2):
                        stress_l_theta = stress_l_modifier_1*np.
                          sin(theta_c)**2 + stress_l_modifier_3*
                          np.cos(theta_c)**2
                elif(theta_c < np.pi/2):
                        stress_l_theta = stress_l_modifier_1*np.
                          sin(theta_c)**2  + stress_l_modifier_4
                          *np.cos(theta_c)**2
                else:
                        print("error calculating what stress_l
```

```
                        should be point 1")
        elif(theta_c < 0):
                if(abs(theta_c) >= np.pi/2):
                        stress_l_theta = stress_l_modifier_2*np.
                          sin(theta_c)**2 + stress_l_modifier_3*
                          np.cos(theta_c)**2
                elif(abs(theta_c) < np.pi/2):
                        stress_l_theta = stress_l_modifier_2*np.
                          sin(theta_c)**2 + stress_l_modifier_4*
                          np.cos(theta_c)**2
                else:
                        print("error calculating what stress_l
                          should be point 2")
        else:
                print("error calculating what stress_l should be
                  point 3")

        GSv = stress_l_theta*(1 + 2.125*math.log(rad/mr))
        #GSr = (stress_l_theta/t_devider)*(math.log(rad/mr))
        #GSt = (stress_l_theta/t_devider)*(1 + math.log(rad/mr))

        values[0] = GSv
    def value_shape(self):
        return (1,)
GSV = vstress(degree=3)


class trans_angles(Expression):
    def eval(self, values, x):
        tol = 10**(-10)
        if x[0] > -tol and x[0] < tol:
            if x[1] > tol:
                w = math.pi
            if x[1] >= -tol and x[1] <= tol:
```

```
                w = 0
            if x[1] < tol:
                w = -math.pi
        else:
            w = math.atan(x[1]/x[0])
            if x[0]<0 and x[1]>=0:
                w = w+math.pi
            if x[0]<0 and x[1]<0:
                w = w+math.pi
            if x[0]>0 and x[1]<0:
                w = w+2*math.pi

        values[0] = math.cos(w)
        values[1] = math.cos(w - math.pi/2)
        #constant as rotation about z axis so always
           perpendicular
        values[2] = 0# math.cos(math.pi/2)
        # roation angle from y to r print CMM
        values[3] = math.cos(w + math.pi/2)
        values[4] = math.cos(w)
        values[5] = 0#math.cos(math.pi/2)
        values[6] = 0#math.cos(math.pi/2)
        values[7] = 0#math.cos(math.pi/2)
        values[8] = 1.0#math.cos(0.0)

    def value_shape(self):
        return (9,)
trans = trans_angles(degree=2)

def end_boundary(x, on_boundary):
    return abs(x[2]) < 0.001

#Elastic constants of wood determined by ultrasound using three
   geometries of specimens cover all 9 elastic constants for E.
```

```
    siligna
E3 = 11.33*1000000000
E2 = E3/6.5
E1 = E3/4.3
V21 = 0.36##Swapping these goes from +x, -y to +x +y.
V12 = V21*E1/E2##
V31 = 0.36#### no change
V13 = V31*E1/E3####
V32 = 0.56##Small change near 0,0
V23 = V32*E2/E3##
Ge23 = E2
Ge31 = Ge23/10.0
Ge12 = Ge23/4.0

cA11 = trans[0]
cA12 = trans[1]
cA13 = 0
cA21 = trans[3]
cA22 = trans[4]
cA23 = 0
cA31 = 0
cA32 = 0
cA33 = 1

#stiffness matrix entries
CM11 = E1 - E1*V12*V21/(E2*(V12*V21/E2 - 1/E2)) - (V13 - V12*(V13
    *V21/E2 + V23/E2)/(V12*V21/E2 - 1/E2))*(E1*V21*(V12*V31/E3 +
    V32/E3)/(E2*(V12*V21/E2 - 1/E2)) - E1*V31/E3)/((V13*V21/E2 +
    V23/E2)*(V12*V31/E3 + V32/E3)/(V12*V21/E2 - 1/E2) - V13*V31/E3
     + 1/E3)
CM12 = -E1*V21/(E2*(V12*V21/E2 - 1/E2)) + (V13*V21/E2 + V23/E2)*(
    E1*V21*(V12*V31/E3 + V32/E3)/(E2*(V12*V21/E2 - 1/E2)) - E1*V31
    /E3)/((V12*V21/E2 - 1/E2)*((V13*V21/E2 + V23/E2)*(V12*V31/E3 +
     V32/E3)/(V12*V21/E2 - 1/E2) - V13*V31/E3 + 1/E3))
```

```
CM13 = -(E1*V21*(V12*V31/E3 + V32/E3)/(E2*(V12*V21/E2 - 1/E2)) -
    E1*V31/E3)/((V13*V21/E2 + V23/E2)*(V12*V31/E3 + V32/E3)/(V12*
    V21/E2 - 1/E2) - V13*V31/E3 + 1/E3)
CM14 = 0.0
CM15 = 0.0
CM16 = 0.0
CM21 = -V12/(V12*V21/E2 - 1/E2) - (V13 - V12*(V13*V21/E2 + V23/E2
    )/(V12*V21/E2 - 1/E2))*(V12*V31/E3 + V32/E3)/((V12*V21/E2 - 1/
    E2)*((V13*V21/E2 + V23/E2)*(V12*V31/E3 + V32/E3)/(V12*V21/E2 -
     1/E2) - V13*V31/E3 + 1/E3))
CM22 = -1/(V12*V21/E2 - 1/E2) + (V13*V21/E2 + V23/E2)*(V12*V31/E3
     + V32/E3)/((V12*V21/E2 - 1/E2)**2*((V13*V21/E2 + V23/E2)*(V12
    *V31/E3 + V32/E3)/(V12*V21/E2 - 1/E2) - V13*V31/E3 + 1/E3))
CM23 = -(V12*V31/E3 + V32/E3)/((V12*V21/E2 - 1/E2)*((V13*V21/E2 +
     V23/E2)*(V12*V31/E3 + V32/E3)/(V12*V21/E2 - 1/E2) - V13*V31/
    E3 + 1/E3))
CM24 = 0.0
CM25 = 0.0
CM26 = 0.0
CM31 = (V13 - V12*(V13*V21/E2 + V23/E2)/(V12*V21/E2 - 1/E2))/((
    V13*V21/E2 + V23/E2)*(V12*V31/E3 + V32/E3)/(V12*V21/E2 - 1/E2)
     - V13*V31/E3 + 1/E3)
CM32 = -(V13*V21/E2 + V23/E2)/((V12*V21/E2 - 1/E2)*((V13*V21/E2 +
     V23/E2)*(V12*V31/E3 + V32/E3)/(V12*V21/E2 - 1/E2) - V13*V31/
    E3 + 1/E3))
CM33 = 1/((V13*V21/E2 + V23/E2)*(V12*V31/E3 + V32/E3)/(V12*V21/E2
     - 1/E2) - V13*V31/E3 + 1/E3)
CM34 = 0.0
CM35 = 0.0
CM36 = 0.0
CM41 = 0.0
CM42 = 0.0
CM43 = 0.0
CM44 = (2*Ge23)
```

```
CM45 = 0.0
CM46 = 0.0
CM51 = 0.0
CM52 = 0.0
CM53 = 0.0
CM54 = 0.0
CM55 = (2*Ge31)
CM56 = 0.0
CM61 = 0.0
CM62 = 0.0
CM63 = 0.0
CM64 = 0.0
CM65 = 0.0
CM66 = (2*Ge12)

#assembling stiffness matrix
CMM = as_matrix([[CM11, CM12, CM13, CM14, CM15, CM16], [CM21,
    CM22, CM23, CM24, CM25, CM26], [CM31, CM32, CM33, CM34, CM35,
    CM36], \
                    [CM41, CM42, CM43, CM44, CM45, CM46], [CM51,
                       CM52, CM53, CM54, CM55, CM56], [CM61, CM62,
                       CM63, CM64, CM65, CM66]])

G11 = cA11**2
G12 = cA12**2
G13 = cA13**2
G14 = cA12*cA13
G15 = cA11*cA13
G16 = cA11*cA12
G21 = cA21**2
G22 = cA22**2
G23 = cA23**2
G24 = cA22*cA23
G25 = cA21*cA23
```

```
G26 = cA21*cA22
G31 = cA31**2
G32 = cA32**2
G33 = cA33**2
G34 = cA32*cA33
G35 = cA31*cA33
G36 = cA31*cA32
G41 = 2*cA21*cA31
G42 = 2*cA22*cA32
G43 = 2*cA23*cA33
G44 = cA22*cA33+cA23*cA32
G45 = cA21*cA33+cA23*cA31
G46 = cA21*cA32+cA22*cA31
G51 = 2*cA11*cA31
G52 = 2*cA12*cA32
G53 = 2*cA13*cA33
G54 = cA12*cA33+cA13*cA32
G55 = cA11*cA33+cA13*cA31
G56 = cA11*cA32+cA12*cA31
G61 = 2*cA11*cA21
G62 = 2*cA12*cA22
G63 = 2*cA13*cA23
G64 = cA12*cA23+cA13*cA22
G65 = cA11*cA23+cA13*cA21
G66 = cA11*cA22+cA12*cA21

G = as_matrix(((G11, G12, G13, G14, G15, G16), (G21, G22, G23,
    G24, G25, G26), (G31, G32, G33, G34, G35, G36), (G41, G42, G43
    , G44, G45, G46), (G51, G52, G53, G54, G55, G56), (G61, G62,
    G63, G64, G65, G66)))

CMF = G.T*CMM*G

V = VectorFunctionSpace(mesh, "Lagrange", 1)
```

```
VV = VectorFunctionSpace(mesh, "Lagrange", 1)
VF = FunctionSpace(mesh, "Lagrange", 1)

c = Expression(("0.0", "0.0", "0.0"), degree=3)
bcs = DirichletBC(VV, c, end_boundary)

domains = CellFunction("size_t", mesh)


du = TrialFunction(VV)            # Incremental displacement
v  = TestFunction(VV)             # Test function
u  = Function(VV)                 # Displacement from previous
   iteration
E = 0.5*(grad(u)+(grad(u)).T)



stress1s = CMF[0,0]*E[0,0] + CMF[0,1]*E[1,1] + CMF[0,2]*(E[2,2])
   + CMF[0,3]*E[1,2] + CMF[0,4]*E[0,2] + CMF[0,5]*E[0,1]
stress2s = CMF[1,0]*E[0,0] + CMF[1,1]*E[1,1] + CMF[1,2]*(E[2,2])
   + CMF[1,3]*E[1,2] + CMF[1,4]*E[0,2] + CMF[1,5]*E[0,1]
stress3s = CMF[2,0]*E[0,0] + CMF[2,1]*E[1,1] + CMF[2,2]*(E[2,2])
   + CMF[2,3]*E[1,2] + CMF[2,4]*E[0,2] + CMF[2,5]*E[0,1] + GSV[0]
stress4s = CMF[3,0]*E[0,0] + CMF[3,1]*E[1,1] + CMF[3,2]*(E[2,2])
   + CMF[3,3]*E[1,2] + CMF[3,4]*E[0,2] + CMF[3,5]*E[0,1]
stress5s = CMF[4,0]*E[0,0] + CMF[4,1]*E[1,1] + CMF[4,2]*(E[2,2])
   + CMF[4,3]*E[1,2] + CMF[4,4]*E[0,2] + CMF[4,5]*E[0,1]
stress6s = CMF[5,0]*E[0,0] + CMF[5,1]*E[1,1] + CMF[5,2]*(E[2,2])
   + CMF[5,3]*E[1,2] + CMF[5,4]*E[0,2] + CMF[5,5]*E[0,1]

#psi = 0.5*((stress1s+0)*E[0,0]+(stress2s+0)*E[1,1]+(stress3s
   +1000)*(E[2,2])+stress4s*E[1,2]+stress5s*E[0,2]+stress6s*E
   [0,1])
# Total potential energy
```

```
Pi = (0.5*((stress1s)*E[0,0]+(stress2s)*E[1,1]+(stress3s)*(E
   [2,2])+stress4s*E[1,2]+stress5s*E[0,2]+stress6s*E[0,1]))*dx

# Compute first variation of Pi (directional derivative about u
   in the direction of v)
F = derivative(Pi, u, v)

# Compute Jacobian of F
J = derivative(F, u, du)

# Solve variational problem
parameters.form_compiler.quadrature_degree = 2
solve(F == 0, u, bcs, J=J)


#plot(u, mode = "displacement", interactive = True)

u_vec = project(u, V).vector().array()
coor_int = interpolate(Expression(("x[0]", "x[1]", "x[2]"),
   degree=3), V).vector().array()
new_coor = coor_int+u_vec
num_of_verts = mesh.num_vertices()
num_of_cells = mesh.num_cells()
dofs_to_vert = np.zeros(num_of_verts, dtype=np.uintp)
vectordofs_to_vert = np.zeros((num_of_verts*3), dtype=np.uintp)
vectordofs_to_subvert = np.zeros((num_of_verts*3),dtype=np.uintp)
cellinds = np.zeros((num_of_cells,4), dtype=np.uintp)
cell_inds = np.zeros((num_of_cells,1), dtype=np.uintp)
dm = VF.dofmap()

dms = [V.sub(i).dofmap() for i in range(3)]
for cell in cells(mesh):
```

```
        cell_ind = cell.index()
        cell_inds[cell_ind] = cell.index()
        vert_inds = cell.entities(0)
        cellinds[cell_ind,:] = vert_inds #retuns the local
          indacies for each cell
        dofs_to_vert[dm.cell_dofs(cell_ind)] = vert_inds
        for i, (dms_i, dmcs_i) in enumerate(zip(dms, dms)):
            vectordofs_to_vert[dms_i.cell_dofs(cell_ind)] =
              vert_inds #gives map for coords to cells, not
              sencitive to xyz position
            vectordofs_to_subvert[dms_i.cell_dofs(cell_ind)] = i
              #gives map for each x,y,z to to particular cells
              for map above
map_mat = np.zeros((len(new_coor),3), dtype=float)
coor_cur = np.zeros((len(new_coor)/3,3), dtype=float)
map_mat[:,0] = vectordofs_to_vert
map_mat[:,1] = vectordofs_to_subvert
map_mat[:,2] = new_coor

for ij in range(0,len(map_mat)):
        if map_mat[ij,1] == 0:
            coor_cur[map_mat[ij,0],0] = map_mat[ij,2]
        if map_mat[ij,1] == 1:
            coor_cur[map_mat[ij,0],1] = map_mat[ij,2]
        if map_mat[ij,1] == 2:
            coor_cur[map_mat[ij,0],2] = map_mat[ij,2]



mesh_coor = mesh.coordinates()

mind = np.where(mesh_coor[:,2]>399)
mind = mind[0]
```

```
theta = 0


top_points = np.zeros((len(mind),2))
cur_points = np.zeros((len(mind),2))
for ii in range(0,len(top_points)):
    top_points[ii,0] = mesh_coor[mind[ii],0]*math.cos(theta) +
       mesh_coor[mind[ii],1]*(-math.sin(theta))
    top_points[ii,1] = mesh_coor[mind[ii],0]*math.sin(theta) +
       mesh_coor[mind[ii],1]*math.cos(theta)
    cur_points[ii,0] = coor_cur[mind[ii],0]*math.cos(theta) +
       coor_cur[mind[ii],1]*(-math.sin(theta))
    cur_points[ii,1] = coor_cur[mind[ii],0]*math.sin(theta) +
       coor_cur[mind[ii],1]*math.cos(theta)

pind = np.where((top_points[:,0] < 0.5) & (top_points[:,0] > 0))
nind = np.where((top_points[:,0] > -0.5) & (top_points[:,0] < 0))

pdiffv = cur_points[pind] - top_points[pind]
ndiffv = cur_points[nind] - top_points[nind]

measure = (-1*(np.mean(ndiffv[:,0])) + (np.mean(pdiffv[:,0])))
print(measure)

with open('tfile_var.csv', 'wb') as fh:
    fh.write(str(measure))
fh.close()

# measurment should be ~6.5-6.7
#comment for script, the origonal test assumes that all strain
   causeing outward movment is longatudinal, however due to the
   material geo, a significant portion may be radial/tangential
```

```
#plot(u, mode = "displacement", interactive = True)
#plot(u[2], mode = "displacement", interactive = True)

#plot(u, mode = "displacement", title = "single, u", interactive
   =True)
#subdomain tut http://fenicsproject.org/documentation/tutorial/
   materials.html
```

Bibliography

Aggarwal, P. and Chauhan, S. (2013). Longitudinal growth strains in five clones of *Eucalyptus tereticornis* Sm. *Journal of Forestry Research*, 24(2):339–343.

Akima, H. and Gebhardt, A. (2016). *akima: Interpolation of Irregularly and Regularly Spaced Data*. R package version 0.6-2.

Alméras, T. and Clair, B. (2016). Critical review on the mechanisms of maturation stress generation in trees. *Journal of The Royal Society Interface*, 13(122):20160550.

Alméras, T., Gril, J., and Yamamoto, H. (2005). Modelling anisotropic maturation strains in wood in relation to fibre boundary conditions microstructure and maturation kinetics. *Holzforschung*, 59(3).

Almras, T. and Clair, B. (2016). Critical review on the mechanisms of maturation stress generation in trees. *Journal of The Royal Society Interface*, 13:20160550.

Alnaes, M. S., Blechta, J., Hake, J., Johansson, A., Kehlet, B., Logg, A., Richardson, C., Ring, J., Rognes, M. E., and Wells, G. N. (2015). The fenics project version 1.5. *Archive of Numerical Software*, 3(100).

Altaner, C. (2018). Relationship between extractive content and natural durability. Personal Communication.

Altaner, C., Murray, T. J., , and Morgenroth, J. (2017). Durable Eucalypts on Drylands: Protecting and Enhancing Value. In Altaner, C., Murray, T. J., and Morgenroth, J., editors, *Conference Proceedings*. New Zealand School of Forestry.

Altaner, C. M. (2015). Developing a quality eucalypt resource at seedling stage. *Australian Forest Grower*, 37(4):33–35.

Apiolaza, L. A. (2008). Improvement Objectives for Short Rotation Forestry. *New Zealand Journal of Forestry*, 52(4).

Apiolaza, L. A. (2009). Very early selection for solid wood quality: screening for early winners. *Annals of Forest Science*, 66(6):601–601.

Apiolaza, L. A., Butterfield, B., Chauhan, S. S., and Walker, J. C. F. (2011a). Characterization of mechanically perturbed young stems: can it be used for wood quality screening? *Annals of Forest Science*, 68(2):407–414.

Apiolaza, L. A., Chauhan, S., Hayes, M., Nakada, R., Sharma, M., and Walker, J. (2013). Selection and breeding for wood quality a new approach. *New Zealand Journal of Forestry*, 58:33.

Apiolaza, L. A., Chauhan, S. S., and Walker, J. C. F. (2011b). Genetic control of very early compression and opposite wood in Pinus radiata and its implications for selection. *Tree Genetics & Genomes*, 7(3):563–571.

Apiolaza, L. A., Van Ballekom, S., Mcconnochie, R., Millen, P., and Walker, J. C. F. (2011c). *Introducing durable species to New Zealand drylands: Genetics of early adaptation of Eucalyptus bosistoana*. Wood technology research centre, Christchurch, New Zealand.

Archer, R. R. (1976). On the distribution of tree growth stresses. *Wood Science and Technology*, 10(4):293–309.

Archer, R. R. (1979). On the distribution of tree growth stresses. *Wood Science and Technology*, 13(1):67–78.

Archer, R. R. (1981). On the distribution of tree growth stresses. *Wood Science and Technology*, 15(3):201–209.

Archer, R. R. (1985). On the distribution of tree growth stresses. *Wood Science and Technology*, 19(3):259–276.

Archer, R. R. (1987a). *Growth stresses and strains in trees*. Springer series in wood science. Springer-Verlag.

Archer, R. R. (1987b). On the origin of growth stresses in trees. *Wood Science and Technology*, 21(2):139–154.

Archer, R. R. (1989). On the origin of growth stresses in trees. *Wood Science and Technology*, 23(4):311–322.

Archer, R. R. and Byrnes, F. E. (1974). On the distribution of tree growth stresses Part I: An anisotropic plane strain theory. *Wood Science and Technology*, 8(3):184–196.

Auguie, B. (2017). *gridExtra: Miscellaneous Functions for Grid Graphics*. R package version 2.3.

Australia, S. (2005). Australian standard AS5604: Timber Natural durability ratings.

Baillères, H., Chanson, B., Fournier, M., Tollier, M. T., and Monties, B. (1995). Structure composition chimique et retraits de maturation du bois chez les clones d'Eucalyptus. *Annales des Sciences Forestières*, 52(2):157–172.

Baker, F. W. G. (1992). *Rapid propagation of fast-growing woody species*. C.A.B. International for CASAFA Wallingford, Oxon, UK.

Bamber, R. K. (1979). The Origin of Growth Stresses. *Forpride Digest*, 8:75–79.

Bamber, R. K. (1987). The Origin of Growth Stresses: A Rebuttal. *IAWA Journal*, 8(1):80–84.

Bamber, R. K. (2001). A general theory for the origin of growth stresses in reaction wood: how trees stay upright. *Iawa Journal*, 22(3):205–212.

Barber, N. F. and Meylan, B. A. (1964). The Anisotropic Shrinkage of Wood. A Theoretical Model. *Holzforschung*, 18(5):146–156.

Barnett, J. R. (1981). *Xylem Cell Development*. Castle House.

Barnett, J. R. and Jeronimidis, G. (2003). *Wood Quality and Its Biological Basis*. Biological sciences series. Blackwell.

Batten Jr, G. and Nissan, A. (1987). Unified theory of the mechanical properties of paper and other H-bond-dominated solids. III. *Tappi journal*, 70(11):137–140.

Bergander, A. and Salmén, L. (2002). Cell wall properties and their effects on the mechanical properties of fibers. *Journal of Materials Science*, 37(1):151–156.

Bhat, K. M. and Florence, E. J. M. (2003). Natural Decay Resistance of Juvenile Teak Wood Grown in High Input Plantations. *Holzforschung*, 57(5).

Biechele, T., Nutto, L., and Becker, G. (2009). Growth strain in *Eucalyptus nitens* at different stages of development. *Silva Fennica*, 43(4).

Blackburn, D., Hamilton, M., Williams, D., Harwood, C., and Potts, B. (2014). Acoustic Wave Velocity as a Selection Trait in Eucalyptus nitens. *Forests*, 5:744762.

Bootle, K. R. (2005). *Wood in Australia : types, properties and uses / Keith R. Bootle*. McGraw-Hill, Sydney. (Keith R.) 2nd ed. Previous ed.: 1983. Includes bibliographical references and index.

Bowyer, J., Shmulsky, R., and Haygreen, J. (2007). *Forest Products and Wood Science: An Introduction*. Wiley.

Boyd, J. D. (1950). Tree growth stresses .3. The origin of growth stresses. *Australian Journal of Scientific Research Series B-Biological Sciences*, 3(3):294–309.

Boyd, J. D. (1972). Tree growth stresses Part V: Evidence of an origin in differentiation and lignification. *Wood Science and Technology*, 6(4):251–262.

Boyd, J. D. (1977). Basic cause of differentiation of tension wood and compression wood. *Australian Forest Research*, 7:121–143.

Boyd, J. D. (1985). The Key Factor in Growth Stress Generation in Trees Lignification or Crystallisation? *IAWA Journal*, 6(2):139–150.

Boyd, J. D. et al. (1950). Tree growth stresses. I. Growth stress evaluation. *Australian Journal of Scientific Research*, 3(3):270–93.

Brodzki, P. (1972). Callose in compression wood tracheids. *Acta Societatis Botanicorum Poloniade*, 41:321–327.

Buchanan, A., Bryant, T., King, A., Simperingham, P., Smith, P., Tan, R., and Walford, B. (2005). Timber Structures Standard Amendments No 1 & 2 & 4 Appended. In NZS 3603:1993. Technical report, Standards New Zealand.

Burdon, R., Kibblewhite, P. R., C. F. Walker, J., A. Megraw, R., Evans, R., and Cown, D. (2004). Juvenile versus mature wood: A new concept, orthogonal to corewood

versus outerwood, with special reference to pinus radiata and p. taeda. *Forest Science*, 50:399–415.

Burgert, I., Eder, M., Gierlinger, N., and Fratzl, P. (2007). Tensile and compressive stresses in tracheids are induced by swelling based on geometrical constraints of the wood cell. *Planta*, 226(4):981–987.

Burgess, J. (2015). Genetic parameter estimates for growth traits of Eucalyptus bosistoana: assessment of two progeny trials in Marlborough, New Zealand. Master's thesis, University of Canterbury.

Cappa, E. P. and Cantet, R. J. (2006). Bayesian inference for normal multiple-trait individual-tree models with missing records via full conjugate Gibbs. *Canadian Journal of Forest Research*, 36(5):1276–1285.

Cappa, E. P., Pathauer, P. S., and Lopez, G. A. (2010). Provenance variation and genetic parameters of Eucalyptus viminalis in Argentina. *Tree Genetics & Genomes*, 6(6):981–994.

Cave, I. D. (1968). The anisotropic elasticity of the plant cell wall. *Wood Science and Technology*, 2(4):268–278.

Ceccarelli, S., Erskine, W., Hamblin, J., and Grando, S. (1994). Genotype by environment interaction and international breeding programmes. *Experimental agriculture*, 30(2):177–188.

Chang, S.-S., Salmén, L., Olsson, A.-M., and Clair, B. (2013). Deposition and organisation of cell wall polymers during maturation of poplar tension wood by FTIR microspectroscopy. *Planta*, 239(1):243–254.

Charlier, L. and Mazeau, K. (2012). Molecular Modeling of the Structural and Dynamical Properties of Secondary Plant Cell Walls: Influence of Lignin Chemistry. *J. Phys. Chem. B*, 116(14):4163–4174.

Chauhan, S. S. (2008). Pairing Test and Longitudinal Growth Strain: Establishing the Association. In *Pairing Test and Longitudinal Growth Strain: Establishing the Association*. Proceedings of the 51st International Convention of Society of Wood Science and Technology November 10-12, 2008 Concepcin, CHILE.

Chauhan, S. S. and Entwistle, K. (2010). Measurement of surface growth stress in Eucalyptus nitens Maiden by splitting a log along its axis. *Holzforschung*, 64(2).

Chauhan, S. S., Sharma, M., Thomas, J., Apiolaza, L. A., Collings, D. A., and Walker, J. C. F. (2013). Methods for the very early selection of Pinus radiata D. Don. for solid wood products. *Annals of Forest Science*, 70(4):439–449.

Chauhan, S. S. and Walker, J. (2004). Relationships between longitudinal growth strain and some wood properties in Eucalyptus nitens. *Australian Forestry*, 67(4):254–260.

Chauhan, S. S. and Walker, J. C. (2011). Wood quality in artificially inclined 1-year-old trees of *Eucalyptus regnans* - differences in tension wood and opposite wood properties. *Can. J. For. Res.*, 41(5):930–937.

Clair, B., Alméras, T., Yamamoto, H., Okuyama, T., and Sugiyama, J. (2006). Mechanical Behavior of Cellulose Microfibrils in Tension Wood in Relation with Maturation Stress Generation. *Biophysical Journal*, 91(3):1128–1135.

Clair, B., Alteyrac, J., Gronvold, A., Espejo, J., Chanson, B., and Almras, T. (2013). Patterns of longitudinal and tangential maturation stresses in *Eucalyptus nitens* plantation trees. *Annals of Forest Science*, 70(8):801–811.

Cosgrove, D. J. (2005). Growth of the plant cell wall. *Nat Rev Mol Cell Biol*, 6:850–61.

Coutts, P. and Grace, J. (1995). *Wind and Trees*. Cambridge University Press.

Cramer, M. (2018). Wachstumsspannungen in Eukalyptus. Master's thesis, Technische Universitat Dresden.

Cullis, B. R., Jefferson, P., Thompson, R., and Smith, A. B. (2014). Factor analytic and reduced animal models for the investigation of additive genotype-by-environment interaction in outcrossing plant species with application to a pinus radiata breeding programme. *Theoretical and Applied Genetics*, 127(10):2193–210.

Davidson, T. C., Newman, R. H., and Ryan, M. J. (2004). Variations in the fibre repeat between samples of cellulose I from different sources. *Carbohydrate Research*, 339(18):2889–2893.

Davies, N., Sharma, M., Altaner, C., and Apiolaza, L. (2015). Screening eucalyptus for growth strain. In *Abstracts of the 8th Plant Biomechanics International Conference*.

Davies, N. T. (2014). Reverse Engineering the Tree. Master's thesis, New Zealand School of Forestry.

Davies, N. T., Apiolaza, L. A., and Sharma, M. (2017). Heritability of growth strain in Eucalyptus bosistoana: a Bayesian approach with left-censored data. *New Zealand Journal of Forestry Science*, 47(1).

De Little, D. et al. (1989). Paropsine chrysomelid attack on plantations of eucalyptus nitens in tasmania. *New Zealand Journal of Forestry Science*, 19(2/3):223–227.

Dieters, M., White, T., and Hodge, G. (1995). Genetic parameter estimates for volume from fuil-sib tests of slash pine (Pinus elliottii). *Canadian Journal of Forest Research*, 25(8):1397–1408.

Dlouh, J., Fournier, M., Jaouen, G., and Almeras, T. (2013). Integrative biomechanics for tree ecology: beyond wood density and strength. *Journal of Experimental Botany*, 64(15):4793–4815.

Donaldson, L. A. and Burdon, R. D. (1995). Clonal variation and repeatability of microfibril angle in pinus radiata. *New Zealand Journal of Forestry Science*, pages 164–174.

Dungey, H. S., Matheson, A. C., Kain, D., and Evans, R. (2006). Genetics of wood stiffness and its component traits in pinus radiata. *Canadian Journal of Forest Research*, 36(5):1165–1178.

Eder, M., Arnould, O., Dunlop, J. W. C., Hornatowska, J., and Salmén, L. (2012). Experimental micromechanical characterisation of wood cell walls. *Wood Science and Technology*, 47(1):163–182.

Entwistle, K., Chauhan, S., Sharma, M., and Walker, J. (2014). The effect of saw kerf width on the value of the axial growth stress measured by slitting a log along its axis. *Wood Material Science & Engineering*, pages 1–12.

Fahlén, J. and Salmén, L. (2005). Pore and Matrix Distribution in the Fiber Wall Revealed by Atomic Force Microscopy and Image Analysis. *Biomacromolecules*, 6(1):433–438.

Faisal, T. R., Rey, A., and Pasini, D. (2013). A multiscale mechanical model for plant tissue stiffness. *Polymers*, 5(2):730–750.

Ferrand, J.-C. (1982). Etude des contraintes de croissance Première partie : méthode de mesure sur carottes de sondage. *Annales des Sciences Forestières*, 39(2):109–142.

Flores, E. S., DiazDelao, F., Friswell, M., and Ajaj, R. (2014). Investigation on the extensibility of the wood cell-wall composite by an approach based on homogenisation and uncertainty analysis. *Composite Structures*, 108:212–222.

Forest Owners Association (2017). Facts and Figures, 2017–2018, New Zealand Plantation Forest Industry. Technical report, New Zealand Forest Owners Association.

Fournier, M., Chanson, B., Thibaut, B., and Guitard, D. (1994). Mesures des déformations résiduelles de croissance à la surface des arbres en relation avec leur morphologie. Observations sur différentes espèces. *Annales des Sciences Forestières*, 51(3):249–266.

Fromm, J. (2013). *Cellular Aspects of Wood Formation*. Plant Cell Monographs. Springer.

Gardiner, B., Barnett, J., Saranpää, P., and Gril, J. (2014). *The Biology of Reaction Wood*. Springer Series in Wood Science. Springer Berlin Heidelberg.

Gelman, A. and Hill, J. (2007). *Data analysis using regression and multilevel/hierarchical models*. Cambridge University Press, Cambridge;New York;.

Gillis, P. P. and Hsu, C. H. (1979). An elastic plastic theory of longitudinal growth stresses. *Wood Science and Technology*, 13(2):97–115.

Gonçalves, R., Trinca, A. J., and Pellis, B. P. (2013). Elastic constants of wood determined by ultrasound using three geometries of specimens. *Wood Science and Technology*, 48(2):269–287.

Greaves, B., Borralho, N. M. G., Raymond, C. A., Evans, R., and Whiteman, P. (1997). Age-age correlations in, and relationships between basic density and growth in Eucalyptus nitens. *Silvae Genetica*, 46(5).

Griffin, A. and Cotterill, P. (1988). Genetic variation in growth of outcrossed, selfed and open-pollinated progenies of Eucalyptus regnans and some implications for breeding strategy. *Silvae Genetica*, 37(3-4):124–131.

Gril, J., Jullien, D., Bardet, S., and Yamamoto, H. (2017). Tree growth stress and related problems. *Journal of Wood Science*, 63(5):411–432.

Gueneau, P. and Chardin, A. (1973). *Growth stresses.* . Cahiers Scientifiques, Centre Technique Forestier Tropical, France.

Gueneau, P. and Kikata, Y. (1973). Growth stresses. . *Bois et forets des tropiques*, 149:21–30.

Gueneau, P. and Saurat, J. (1974). *Growth stresses – forest measurements*. Rapport, Centre Technique du Bois France.

Guitard, D., Masse, H., Yamamoto, H., and Okuyama, T. (1999). Growth stress generation: a new mechanical model of the dimensional change of wood cells during maturation. *Journal of Wood Science*, 45(5):384–391.

Hadfield, J. (2014). MCMCglmm Course Notes. [Online accessed May 2018].

Hadfield, J. D. (2010). MCMC Methods for Multi-Response Generalized Linear Mixed Models: The MCMCglmm R Package. *Journal of Statistical Software*, 33(2):1–22.

Hamilton, M. and Potts, B. (2008). Eucalyptus nitens genetic parameters. *New Zealand Journal of Forestry Science*, 38:102119.

Harju, A. M., Venlinen, M., Laakso, T., and Saranp, P. (2009). Wounding response in xylem of Scots pine seedlings shows wide genetic variation and connection with the constitutive defence of heartwood. *Tree Physiology*, 29(1):19–25.

Harrington, J. J. (2002). *Hierarchical modelling of softwood hygro-elastic properties*. PhD thesis, University of Canterbury.

Hein, P. R. G., Bouvet, J.-M., Mandrou, E., Vigneron, P., Clair, B., and Chaix, G. (2012). Age trends of microfibril angle inheritance and their genetic and environmental correlations with growth density and chemical properties in Eucalyptus urophylla S.T. Blake wood. *Annals of Forest Science*, 69:681–691.

Hejnowicz, Z. (1967). Some observations on the mechanism of orientation movement of woody stems. *American journal of Botany*, pages 684–689.

Henderson, C. (1985). Equivalent Linear Models to Reduce Computations. *Journal of Dairy Science*, 68(9):2267–2277.

Henson, M., Boyton, S., Davies, M., Joe, B., Kangane, B., Murphy, T. N., Palmer, G., and Vanclay, J. K. (2004). Genetic parameters of wood properties in a 9 year old E. dunnii progeny trial in NSW, Australia. In *Eucalyptus in a Changing World*, pages 83–83.

Hepworth, D. (1998). Modelling the Mechanical Properties of Xylem Tissue from Tobacco Plants (Nicotiana tabacum'Samsun') by Considering the Importance of Molecular and Micromechanisms. *Annals of Botany*, 81(6):761–770.

Hodge, G. R. and White, T. L. (1992). Genetic Parameter Estimates for Growth Traits at Different Ages in Slash Pine and some Implications for Breeding. *Silvae Genetica*, 41.

Houtman, C. J. and Atalla, R. H. (1995). Cellulose-lignin interactions (A computational study). *Plant physiology*, 107(3):977–984.

Hung, T. D., Brawner, J. T., Meder, R., Lee, D. J., Southerton, S., Thinh, H. H., and Dieters, M. J. (2014). Estimates of genetic parameters for growth and wood properties in *Eucalyptus pellita* F. Muell. to support tree breeding in Vietnam. *Annals of Forest Science*, 72(2):205–217.

Jacobs, M. R. (1945). *The growth stresses of woody stems*. Commonwealth of Australia Department of national development forestry and timber bureau.

Jacobs, M. R. (1965). *Stresses and strains in tree trunks as they grow in length and width*. Commonwealth of Australia Department of national development forestry and timber bureau.

Jin, K., Qin, Z., and Buehler, M. J. (2015). Molecular deformation mechanisms of the wood cell wall material. *Journal of the mechanical behavior of biomedical materials*, 42:198–206.

Jones, E., Oliphant, T., Peterson, P., et al. (2001). SciPy: Open source scientific tools for Python. [Online accessed May 2018].

Kamarudin, N. (2014). *A new technology for measuring growth stress in Eucalypts*. PhD thesis, University of Melbourne.

Kikata, Y. (1972). The efect of lean on level of growth stresses in pinus densiflora. *Journal of the Japan Wood Research Society*, 18(9):443–449.

Kikata, Y. and Miwa, K. (1977). A modified hole drilling technique for determining residual stresses (growth stresses) in tree trunks. *Journal of the Society of Materials Science Japan*, 26(284):429–432.

Kim, J. S., Awano, T., Yoshinaga, A., and Takabe, K. (2011). Ultrastructure of the innermost surface of differentiating normal and compression wood tracheids as revealed by field emission scanning electron microscopy. *Planta*, 235(6):1209–1219.

Kingsbury, N. (2009). *Hybrid: the history and science of plant breeding*. University of Chicago Press.

Koehler, A. (1933). A new hypothesis as to the cause of shakes and rift cracks in green timber. *Journal of Forestry*, 31(5):551–556.

Kojima, M., Becker, V. K., and Altaner, C. M. (2011). An unusual form of reaction wood in Koromiko [Hebe salicifolia G. Forst. (Pennell)] a southern hemisphere angiosperm. *Planta*, 235(2):289–297.

Kokutse, A. D., Stokes, A., Baillères, H., Kokou, K., and Baudasse, C. (2006). Decay resistance of Togolese teak (Tectona grandis L.f) heartwood and relationship with colour. *Trees*, 20(3):403–403.

Kruschke, J. (2014). *Doing Bayesian data analysis: A tutorial with R, JAGS, and Stan.* Burlington, MA: Academic Press.

Kübler, H. (1959a). Studien ber Wachstumsspannungen des HolzesErste Mitteilung: Die Ursache der Wachstumsspannungen und die Spannungen quer zur Faserrichtung. *Holz als Roh- und Werkstoff*, 17(1):1–9.

Kübler, H. (1959b). Studien ber Wachstumsspannungen des HolzesZweite Mitteilung Die Spannungen in Faserrichtung. *Holz als Roh- und Werkstoff*, 17(2):44–54.

Kübler, H. (1983). Mechanism of frost crack formation in trees–a review and synthesis. *Forest Science*, 29(3):559–568.

Kübler, H. (1987). Growth stresses in trees and related wood properties. *Forestry Abstacts*, 48(3):131–189.

Lasserre, J., Mason, E., Watt, M., and Moore, J. (2009). Influence of initial planting spacing and genotype on microfibril angle, wood density, fibre properties and modulus of elasticity in *Pinus radiata* d.don corewood. *Forest Ecology and Management*, 258:1924–1931.

Li, C., Weng, Q., Chen, J.-B., Li, M., Zhou, C., Chen, S., Zhou, W., Guo, D., Lu, C., Chen, J.-C., Xiang, D., and Gan, S. (2016). Genetic parameters for growth and wood mechanical properties in *Eucalyptus cloeziana* F. Muell. *New Forests*, 48:33–49.

Li, Y., Apiolaza, L. A., and Altaner, C. (2018). Genetic variation in heartwood properties and growth traits of eucalyptus bosistoana. *European journal of forest research*, 137(4):565–572.

Li, Y., Suontama, M., Burdon, R., and Dungey, H. (2017). Genotype by environment interactions in forest tree breeding: review of methodology and perspectives on research and application. *Tree Genetics & Genomes*, 13(3):1.

Lopez, G. A., Potts, B. M., Vaillancourt, R. E., and Apiolaza, L. A. (2003). Maternal and carryover effects on early growth of eucalyptus globulus. *Canadian Journal of Forest Research*, 33(11):2108–2115.

Lunn, D., Jackson, C., Best, N., Thomas, A., and Spiegelhalter, D. (2012). *The BUGS book: A practical introduction to Bayesian analysis*. CRC press.

Madhibha, T., Murepa, R., Musokonyi, C., and Gapare, W. (2013). Genetic parameter estimates for interspecific Eucalyptus hybrids and implications for hybrid breeding strategy. *New Forests*, 44(1):63–84.

Mark, R. (1967). *Cell wall mechanics of tracheids*. Yale University Press.

Marra, A. A. (1992). *Technology of Wood Bonding Principles in Practice*. Van Nostrand Reinhold.

Martley, J. F. (1928). Theoretical calculation of the pressure distribution on the basal section of a tree. *Forestry*, 2(1):69–72.

Mason, E. G. (2006). Interactions between influences of genotype and grass competition on growth and wood stiffness of juvenile radiata pine in a summer-dry environment. *Canadian Journal of Forest Research*, 36(10):2454–2463.

Mattheck, C. and Kübler, H. (1997). *Wood: the internal optimization of trees*. Springer.

Meinzer, F. C., Lachenbruch, B., and Dawson, T. E. (2011). *Size- and Age-Related Changes in Tree Structure and Function*. Springer Netherlands.

Mellerowicz, E. J., Immerzeel, P., and Hayashi, T. (2008). Xyloglucan: The Molecular Muscle of Trees. *Annals of Botany*, 102(5):659–665.

Mihai, G. and Mirancea, I. (2016). Age trends in genetic parameters for growth and quality traits in Abies alba. *iForest - Biogeosciences and Forestry*, 9(6):954–959.

Mishnaevsky, Jr., L. and Qing, H. (2008). Micromechanical modelling of mechanical behaviour and strength of wood: State-of-the-art review. *Computatioal Materials Science*, 44(2):363–370.

Mishra, G. (2018). *Heartwood formation and the chemical basis of natural durability in Eucalyptus bosistoana.* PhD thesis, Forestry Science.

Mora, F. and Serra, N. (2014). Bayesian estimation of genetic parameters for growth stem straightness, and survival in Eucalyptus globulus on an Andean Foothill site. *Tree Genetics & Genomes*, 10:711–719.

Munch, E. (1938). Statik und Dynamic des schraubigen Baues der Zellwand besonders des Druck- und Zugholzes. *Flora*, 32:357–424.

Muneri, A., Leggate, W., and Palmer, G. (1999). Relationships between surface growth strain and some tree wood and sawn timber characteristics of Eucalyptus cloeziana. *The Southern African Forestry Journal*, 186(1):41–49.

Murphy, T. N., Henson, M., and Vanclay, J. K. (2005). Growth stress in *Eucalyptus dunnii*. *Australian Forestry*, 68(2):144–149.

Myszewski, J. H., Bridgwater, F. E., Lowe, W. J., Byram, T. D., and Megraw, R. A. (2004). Genetic Variation in the Microfibril Angle of Loblolly Pine From Two Test Sites. *Southern Journal of Applied Forestry*, 28(4):196–204.

Naranjo, S. S., Moya, R., Chauhan, S., and Moya, R. (2012). Early genetic evaluation of morphology and some wood properties of *Tectona grandis* L. clones. *Silvae Genet*, 61:58–65.

Nicholson, J. E. (1971). A rapid method for estimating longitudinal growth stresses in logs. *Wood Science and Technology*, 5(1):40–48.

Niklas, K. and Spatz, H. (2012). *Plant Physics*. University of Chicago Press.

Nissan, A. H. (1987). Unified theory of the mechanical properties of paper and other H-bond-dominated solids. II. *Tappi journal*, 70(10):128–131.

Nissan, A. H. and Batten, G. L. (1997). The link between the molecular and structural theories of paper elasticity. *Tappi journal*, 80(4):153–158.

Okuyama, T. (1993). Growth stresses in tree. *J. Jpn. Wood Res. Soc.*, 39:747–756.

Okuyama, T., Kawai, A., Kikata, Y., and Yamamoto, H. (1986). *The growth stresses in reaction wood*. Proc. 18th IUFRO World Congress, Yugoslavia, Div. 5 For. Proc.

Okuyama, T., Sasaki, Y., Kikata, Y., and Kawai, N. (1981). The seasonal change in growth stresses in the tree trunk. *Journal of the Japan Wood Research Society*, 27(5):350–155.

Okuyama, T., Takeda, H., Yamamoto, H., and Yoshida, M. (1998). Relation between growth stress and lignin concentration in the cell wall: Ultraviolet microscopic spectral analysis. *Journal of Wood Science*, 44(2):83–89.

Okuyama, T., Yamamoto, H., Iguchi, M., and Yoshida, M. (1990). Generation process of growth stresses in cell-walls .2. Growth stresses in tension wood. *Mokuzai Gakkaishi*, 36(10):797–803.

Okuyama, T., Yamamoto, H., Yoshida, M., Hattori, Y., and Archer, R. (1994). Growth stresses in tension wood: role of microfibrils and lignification. *Annales des Sciences Forestières*, 51(3):291–300.

Osorio, L., White, T., and Huber, D. (2003). Age–age and trait–trait correlations for Eucalyptus grandis Hill ex Maiden and their implications for optimal selection age and design of clonal trials. *Theoretical and Applied Genetics*, 106(4):735–743.

Pilate, G., Chabbert, B., Cathala, B., Yoshinaga, A., Leplé, J.-C., Laurans, F., Lapierre, C., and Ruel, K. (2004). Lignification and tension wood. *Comptes Rendus Biologies*, 327(9-10):889–901.

Plummer, M. (2015). RJAGS: Interface to the JAGS MCMC library.

Polge, H. and Thiercelin, F. (1979). Growth stress appraisal through increment core measurements. *Wood Science*, 12(2):86–92.

Potts, B. M., Vaillancourt, R. E., Jordan, G., Dutkowski, G., McKinnon, G., Steane, D., Volker, P., Lopez, G., Apiolaza, L., Li, Y., et al. (2004). Exploration of the Eucalyptus globulus gene pool. In *Eucalyptus in a Changing World. Proc. IUFRO*.

Poynton, R. J. (1979). *Tree Planting in Southern Africa: The eucalypts*, volume 1 of *Tree Planting in Southern Africa*. Department of Forestry, Department of Forestry, South Africa.

Qiu, D., Wilson, I. W., Gan, S., Washusen, R., Moran, G. F., and Southerton, S. G. (2008). Gene expression in Eucalyptus branch wood with marked variation in cellulose microfibril orientation and lacking G-layers. *New Phytologist*, 179(1):94–103.

R Core Team (2017). *R: A Language and Environment for Statistical Computing*. R Foundation for Statistical Computing, Vienna, Austria.

Raymond, C., Kube, P., Pinkard, L., Savage, L., and Bradley, A. (2004). Evaluation of non-destructive methods of measuring growth stress in Eucalyptus globulus: relationships between strain wood properties and stress. *Forest Ecology and Management*, 190(2-3):187–200.

Raymond, C. A. (2002). Genetics of Eucalyptus wood properties. *Annals of Forest Science*, 59:525531.

Raymond, C. A. and Cotterill, P. P. (1990). Methods of assessing crown form of *Pinus radiata*. *Silvae Genetica*, 39(2):67–71.

Retief, E. C. L. and Stanger, T. K. (2009). Genetic control of wood density and bark thickness and their correlations with diameter, in pure and hybrid populations ofEucalyptus grandisandE. urophyllain South Africa. *Southern Forests: a Journal of Forest Science*, 71:147–153.

Ribes, A. and Caremoli, C. (2007). Salome platform component model for numerical simulation. In *31st Annual International Computer Software and Applications Conference - Vol. 2 - (COMPSAC 2007)*. IEEE.

Ross, R. J. and USDA Forest Service., F. P. L. (2010). Wood handbook : wood as an engineering material. Technical report, Forest Products Laboratory.

Ruelle, J., Beauchêne, J., Prévost, M. F., Clair, B., and Fournier, M. (2006). Tension Wood and Oppositewood in 21 Tropical Rain Forest Species. *IAWA Journal*, 27(4):341–376.

Salmén, L. (2014). Wood morphology and properties from molecular perspectives. *Annals of Forest Science*, 72(6):679–684.

Sangha, A. K., Petridis, L., Smith, J. C., Ziebell, A., and Parks, J. M. (2011). Molecular simulation as a tool for studying lignin. *Environmental Progress & Sustainable Energy*, 31(1):47–54.

Saranpaa, P., Gril, J., Gardiner, B. A., and Barnett, J. (2014). *The Biology of Reaction Wood*. Springer Series in Wood Science. Springer, Berlin.

Saurat, J. and Guneau, P. (1976). Growth stresses in beech. *Wood Sci.Technol.*, 10(2):111–123.

Schberl, J. (1997). NETGEN An advancing front 2D/3D-mesh generator based on abstract rules. *Computing and Visualization in Science*, 1(1):41–52.

Senn, S., Holford, N., and Hockey, H. (2012). The ghosts of departed quantities: approaches to dealing with observations below the limit of quantitation. *Statistics in Medicine*, 31(30):4280–4295.

Sharma, M. (2013). *New Approaches to Wood Quality Assessment*. PhD thesis, Forestry Science.

Sharma, M., Apiolaza, L. A., Chauhan, S., Mclean, J. P., and Wikaira, J. (2015). Ranking very young Pinus radiata families for acoustic stiffness and validation by microfibril angle. *Annals of Forest Science*, 73(2):393–400.

Silva, J. C. e., Borralho, N. M. G., Arajo, J. A., Vaillancourt, R. E., and Potts, B. M. (2008). Genetic parameters for growth wood density and pulp yield in Eucalyptus globulus. *Tree Genetics & Genomes*, 5:291305.

Smith, D. M., Larson, B. C., Kelty, M. J., and Ashton, P. M. S. (1997). *The Practice of Silviculture: Applied Forest Ecology*. John Whiley and Sons, 9 edition.

Soria, F., Basurco, F., Toval, G., Silió, L., Rodriguez, M. C., and Toro, M. (1998). An application of Bayesian techniques to the genetic evaluation of growth traits in Eucalyptus globulus. *Canadian Journal of Forest Research*, 28(9):1286–1294.

Stackpole, D. J., Vaillancourt, R. E., de Aguigar, M., and Potts, B. M. (2009). Age trends in genetic parameters for growth and wood density in Eucalyptus globulus. *Tree Genetics & Genomes*, 6(2):179–193.

Standards New Zealand (2005). New Zealand standard NZS3622:2004: Verification of Timber Properties.

Sugiyama, K., Okuyama, T., Yamamoto, H., and Yoshida, M. (1993). Generation process of growth stresses in cell walls: Relation between longitudinal released strain and chemical composition. *Wood Sci.Technol.*, 27(4).

Sun, Z., Zhao, X., Wang, X., and Ma, J. (2014). Multiscale modeling of the elastic properties of natural fibers based on a generalized method of cells and laminate analogy approach. *Cellulose*, 21(3):1135–1141.

Suontama, M., Low, C. B., Stovold, G. T., Miller, M. A., Fleet, K. R., Li, Y., and Dungey, H. S. (2015). Genetic parameters and genetic gains across three breeding cycles for growth and form traits of Eucalyptus regnans in New Zealand. *Tree Genetics & Genomes*, 11.

Taiz, L. and Zeiger, E. (2006). *Plant Physiology*. Sinauer Associates.

Timell, T. (1969). The chemical composition of tension wood. *Svensk Papp Tidn*, 72:173–81.

Timell, T. (1986). *Compression Wood in Gymnosperms*. Springer.

Tyerman, S. D., Niemietz, C. M., and Bramley, H. (2002). Plant aquaporins: multifunctional water and solute channels with expanding roles. *Plant Cell and Environment*, 25(2):173–194.

Valencia, J., Harwood, C., Washusen, R., Morrow, A., Wood, M., and Volker, P. (2010). Longitudinal growth strain as a log and wood quality predictor for plantation-grown Eucalyptus nitens sawlogs. *Wood Science and Technology*, 45:1534.

van Ballekom, S. and Millen, P. (2017). NZDFI: Achievements, Constraints and Opportunities. In *Durable Eucalypts on Drylands: Protecting and Enhancing Value*. University of Canterbury.

Van Belle, G. (2011). *Statistical rules of thumb*, volume 699. John Wiley and Sons.

Vargas-Reeve, F., Mora, F., Perret, S., and Scapim, C. A. (2013). Heritability of stem straightness and genetic correlations in Eucalyptus cladocalyx in the semi-arid region of Chile. *Crop Breeding and Applied Biotechnology*, 13(2):107–112.

Walker, J. (1993). *Primary Wood Processing: Principles and Practice*. Chapman & Hall.

Walker, J. (2006). *Primary Wood Processing: Principles and Practice*. SpringerLink: Springer e-Books. Springer.

Walker, J. (2014-2018). Sustainable farming fund project 407602 metings and nzdfi metings. unpublished.

Wang, N., Liu, W., and Peng, Y. (2013). Gradual transition zone between cell wall layers and its influence on wood elastic modulus. *Journal of Materials Science*, 48(14):5071–5084.

Wardrop, A. B. (1965). *The formation and function of reaction wood*. Syracuse University Press, Syracuse, NY.

Watanabe, K., Yamashita, K., and Noshiro, S. (2011). Non-destructive evaluation of surface longitudinal growth strain on Sugi (Cryptomeria japonica) green logs using near-infrared spectroscopy. *Journal of Wood Science*, 58(3):267–272.

Watt, M. P., Blakeway, F. C., Mokotedi, M. E. O., and Jain, S. M. (2003). Micropropagation of Eucalyptus. In *Micropropagation of Woody Trees and Fruits*, pages 217–244. Springer Netherlands.

White, T. L., Adams, W. T., and Neale, D. B. (2007). *Forest genetics*. CABI.

Wickham, H. (2016). *ggplot2: Elegant Graphics for Data Analysis*. Springer-Verlag New York.

Wilhelmy, V. and Kübler, H. (1973). Probe for measurement of strains inside solid bodies. *Experimental Mechanics*, 13(3):142–144.

Wu, H., Ivkovi, M., Gapare, W., Matheson, A., Baltunis, B., Powell, M., and A. McRae, T. (2008). Breeding for wood quality and profit in radiata pine: A review of genetic parameters. Technical report, CSIRO Forestry and Forest Products.

Wu, H., Powell, M., L. Yang, J., Ivkovi, M., and A. McRae, T. (2007). Efficiency of early selection for rotation-aged wood quality traits in radiata pine. *http://dx.doi.org/10.1051/forest:2006082*, 64:2019–2029.

Xu, P. and Walker, J. C. F. (2004). Stiffness gradients in radiata pine trees. *Wood Science and Technology*, 38(1):1–9.

Yamamoto, H. (1998). Generation mechanism of growth stresses in wood cell walls: roles of lignin deposition and cellulose microfibril during cell wall maturation. *Wood Science and Technology*, 32(3):171–182.

Yamamoto, H. (2002). Origin of the Biomechanical Properties of Wood Related to the Fine Structure of the Multi-layered Cell Wall. *Journal of Biomechanical Engineering*, 124(4):432.

Yamamoto, H. (2007). Tree growth stress and its related problems. In *Compromised wood workshop*. University of Canterbury.

Yamamoto, H. and Almèras, T. (2007). A mathematical verification of the reinforced-matrix hypothesis using the Mori-Tanaka theory. *Journal of Wood Science*, 53(6):505–509.

Yamamoto, H. and Okuyama, T. (1988). Analysis of the generation process of growth stresses in cell-walls. *Mokuzai Gakkaishi*, 34(10):788–793.

Yamamoto, H., Okuyama, T., Sugiyama, K., and Yoshida, M. (1992). Generation process of growth stresses in cell-walls: Action of the cellulose microfibril upon the generation of the tensile stresses. *Mokuzai Gakkaishi*, 38(2):107–113.

Yamamoto, H., Okuyama, T., and Yoshida, M. (1993). Generation process of growth stresses in cell-walls .5. Model of tensile-stress generation in gelatinous fibres. *Mokuzai Gakkaishi*, 39(2):118–125.

Yamamoto, H., Okuyama, T., and Yoshida, M. (1995). Generation process of growth stresses in cell-walls .6. Analysis of growth stress generation by using a cell model having 3 layers (S1, S2 and I+P). *Mokuzai Gakkaishi*, 41(1):1–8.

Yamamoto, H., Okuyama, T., Yoshida, M., and Sugiyama, K. (1991). Generation process of growth stresses in cell walls: Growth stresses in compression wood. *Mokuzai Gakkaishi*, 37:94–100.

Yang, J. L., Baillères, H., Evans, R., and Downes, G. (2006). Evaluating growth strain of Eucalyptus globulus Labill. from SilviScan measurements. *Holzforschung*, 60(5).

Yang, J. L., Baillères, H., Okuyama, T., Muneri, A., and Downes, G. (2005). Measurement methods for longitudinal surface strain in trees: a review. *Australian Forestry*, 68(1):34–43.

Yang, J. L., Fife, D., Waugh, G., Downes, G., and Blackwell, P. (2002). The effect of growth strain and other defects on the sawn timber quality of 10 year old *Eucalyptus globulus* Labill. *Australian Forestry*, 65(1):31–37.

Yang, J.-L. and Waugh, G. (2001). Growth stress, its measurement and effects. *Australian Forestry*, 64(2):127–135.

Yin, J., Song, K., Lu, Y., Zhao, G., and Yin, Y. (2015). Comparison of changes in micropores and mesopores in the wood cell walls of sapwood and heartwood. *Wood Science and Technology*, 49(5):987–1001.

Yoshida, M. and Okuyama:, T. (2002). Techniques for Measuring Growth Stress on the Xylem Surface Using Strain and Dial Gauges. *Holzforschung*, 56(5).

Yoshizawa, N., Satoh, M., Yokota, S., and Idei, T. (1992). Formation and structure of reaction wood in Buxus microphylla var. insularis Nakai. *Wood Sci.Technol.*, 27(1).

Zhan, T., Lu, J., Zhou, X., and Lu, X. (2014). Representative volume element (RVE) and the prediction of mechanical properties of diffuse porous hardwood. *Wood Science and Technology*, 49(1):147–157.

Zhang, L. and LeBoeuf, E. J. (2009). A molecular dynamics study of natural organic matter: 1. Lignin kerogen and soot. *Organic Geochemistry*, 40(11):1132–1142.